3D longitudinal evaluation of facial morphology of the surgically managed unilateral cleft lip and palate (UCLP) cases.

Dhelal Hatem Nsaif Al-Rudainy

B.D.S., M.Sc. Orthodontics

Submitted in fulfilment of the requirement for the degree of Doctor of Philosophy

To

Glasgow Dental School, College of Medical, Veterinary and Life Sciences

April 2018

I dedicate this work to the people of Iraq, my beloved home.

Summary

Introduction

Modern society is passionate about beauty and aesthetics. According to a 2016 survey by the International Society of Aesthetic and Plastic Surgery, the demand for aesthetic surgery is more than ever. People's perception and awareness of facial aesthetics has increased. Orofacial cleft is the most common facial dysmorphology, with prevalence about 1.46:1000 in Scotland. The aim of the initial surgical repair of cleft lip is to improve facial aesthetics and function, without interrupting facial growth. Nevertheless, facial asymmetry is a stigma in cleft patients, and revision surgery due to a patient or their parents' dissatisfaction with the outcomes is not uncommon.

Objective evaluation of facial asymmetry after primary surgical repair is valuable. It is an indication of the success of surgery, and it informs the surgeon of the magnitude and location of residual asymmetry. The evaluation of facial asymmetry has evolved significantly from landmark-based assessment to surface-based analysis. The latter provides a comprehensive evaluation of facial asymmetry by superimposing the original 3D model on its mirror copy. This permits the quantification and the visualisation of the disparity between the two halves of the face.

Many studies evaluated facial asymmetry a few years after primary surgical repair. Longitudinal monitoring and quantifying of facial shape changes can potentially guide the surgeon to the optimal surgical technique. Only a few studies evaluated facial asymmetry before and after primary surgery, and their analysis was dependent on a set of facial landmarks that did not describe the asymmetry of facial surfaces between these landmarks. Unfortunately, the existing literature does not provide comprehensive longitudinal evaluation of facial asymmetry of cleft patients, and the impact

of facial expression on residual facial asymmetry has not been fully investigated.

Aim

The aim of this study was the longitudinal evaluation of facial asymmetry of UCLP patients using an advanced facial analysis tool, and to compare the postoperative residual asymmetry with the control group. The study was carried out to assess the impact of growth and facial expression on residual facial asymmetry.

Methodology

This study was carried out on 30 UCLP patients. All the patients were Caucasian and underwent the same surgical protocol, which was carried out by the same surgeon at the Royal Hospital of Sick Children, Edinburgh. 3D facial images were captured for the patients, before surgery, at about 4 months after surgery and at four-year follow-up, at rest and at maximum smile using 3dMDface system. Historical data of 70 3D facial images of six-month-old non-cleft infants were also analysed in this study.

Facial asymmetry was evaluated using a generic mesh. A generic facial mesh is a mathematical facial mask that consists of 7,190 vertices. The mesh was conformed on each 3D facial image. The conformed meshes were utilised to evaluate facial asymmetry using two methods: the average asymmetry, the total and regional facial asymmetry. The average asymmetry method involved the creation of four average faces for cleft patients: an average preoperative face, an average postoperative face, and two average faces at the four-year follow-up (one at rest and one at a maximum smile). The fifth average face was that of six-month-old non-cleft infants. A mirror copy for each average 3D facial model was created by reflecting it on a lateral

arbitrary plane. The original and mirror models were superimposed, the absolute distances between corresponding points on the two surfaces were calculated and analysed in three directions (mediolateral, vertical and anteroposterior), to quantify facial asymmetry. The results were displayed in colour-coded maps.

Asymmetry scores were obtained by calculating the median of the absolute distances between corresponding points for the total face, upper lip and nose. The asymmetry scores in the mediolateral, vertical and anteroposterior directions were also quantified. Statistical tests were applied to detect significant differences in asymmetry scores of the total face and each facial region between study groups (before surgery, after surgery and at four-year follow-up), and between surgically managed cleft group and the control group. The correlations of asymmetry scores of the total face, nose and upper lip before surgery, after surgery and at four-year follow-up were also investigated.

Results

Facial asymmetry in cleft patients was dramatically improved after surgery. However, the postoperative residual asymmetry of UCLP patients was significantly higher than the non-cleft infants in the three directions. Furthermore, facial asymmetry increased during growth, with main impact on the nose. Facial expressions accentuated the residual asymmetry. Specifically, there was considerable shifting of the upper lip toward the scar tissue of the affected side. The residual asymmetry of the nose at the four-year follow-up was correlated to initial nasal asymmetry and residual nasal postoperative asymmetry. The anteroposterior deficiency of the upper lip, nose and paranasal area was pronounced in the cleft group at all time intervals due to insufficient bony support of the cleft maxilla.

Conclusions

Cleft patients and their parents should be informed of the likelihood of residual asymmetry following surgery. Refinements in primary surgery are necessary. The superficial and deep fibres of the orbicularis muscle have to be accurately repaired according to the direction of the muscle fibres to avoid the shifting of the philtrum of the upper lip toward the scar tissue on the affected side. The orbicularis oris muscle has to be adequately dissected and rotated in the downward direction to eliminate the residual vertical deficiency at the corner of the mouth on the affected side. An incision in the internal lateral side of the nose should be considered to reduce this deficiency. The levator labii superioris alaeque nasi muscle of the cleft side has to be reflected and sutured to the corresponding muscle fibres on the other side, to avoid the residual shifting of the nose to the non-cleft side, and to eliminate the residual vertical deficiency of the alar base on the cleft side during smiling. Revision surgery should be delayed until completion of growth. Before lip revision surgery, it is necessary to evaluate the residual asymmetry when the face is at rest and during facial expressions. Consideration should be given to initial nasal asymmetry and residual postoperative nasal asymmetry. Patients should be informed about the expected need for revision surgery including rhinoplasty. We were able for the first time to quantify facial asymmetry in three directions which provided an insight into the cause of the residual facial asymmetry at rest and at maximum smile. The generic mesh is an innovative tool for the assessment of facial asymmetry.

Contents

List of tables

List of figures

Acknowledgements

"Praise to Allah, who has guided us to this; and we would never have been guided if Allah had not guided us" [Al-A'raf 43]. Thanks to Allah, Almighty, for giving me the strength to complete this study.

My deepest gratitude to my principle supervisor Professor Ashraf Ayoub for his support, dedication and guidance in all stages of this study. I could not imagine having a better supervisor for my PhD.

I am indebted to my co-supervisors Dr Xi Ju and Dr Mehendale; Dr Xi Ju for his impressive software programming knowledge, which remarkably contributed to the quality of this project, and Dr Mehendale for her positive input to this study and generosity in providing this study with patient images.

I am grateful to Mrs Orla Duncan and Mr Steve Stanton for their limitless help and the time they gave to support this study. Mrs Duncan assisted sincerely and without hesitation in the prospective part of this study. Without her help, this part of this study would never have seen the light of day. Mr Stanton's professionalism in image capturing, especially with children, had a significant impact on the success of this study. Thank you to both of you.

I would also like to thank the children and families who enrolled in this study; I really appreciate the time and effort you spent in returning to take the images.

I would like to express my appreciation to the Children's Clinical Research Facility (CRF) Edinburgh, especially Ms Kay Riding and Ms Jane Andrews for their help in this study, and the Glasgow Dental School Office, especially Mrs

Martha Millard, Ms Evelyn Wallace and Ms Tracy McArthur, for the administrative work they did with NHS Lothian. I also wish to thank Mrs Liz Scott for her cooperation and administrative help.

Many thanks are additionally extended to Dr Gillgrass and Mr Benington for their valuable time and comments in the clinics. Thank you to all members of the cleft teams in Edinburgh and Glasgow for making me feel part of your team.

My deepest gratitude and appreciation also go to my financial sponsor the Higher Committee for Educational Development in Iraq (HCED) for nominating me to study abroad and funding my scholarship.

An important thank you goes to my mum and dad whose unlimited love throughout my study has encouraged me and helped me confront any difficulties I encountered. Without their contributions I would not have been able to complete this study. Warm thanks to my lovely sisters and brother Maha, Farah and Ali for their continuous emotional support.

I would also like to thank my husband for his endless inspiration and support and my lovely, brave sons Mustafa and Ali, who missed their mum for a long time.

During my PhD journey, I met many people in Edinburgh and Glasgow who participated in the success of this study. Thank you to all of you.

Thank you,

Dhelal.

Author's Declaration

I declare that, except where explicit reference is made to the contribution of others, that this thesis is the result of my own work and has not been submitted for any other degree at the University of Glasgow or any other institution.

Signature

Printed name: Dhelal Al-Rudainy

April 2018

List of abbreviations

Abbreviations	Full names
UCLP	Unilateral cleft lip and palate
UCL	Unilateral cleft lip
BCLP	Bilateral cleft lip and palate
CP	Cleft palate
UCLA	Unilateral cleft lip and alveolus
CL(P)	Cleft lip with or without cleft palate
3D	Three dimensions
mm	Millimetre
ms	Millisecond
R	Right
L	Left
LLip	Lower lip
ULip	Upper lip
ICP	Iterative Closest Point
SD	Standard deviation
Pre	Preoperative
Post	postoperative
Correl.	Correlation
Coeffi.	Coefficient
Min	Minimum
Max	Maximum

Chapter one

Literature review

1 Chapter one: Literature review

Introduction

Cleft of the orofacial region is the most common craniofacial dysmorphology. It requires surgical correction to restore the normal facial aesthetics and functions. Many surgical techniques have been developed and applied worldwide. The main outcome measures are the improved facial appearance and patients' satisfaction.

1.1 Orofacial cleft

1.1.1 Cleft prevalence

The overall prevalence of orofacial cleft is about one in 700 live infants (Mossey and Modell, 2012), Cleft prevalence in the UK is in line with this (Fitzsimons et al., 2012). Unilateral cleft lip and palate (UCLP) is the most frequently occurring type of cleft, while BCLP is the lowest form. cleft lip with or without cleft palate CL(P) is more often found in males, while females are more susceptible to cleft palate(CP). The cleft affects the left side of the face more than the right side (Mossey et al., 2009; Mossey and Modell, 2012).

The prevalence of orofacial cleft in Scotland is 1.46:1000, with 0.77:1000 for CL(P) and 0.69:1000 for CP recorded (Clark et al., 2003). Approximately 80 to 100 patients are born with orofacial cleft in Scotland each year (Williams et al., 2001). According to the Cleft Care Scotland's 2015/2016 annual report, 1,435 patients were recorded as requiring cleft care in Scotland from 2000 to 2016 (Figure 1.1), of which 285 patients were UCLP (quote from CCS Report).

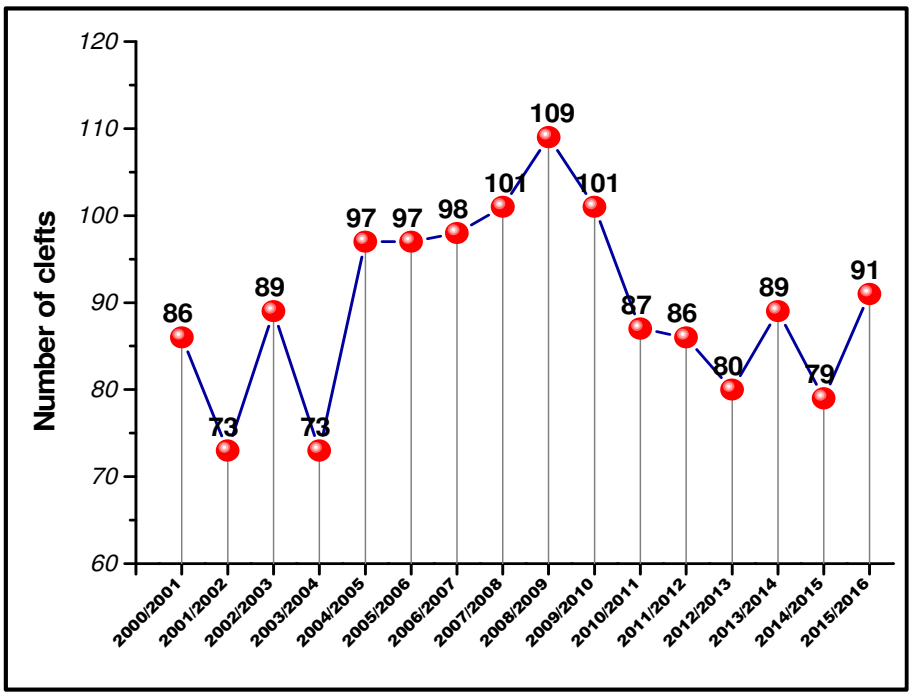

Figure 1.1: Number of cleft cases in Scotland from 2000 to 2016 according to the Cleft Care Scotland 2015/2016 annual report.

The 2014/2015 Cleft Care Scotland report, which is the most up to date report providing information of cleft births by health board of residence, identified 78 cleft cases. The highest number of cleft cases, 21 patients, was reported in Greater Glasgow and Clyde, followed by Lanarkshire and Tayside, where nine cases were reported. Only five patients were registered in Lothian (Figure 1.2).

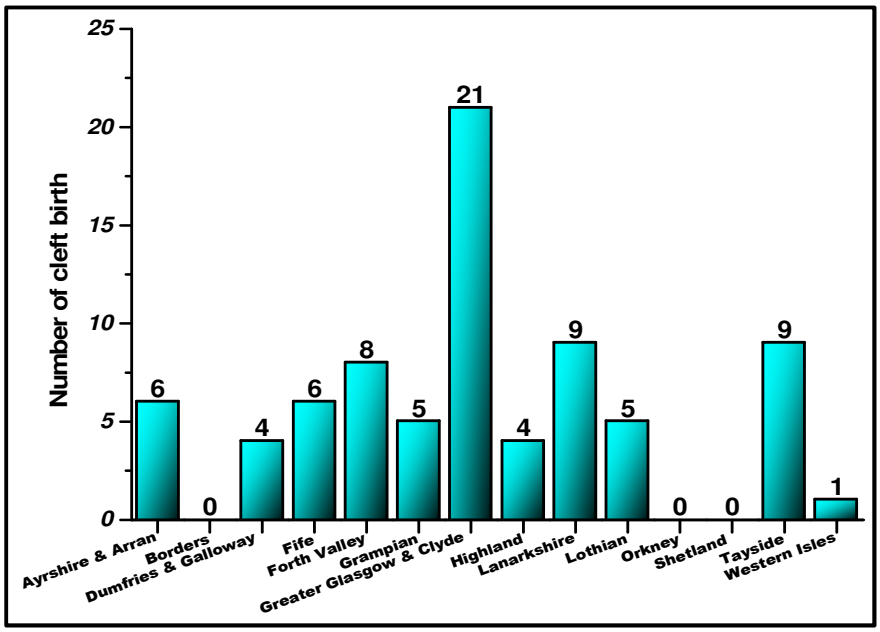

Figure 1.2: Cleft births by health board of residence according to the Cleft Care Scotland 2014/2015 annual report.

1.1.2 Classification of cleft lip and palate

Various systems have been developed for the classification of cleft lip and palate. The main objective in developing these classifications is to categorise cleft deformities into groups according to their features. The **Veau classification** was one of the earliest systems to be introduced, it was developed by Veau and Borel in 1931. This system divides cleft deformities into four groups depending on the extent of the cleft: *Group I* includes cleft deformities in the soft palate only; *Group II* consists of clefts in both the hard and soft palate, that do not extend beyond the incisive foramen; *Group III* describes cleft dysmorphology where the clefts extend beyond the incisive foramen, including the alveolar ridge and the upper lip. *Group IV* includes bilateral clefts that extend from the soft palate to the upper lip. The main

drawback of this system is that it does not differentiate between complete and incomplete bilateral clefts (Wang et al., 2014).

The **Kernahan system**, proposed in 1971, provides a diagram for classifying clefts. The shape of this diagram is the letter "Y" (Figure 1.3), which is divided into nine areas. The "U" part of this letter representing six areas including the right and left nasal floor (areas one and four), lip (areas two and five), and alveolae (areas three and six). The straight part of the letter "Y" includes three areas: one representing the primary palate (area seven), while the secondary palate bilaterally is represented by areas eight and nine. The area affected by the cleft is marked on the diagram on the representing site. This system was a modification of the original classification developed by Kernahan and Stark in 1958.

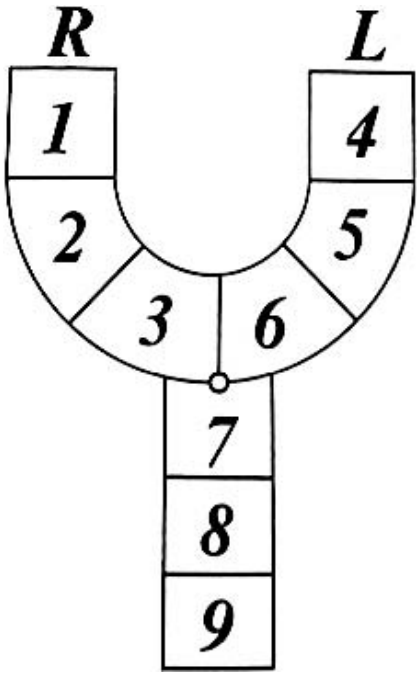

Figure 1.3: The "Y" diagram as described by Kernahan, quoted from Allori et al., 2017.

Another popular approach for classifying cleft lip and palate is the **LAHSHAL system** (Kriens, 1989). In this system, the capital letters represent the anatomical areas of the lip and palate from the right side to the left side: L for lip, A for alveolus, H for hard palate, and S for the soft palate (Figure 1.4). Under this system, the cleft is described by the letter where the cleft is present. For example, the letters "LA" designate a unilateral cleft of the lip and alveolus on the right side. This system is simple, precise and flexible. It is considered as a potentially useful system in describing orofacial clefts (McBride et al., 2016). In 1995, according to the recommendation of the Royal College of Surgeons of England the second letter H was removed, so the classification became LAHSAL instead of LAHSHAL (McBride et al., 2013). Attempts to use numerical classification systems have been reported (Schwartz et al., 1993; Liu et al., 2007). These systems can be utilised for immediate computerised analysis of cleft data. No universal classification system has yet been developed from the various systems proposed, and efforts to establish such a system continue (Wang et al., 2014).

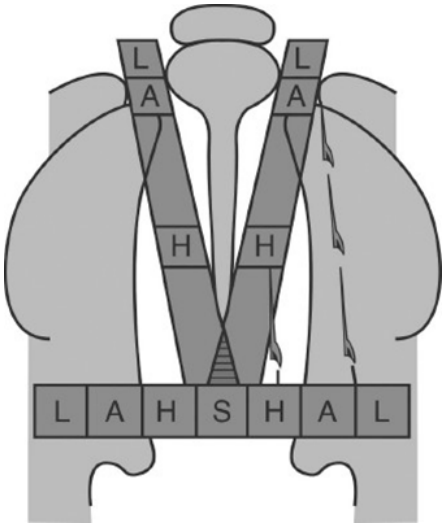

Figure 1.4: LAHSHAL diagram (McBride et al., 2016)

1.1.3 Facial morphology of cleft infants

1.1.3.1 Morphology of the upper lip

The dysmorphology in cleft infants includes the upper lip, the nose and the underlying structures (Laberge, 2007). There is a conflict whether this dysmorphology is due to tissue deficiency, or tissue dysmorphology owing to abnormal muscular attachments and disrupted anatomy (Schendel, 2000). Volumetric measurements using CBCT scan helps to measure bony and soft tissue deficiency (Kasaven et al., 2017).

The main feature of the anatomy of the complete unilateral cleft is tissue deficiency in the upper lip extending to the nose. The cleft divides the upper lip into short medial and lateral sides. The philtral column appears on the medial side only. The vermilion on the medial side is narrow. On the lateral side the vermilion and the redline are parallel to each other and then converge as they reach the cleft area. The highest point of the vermilion is known as Noordhoff's point, where the white role of the lateral vermilion represents the absent Cupid's bow peak (Noordhoff, 1984).

The orbicularisoris muscle normally displays horizontal continuity. However, in a unilateral cleft lip and palate this muscle is disrupted in an oblique direction along the cleft margin and the muscle bundles are inserted in the columella on the non-cleft side, while on the cleft side they are inserted at the base of the nasal bone (Laberge, 2007). Fára (1968) described the orbicularis muscle fibres' arrangement as a marked bundle running nearby the margin of the cleft, while Dado and Kernahan (1985) suggested that the fibres were disorganised and run in different directions.

1.1.3.2 Morphology of the nose

The morphology of the cleft nose is attributed to the abnormal insertion of the orbicularisoris muscle, which creates unequal forces (Kaufman et al., 2012). On the non-cleft side, the columella and the caudal part of the nasal septum were pulled in a lateral direction. While the alar base on the cleft side is retracted laterally and inferiorly. The nasal dome on the cleft side is wide; the tip is less prominent and is shifted toward the non-cleft side. Furthermore, the bony support for the nasal base is insufficient and retracts the alar base posteriorly (Tse, 2013). The asymmetry of the lateral nasal cartilage has contributed to the retraction of the alar base by an imbalance of the pulling forces of the muscle rather than by primary dysmorphology of the cartilage (Kaufman et al., 2012). Numerous studies show that the lower nasal cartilages on both sides of the cleft do not differ significantly in their size or dimensions (Park et al., 1998; Li et al., 2002). A deviation of the anterior nasal spine and the anterior caudal part of the nasal septum toward the non-cleft side is characteristic. The medial crus is shorter in the cleft side, while the lateral crus is longer (Laberge, 2007). The premaxilla is rotated in an outward direction and protruded in the non-cleft side (Gomez et al., 2012). In the case of an incomplete cleft lip, where the defect does not include the total height of the upper lip, a band of soft tissue, called Simonart's band, transverses the lip. This band consists of skin and is devoid of muscle fibres (Tse, 2013).

1.1.4 Cleft lip and palate management

1.1.4.1 Non-surgical management

The management of cleft patients starts from birth and continues until adulthood (Habel et al., 1996). The management is multidisciplinary and the team includes a surgeon, audiologist, orthodontist, speech pathologist, otolaryngologist, psychologist, geneticist and paediatrician (Fox and Stone, 2013; James et al., 2014). Immediately after birth, breathing and feeding of cleft infants require special care. Compressible bottles, modified or artificial nipples, and palatal obturators are usually utilised to help cleft infants to overcome feeding difficulties (Reid, 2004). Lip adhesion may be considered in severe cases. This technique allows a surgical approximation of the sides of the cleft without functional reconstruction of the defective tissue. The method is not a preferred choice as it causes extensive scar tissue that interferes with function and any other lip revision procedures (Scrimshaw, 1979; Salyer et al., 2004; Salyer et al., 2009). A common and efficient approach for the reduction of cleft gap is lip taping. In this technique, a strip of tape is placed with tension on the lip crossing the gap from one cheek to the other (Nahai et al., 2005). Active and passive pre-surgical orthopaedic appliances have been applied to minimise the size of the cleft (Suri and Tompson, 2004). Pre-surgical orthopaedic moulding has been considered for wide unilateral cleft cases. This approach helps to improve the position and the form of the maxillary skeleton that reduces the gap of the cleft and improve facial asymmetry. It also minimises excessive post-operative tension on the lip, which can lead to wound dehiscence (Sierra and Turner, 1995). There are two types of moulding available depending on the effect of the moulding procedure, that is whether it includes the alveolus only or whether it extends to the nose. These are: alveolar mouldings and nasoalveolar mouldings. The latter involves the application of a nasal stent to correct the

length of the columella and the position of nasal cartilages (Maull et al., 1999; Suri and Tompson, 2004).

Despite the favourable effect of using pre-surgical orthopaedic moulding in reducing the cleft width by the realignment of the maxillary segment, the long-term effect of these appliances on maxillary growth remains uncertain (Kuijpers-Jagtman and Long, 2000; Schendel, 2000; Clark et al., 2011). Moreover, these appliances are expensive and can be a burden to the patient and their family.

1.1.4.2 Surgical management

1.1.4.2.1 Techniques for surgical correction of cleft lip

Many different techniques have been developed for the surgical correction of cleft lip. The type of technique to be applied for each cleft case is the surgeon's decision, and will be based on the degree of cleft dysmorphology as well as the skills of the surgeon (Reddy et al., 2008). The first successful surgical correction of cleft lip was performed by a Chinese physician in 390 AD (Boo-Chai, 1966). The first half of the twentieth century saw the development of the earliest surgical technique, in which the surgical repair of cleft lip was achieved by a simple straight-line closure. However, this technique results in the shortening of the upper lip post-surgically (Burt and Byrd, 2000). Since then, many attempts to overcome this disfiguring condition have been reported. Rose (1833) and Thompson (1912) advocated making an incision along the cleft sides to increase the length of the lip during the straight closure of the cleft defects. However, these techniques were not suitable for severe cleft defect (Balaji, 2013). In 1952, Tennison developed the "triangular flap" technique in which a triangular flap is rotated in the lower third of the lip from one side of the cleft to the other side. This technique is a modification of the LeMesurier technique (1949), the long-term follow-up of the latter technique showed unfavourable results: the

hanging of the upper lip and the increasing of its length. Tennison later modified the incision on the lateral part to reach the Cupid's bow peak. Tennison's technique provided good results, yet it required a mathematical calculation for the exact measurements during the surgical repair of the lip, and it does not include simultaneous correction of the nasal dysmorphology (Balaji, 2013). In 1957, Millard addressed the drawbacks of the surgical repair of the cleft lip and developed a new surgical technique, the rotational advancement flap technique. In this technique, a flap is rotated in the upper third of the lip in a downward direction to increase lip length. This technique has become the preferred choice as it is simple and shows satisfactory post-operative results (Tibesar et al., 2009). Subsequently modifications of Millard's technique have been introduced to reduce the residual deformities and further improve in the quality of the surgical repair of the cleft lip (Roussel et al., 2015).

1.1.4.2.1.1 Millard's rotational advancement flap technique

This technique is based on the assumption that the cleft defect is in the upper part of the lip and is not in the lower third of the lip (Balaji, 2013). Therefore, to correct the defect, an incision is made from the top of the Cupid's bow toward the philtral column in the non-affected side, and the philtrum is rotated in a downward direction toward the lateral segment. Unlike other techniques, the main bulk of this flap is carried out in the non-defect part (the medial part) to close the cleft's gap and to overcome the problem of lip shortening, which is the main complication of cleft repair. The gap that is created by the rotation of the medial part in a downward direction is closed by the advancement of the lateral flap from the lateral segment toward the medial side; it also corrects the dysmorphology of the nose by narrowing the nasal floor and decreasing the flaring of the nasal ala (Tse, 2013). A c-flap in the medial part of the nasal floor is made for nasal floor closure and to increase the length of the short columella. The benefits

of this technique are that it preserves the philtrum dimple and decreases the amount of post-operative scarring (Burt and Byrd, 2000). In 1968, Millard refined his surgery by adding extensions to facilitate the repair of wide clefts. Despite the success of Millard's approach, the resulting scar tissue crossing the upper part of the lip was a disadvantage that required further surgical modifications. In 1987, Mohler modified Millard's technique to minimise the scar tissue. In his modification, the rotational incision was extended back to the columella with back-cut ends at the columella lip junction. The results of this modification were not only reduction of the scar tissue in the upper part of the lip, but also an increase in the length of the lip (Demke and Tatum, 2011; Tse, 2013).

1.1.4.2.1.2 Surgical correction of nasal defect (McComb's technique)

The timing of nasal surgical correction in cleft cases was controversial. Initially, it was accepted that nasal dysmorphology correction in the early months of a child's life will affect the mid-face growth, caused by the surgical dissection of the nasal septum. However, another view encourages surgical correction during the primary lip surgery as the delay will lead to unsatisfactory growth of the nose, and delaying the nasal surgery will have a psychological impact on patients (Thomas, 2009; Campbell et al., 2010; Kaufman et al., 2012; Shkoukani et al., 2013). In 1996, McComb and Coghlan published a longitudinal study that confirmed that early correction of the nasal dysmorphology does not interfere with mid-face growth as the nasal surgery can be accomplished by repositioning the lower alar cartilage without resection. In 1975, McComb published his primary technique for rhinoplasty. In this technique, the skin of the nose is detached from the nasal cartilages in the cleft side using sharp scissors, which are passed through the pre-existing medial and lateral incisions from the primary lip surgery. The separation of the skin extends from the nasal rim upward to the ala and medially to the nasal dome and moves in an upward direction to the nasion

level. A medial suture that extends from the intercrual angle of the alar cartilage to the nasion is used to suspend the cartilage in the new, correct position. Suturing the nasal floor helps to re-establish the shape of the nose and improve its symmetry (Kaufman et al., 2012). If necessary, the lifting suture can be adjusted following the lip repair.

1.1.4.2.1.3 Surgical correction of palatal defect

The surgical repair of cleft palate includes the closure of the hard and soft palate. To help decrease post-operative complications, the procedure must consider the reconstruction of three layers: nasal layer, muscular layer and oral mucosal layer (Farronato et al., 2014). Palatal repair can be achieved in one or two stages. In one-stage repair, both the hard and the soft palate are closed in a single operation. In contrast, the two-stage protocol includes the repair of the soft palate and the hard palate in two separate operations. The first operation is for the closure of soft palate, and the second one is for hard palate closure (Berkowitz, 2013). One of the earlier techniques for palatal repair was Von Langenbeck palatoplasty (1861), in this technique, two mucoperiosteal flaps are mobilised medially for palate closure (Campbell et al., 2010). This technique is easy to perform but cannot provide the required palatal length, and it is usually indicated for cleft palate only (Farronato et al., 2014). To ensure the normal physiological function of the hard palate, it is crucial to produce a long mobile soft palate during palatal reconstruction. The technique was modified in 1936 by Wardill and Kilner to produce VY pushback palatoplasty, where the flaps are pushed in a posterior position to provide the adequate anteroposterior length required of the palate (Campbell et al., 2010). However, the main drawback of this approach was the denuding of the palatal bone anteriorly, which can interrupt mid-facial growth (LaRossa, 2000).

Furlow's (1995) "double-opposing Z-plasty" includes two opposing Z-plasties based in the cleft midline and continuing to the soft palate (Furlow, 1995). This technique provides excellent palatal lengthening, as the placement of the zigzag incision, rather than a straight incision, can increase the length between two points. Z-plasty reduces post-operative complications (Gunther et al., 1998), and reduces the amount of exposed palatal bone, resulting in less scar tissue in comparison with other techniques. As a result, the mid-facial growth is less affected with this technique. Nevertheless, it is considered a time-consuming surgery (Ravishanker, 2006), and difficult to perform (Spauwen et al., 1992).

In vomer flap palatoplasty, the mucoperiosteum of the vomer bone is utilised for the closing of the cleft palate. This type of palatoplasty is usually used in the construction of the nasal layer, as the colour and texture of vomer mucosa match the nasal mucosa. Using this flap for the closing of the oral defect is not uncommon. However, it has to cover the size of the palatal defect (Agrawal and Panda, 2006).

1.1.4.2.2 The timing of surgery

Various primary surgical protocols are available and applied worldwide. There is no consensus on optimal time for primary surgery, and the time of surgery is usually at the surgeon's discretion, with the general health of the patient, psychosocial factors, facial growth and speech being considered (Agrawal and Panda, 2011). The primary lip surgery is usually performed when a child is three to six months of age. Proper surgical reconstruction of the lip can be achieved at 10-12 weeks old when the lip musculature is well developed. Moreover, the aesthetic outcomes of surgery conducted before a child is ten weeks old (neonatal repair) are no worse than when surgery is conducted at three months old (Goodacre et al., 2004). However, the psychological effect would be better.

The timing of palatal surgery is controversial and there is considerable debate in the literature regarding this issue. On the one hand, it has been suggested that early surgical repair of palatal cleft disturbs mid-facial growth due to the denuded bone and subsequent scar tissue formation (Gillies and Fry, 1921). On the other hand, delayed palatal surgery showed favourable growth outcomes (Friede and Enemark, 2001; Friede, 2007), but high rates of poor speech outcomes have been documented (Chapman et al., 2008). A normally functioning palate must exist at the time when the child starts to speak. The NIH international randomised study resolved this debate by comparing the outcomes of palatal surgery at 6 months and at 1 year old; early palatal closure at about six months is the recommended protocol (Semb et al., 2017). Modifying the palatal repair surgical technique and thus decreasing the amount of scar tissue can avoid unfavourable mid-facial growth (Campbell et al., 2010).

1.1.5 Facial growth and development

1.1.5.1 Normal growth and development of child's face

There are several theories explaining craniofacial growth: the functional matrix theory (Moss and Young, 1961), the cartilaginous theory (Scott, 1954, 1958), sutural theory (1940s), and bone remodelling theory (1930s) (Carlson, 2005). The contributions of these theories are different on various parts of the face. Furthermore, the growth of the face is differential, i.e. parts of the face (hard and soft tissues) grow at different rates and at different times (Proffit et al., 2013). The forehead in a normal child's face is protruded, and in the first few years of life, the growth of the cranial cavity is faster than the growth of the face. At this time, it is about 90% of its total size, and thus the proportional size of the forehead becomes smaller (Sharma et al., 2014).

Typically, infants have flat faces with prominent cheeks and large eyes. The teeth are yet to erupt, and the upper and lower jaws have not fully grown yet. These features are responsible for the short vertical dimension of the face. The growth of the face is mainly attributed to the growth of the nasomaxillary complex and the growth of the mandible (Sharma et al., 2014).

According to Scott (1954), the cartilage of the nasal septum is the primary centre that regulates the growth of the mid-facial region in early childhood, and its growth thrusts the facial bone, excluding the mandible, in a downward and forward direction away from the cranial base. A secondarily downward and forward displacement of the nasomaxillary complex is attributed to the anteroposterior growth of the cranial base by the ossification of the sphenoccipital synchondrosis (Premkumar, 2011).

At birth, the mandible is characterised by its retruded position in relation to the rest of the face (Sharma et al., 2014). It consists of two halves that are separated in the midline. By the end of a child's first year, ossification has united these two halves to form one bone. Cartilaginous growth plays an important role in mandibular growth; the cartilage at the top of the condyle at the temporomandibular joint (TMJ) is considered the major factor in the vertical growth of the mandible (Karad, 2014).

In early childhood, the nose is short and rounded and the nasal bridge is short and concave. The nose grows in forward and downward directions (Sharma et al., 2014). By the age of five years, the height and the width of the nose reach between 79% and 87.1% of their adult size respectively. The vertical growth of the upper lip shows rapid increase in the first year of child's life, it reaches 80.2% of its adult size for both sexes (Farkas et al., 1992b).

An anthropometric study by (Farkas et al., 1992a) noted that an early vertical growth spurt of the face was between one to four years old, while the early

growth spurt of the width of the face was observed as according between three to four years old. By five years old, the facial development is mostly completed, having reached 82.2% to 92% of total facial development.

1.1.5.2 Facial growth of cleft children

Mid-facial growth disturbance is a characteristic facial morphology of cleft patients, and it is mainly attributed to growth restriction in the maxilla rather than the mandible (Scheuer et al., 2001). Three general factors are deemed responsible for facial growth disturbance in cleft patients: intrinsic deficiencies, functional distortion, and iatrogenic factors (Ross, 1987).

The effect of primary surgery on facial growth disturbance is controversial. The effect of palatal surgery on maxillary growth has attracted the attention of many studies. It is widely accepted that that maxillary deficiency is mainly related to palatal surgery (Kuijpers-Jagtman and Long, 2000). The scar tissue formed after palatal surgery inhibits the sagittal, transverse and vertical growth of the maxilla (Ross, 1987). The effect of lip surgery might be localised to the development of the anterior part of the dental arch by applying persistent pressure, which leads to an anterior crossbite (Huang et al., 2002).

However, there is some evidence that cheiloplasty is responsible for maxillary growth restriction (Filho et al., 1996 ; Li et al., 2006), and proper reconstruction of the perioral and perinasal muscle is necessary for appropriate maxillary growth potential (Joos, 1995).

1.2 3D imaging of cleft lip

Different techniques have been developed for capturing facial soft tissue and hard tissue data and producing 3D facial models. These techniques have helped to overcome the shortcomings of the 2D methods (photographs, cephalometrics) and direct anthropometry. The standard 2D photograph is difficult to standardise and does not provide an accurate representation of the 3D face. Direct anthropometry, which has been attempted in the past, requires that the patient attend the clinic for direct facial measurements. This is time-consuming and requires a high level of patient cooperation, something that is not possible with infants (Wong et al., 2008; Dindaroğl et al., 2016).

In the literature, four main types of 3D imaging systems have been used to capture facial morphology of cleft patients: cone-beam computed tomography (CBCT), laser scanner, structured light scanner and stereophotogrammetry.

1.2.1 Cone-beam computed tomography (CBCT)

Cone-beam computed tomography (CBCT) is 3D radiographic imaging of the craniofacial region. It is also known as “digital volume topography”. Its development in the 1990s represented a shifting from 2D radiographs (2D cephalometric, panoramic) to 3D volumetric radiographs. CBCT is a modification of the computed tomography (CT) scanner usually used in medical practice. CT scanners are large and produce a fan-shaped beam of radiation. CBCT has been modified to be smaller in size and emits a conically shaped scanning beam to reduce the amount of scattered radiation. The CBCT device comprises a source of X-ray beam that is opposed by a sensor for standardised 2D radiographic capturing (Kau et al., 2005a). Two types of detectors can be utilised in the sensor unit: either an amorphous silicon flat

panel detector or an image intensifier with charge-couple device. The latter is not common, is responsible for the detector's large size and produces circular radiographic images. The flat panel detector is simple and is the most common detector type. The images produced using this type of detector have a rectangular shape. However, it requires regular calibration (Scarfe et al., 2012). According to the size of the scanned object, which is usually called the "field of view" (FOV), CBCT can be classified as large, medium and small. The large FOV can capture the whole facial skeleton, the medium FOV can be utilised to capture both jaws together, while the small FOV is used for scanning a single jaw or small section of the facial skeleton (Kau and Richmond, 2010).

The X-ray source and the sensor are simultaneously revolved around the vertical axis of the patient's head while the patient stands or sits on a chair. The position of the head is usually standardised using laser markers and stabilising aids. During the rotational path, the X-ray source penetrates the region of interest from different angles while multiple radiographic basis images are captured. The device can perform a complete 360^0 rotation or a partial rotation of a 180^0 arc or more. Scanning time varies between devices, ranging from 5.4 seconds to 40 seconds. The X-ray pulses are transmitted at intervals, allowing a time for the captured data to be transferred from the detector to data storage and allowing for the X-ray source to shift into a new position (Nemtoi et al., 2013).

A full set of basis images is called "projection data" and can range from 150 to over 1,000 images. The digital set of 2D radiographic images is used to construct a 3D visualised model using the primary construction process and secondary construction process. In the primary construction process, a software algorithm converts the digital radiographic basis images into a 3D volumetric dataset that consists of cuboids as volumetric elements, with each element called a "voxel". The process takes several minutes to complete

depending on the number of captured images. In the secondary construction process, orthogonal visual images are provided. The voxel size determines image quality: the smaller the voxel size, the higher the image resolution. The size of a voxel can be made smaller by increasing the capturing time. A longer rotational path will capture a higher number of basis images with smaller voxel units, producing a higher resolution 3D model. Bone density has to be considered during image capturing. Higher kV is necessary for penetrating dense bones and producing better image quality. However, the amount of radiation emitted will also be greater (Scarfe et al., 2017).

Although CBCT is excellent in the imaging of hard tissue, the soft tissues are of poor contrast due to the inherent noise of the device, and it is unable to map the muscles and their attachments. Furthermore, it cannot capture skin texture (Kau et al., 2005a). Image artefacts are another limitation of CBCT. Artefacts such as streaking, shading and distortion are usually produced due to the presence of metallic restorations, fixed orthodontic appliances or implants that affect the quality of the images (Kamburoğlu et al., 2013).

The main drawback of CBCT is the high radiation dose delivered by the device, which exceeds that delivered by a panoramic radiograph or a full mouth periapical radiograph (Mah et al., 2003). X-radiation is potentially carcinogenic, especially in children, whose growing organs are more sensitive to radiation, and the accumulative effect of radiation will be greater (Brody et al., 2007). There is widespread awareness of the impact of CBCT use on children. The organ dose (amount of radiation delivered to the organ) with CBCT, especially for the salivary gland, is 30% higher in children than in adolescents (Theodorakou et al., 2012). With the same exposure, the mortality risk in children increases from three to five times higher in comparison with adults. The risk increases with the increase in radiation dose, and there is no safe limit for exposure to radiation. Repeated exposure will accumulatively increase the risk of cancer initiation (Scarfe et al., 2017).

Few studies have utilised 3D radiographic imaging to evaluate skeletal facial asymmetry of cleft patients after surgery (Suri et al., 2008; Li et al., 2011), or before and after primary lip surgery of cleft infants (Fisher et al., 1999; Seidenstricker-kink et al., 2008).

1.2.2 Laser scanning

Until 1989, the application of 3D image capturing by laser scanners was limited to industrial purposes. Since then, low-power lasers have been utilised for 3D facial scanning. The first 3D laser facial scanner consisted of a laser beam source and a video camera, which were fixed on a platform, with the patient sitting on a rotating chair. The chair's rotation was computerised and uniform, with the laser beam striking the face as a vertical line for about 20 seconds. A soft head strap was utilised to fix the forehead to the headrest of the chair. The images produced by this system consisted of 20,000 points, and without texture (Moss et al., 1989). Nowadays, a wide variety of commercial 3D facial scanners are available: the scanner can be fixed (Božič et al., 2010), portable (thus providing flexibility to be moved from one place to another) (Kusnoto and Evans, 2002), or mobile, where the laser scanner is a hand-held scanner (Harrison et al., 2004). Despite the varieties of laser scanning, the basic principle for all 3D scanning is based on a triangulation method. In this method, the triangle is formed by the laser beam source, camera and object, and the distance between the laser source and camera is known and fixed. Changing the triangulation angle is achieved due to the difference in the object's surface height. The video camera monitors and measures the changing of this angle during scanning and calculates the third dimension.

3D facial scanning proved to be an accurate method for capturing facial data. The scanners have been equipped with high-quality video cameras, and the final 3D output models of certain scanners can be with skin texture (Kau et

al., 2005b). It was used in some studies of cleft patients (Duffy et al., 2000; Djordjevic et al., 2014a). However, the patient needs to avoid any movement during scanning, which takes about eight seconds, to prevent image capturing errors, and this might not be achieved (Al-Omari et al., 2005). Furthermore, safety has to be considered, especially for children. In particular, patients should close their eyes during scanning process to avoid direct exposer to the laser beam which may cause thermal retinal damage. Thus, facial laser scanning has not been deemed appropriate for capturing the facial data of infants, with or without a cleft.

Dynamic optical-tracked laser imaging

An attempt was made by Schwenzer-Zimmerer et al. in 2009 for facial scanning of cleft infants before and after primary lip surgery using dynamic optical-tracked laser imaging. This scanner is a mobile hand-held laser scanner (Figure 1.5). The scanning procedure is recorded by moving the hand in straight lines several times over the object to be imaged, with the 3D model being constructed layer by layer through an accumulation process. The laser beam, class 2 type, was safe for the eyes and captured the face in 15 seconds. The procedure required that the infants be under general anaesthetic to prevent imaging errors due to movement. The images were obtained before and after primary lip repair. The advantage of this method was that the scanning process was directly controlled, while the image was being created. This helped to avoid the omission of the undercut regions. However, the fact that the infants are under general anaesthetic during imaging is a shortcoming of this method, as an alteration of the nasolabial region during sleeping has been proven. Under general anaesthesia, the child's nasal breathing would be stopped, and the nasolabial muscles would be relaxed, which will lead to an increase in the vermillion height and a decrease in the medial cleft region measurements (Morioka et al., 2015).

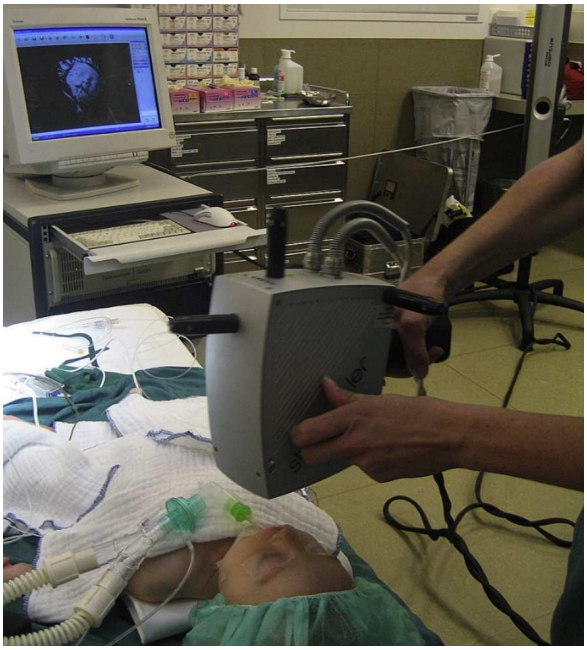

Figure 1.5: Dynamic optical tracked laser system, the hand-held laser scanner is scanning the cleft infant face at the theatre room before surgery (Schwenzer-Zimmerer et al., 2009).

1.2.3 Structured light scanner

In this technique, narrow bands of light that are projected on to an object are distorted on its surface. The bending of these bands follows the surface morphology of the object on which it is projected (Figure 1.6). This bending is utilised for the precise identification of the location of surface points on the object. This scanner needs only one camera to capture the 3D image. The position of the illuminated points on the image are compared to their position on the light projection plane; providing essential information for the 3D coordinates of the points of the target object, which are computed by triangulation (Nguyen et al., 2000; Ma et al., 2009). This technique is simple to use, but the narrow field of view and the low resolution of the images

provided by this system are the main disadvantages. Furthermore, a high-density image production necessitates illuminating the object multiple times by the light pattern, which increases image acquisition time and the possibility of head movement during image capturing. An example of a structured light scanner that was employed in 3D image capturing of infants with cleft is the "three-dimensional sensing system (3DSS)".

Three-dimensional sensing system (3DSS)

This system is considered a combination of the structured light technique with stereophotogrammetry. The device consists of two cameras with a structure light projector. Th camera pair record the light reflected from the infant's face simultaneously. The 3D model of the face is built mathematically, based on the triangulation of all the points captured by the pair of cameras. Due to the slow scanning speed of this system, the cleft infants being imaged (aged three to three-and-a-half months old) had to be asleep to control involuntary movements. Nonetheless, the breathing of infants while sleeping had an effect on image quality (Li et al., 2013). Capturing the images for the infants while they were asleep is not practical.

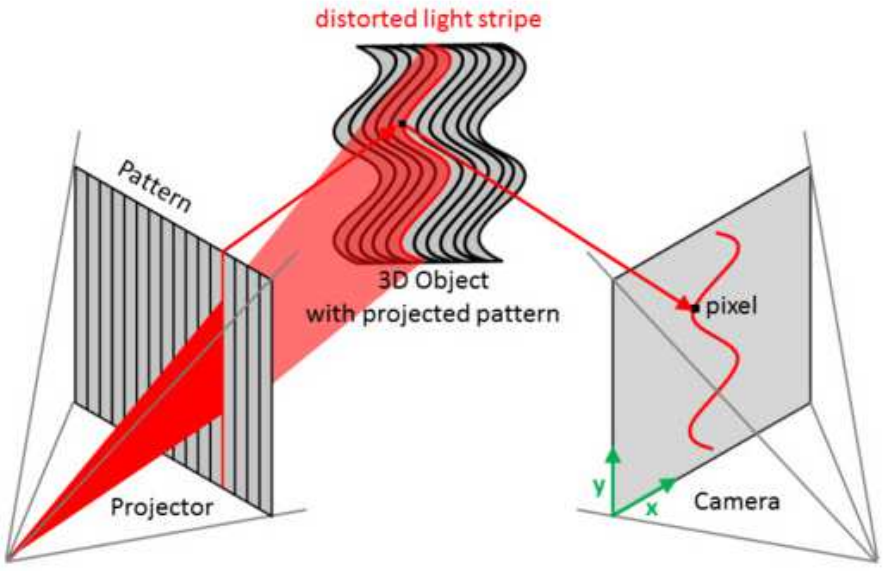

Figure 1.6: Structure light technique. A diagram illustrates how the distorted light patterns, which are projected on the 3D surface, help in precise identification of the location of surface points on the object (Tzou et al., 2014).

1.2.4 Stereophotogrammetry

1.2.4.1 Overview

Stereophotogrammetry is a safe, non-invasive technique for capturing facial data. The concept of this technique is based on capturing the face by using two (or more) cameras simultaneously. The disparities between the captured images (right and left) help to measure the third dimension through a triangulation algorithm. According to Burke and Beard (1967), the first clinical application of stereophotogrammetry in medicine was performed by Thalmann-Degan in 1944. At that time, three-dimensional imaging was based on stereoscopy. Two facial photographs (stereo images) were captured for the face that was standardised in a frame while the patient was lying down. The right and left cameras were covered by red and blue sheets alternately. Projectors were utilised to draw a contoured map of the face. This map described the main terrain of the face (eyes, nose, mouth) by drawing precise contour lines. These lines were separated by a fixed distance (usually 2mm to 5mm) and were identified by numbers, which were drawn in sequence starting from the nose and moving outward towards the peripheries. The anteroposterior depth was presented by differences in the contour level. The method accurately maps facial contours and dimensions, but the output image lacked 3D coordinates. From that point on, additional techniques were developed, ultimately leading to the creation of current digital stereophotogrammetry.

Nowadays, 3D facial models represent the real face of the patient and can be manipulated for diagnosis, treatment planning and evaluation of surgical outcomes (Hajeer et al., 2004b). Stereophotogrammetry has several advantages and broad applications in medicine and in dentistry. The time required by this technique for image acquisition is less than one millisecond,

and it is highly accurate and reliable for the analysis of face morphology (Ayoub et al., 2003; Khambay et al., 2008).

Stereophotogrammetry has been chosen to capture facial data in many studies of cleft lip and/or palate patients. This is especially the case for children, where the acquisition time is crucial. An earlier attempt at using stereophotogrammetry for the assessment of cleft patients was in 1994 conducted by Ras et al. In their study, two semi-metric cameras were held by a frame. The distance between the two cameras was 50cm, with a convergence angle of 15^0. A flash spot was placed between the two cameras, and the registration of the two photographs was assisted by using a grid, which was projected on the patient's face to help in the determination of the third dimension. However, the images produced by this system were uncoloured, and the system did not provide full coverage of the face.

1.2.4.2 General principles of stereophotogrammetry

The stereophotogrammetric system usually consists of two cameras, separated by a certain distance. These cameras are fixed at the same level and angulated to properly cover the face. The patient is usually placed centrally in relation to the cameras, so that each point on the object surface can be captured from two different perspectives. The two captured images are overlapped by about 70%, and the points captured by the right camera will be shifted in position by a given number of pixels in the image captured by the left camera. The differences in the views provided by the two cameras are calculated by subtracting the differences in positions of the points as demonstrated by the disparity map. The construction of this map is a challenging process as for each pixel in the right image a corresponding pixel in the left image must be identified. Once correspondence is obtained, the 3D surface model can be constructed using a triangulation algorithm where the two cameras and the object form a triangle, with the distance between

the cameras and the distance of the object from the cameras being known (Figure 1.7). A computer connected to the system is responsible for completing these complicated mathematical calculations. The third dimension is calculated according to the following formula (Wu et al., 2004):

$$depth\ (z) = df/\ (x2 - x1)$$

Where d is the baseline length between two cameras, f is the focal length of the two cameras, and x2-x1 is the stereo disparity.

The output 3D model can be displayed by different modalities including the wireframe model, shaded model and photo-realistic model. The photo-realistic model can be gained by mapping the colour textured facial images, which are captured by stereo pair textural cameras, on the 3D model.

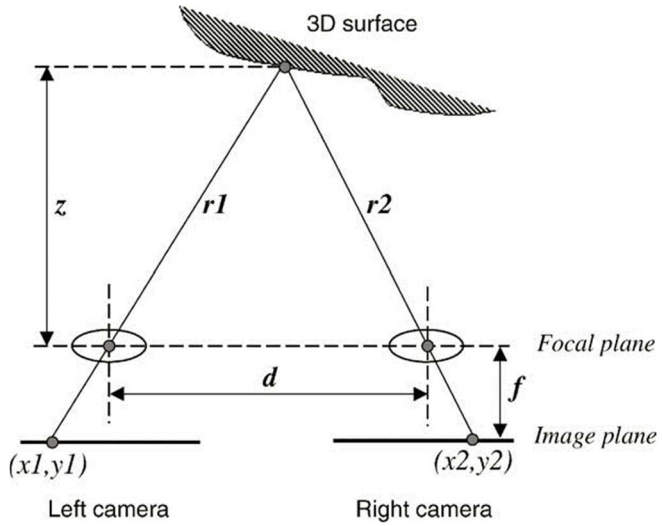

Figure 1.7: A diagram illustrates the triangulation concepts in stereophotogrammetry. The third dimension (z) of each pixel can be calculated from distance between the two cameras (d), (f) the focal length of the cameras, and the stereo disparity of each pixel (x2-x1), which was obtained from the disparity in pixel position in the captured images from the two cameras, quoted from Wu et al., 2004.

1.2.4.3 Types of stereophotogrammetry

3D image construction relies on measuring the distances between the correspondences of the two captured images, which are captured by two camera sets. The triangulation algorithm is applied to determine the 3D dimensions of all the surface points of an object. Stereophotogrammetry is classified as being passive, active and hybrid according to how correspondence is achieved. In passive stereophotogrammetry, the light source that is projected on to the target object is natural light, and the cameras that capture the object are of a high resolution to use natural skin texture as the corresponding points on the two images (Figure 1.8). Lighting during image capturing is essential to avoid shiny surfaces and to ensure accurate and non-distorted 3D image production. An example of passive stereophotogrammetry is the Di3D 3D surface capture system (Batlle et al., 1998; Pallanch, 2011).

In active stereophotogrammetry, structured light patterns are projected on to the object to be captured (Figure 1.9). This sharpens the captured images to allow the triangulation algorithm to be applied. The light patterns on the surface of the target object help to identify the accurate location of the surface points, which facilitate the corresponding triangulation process (Batlle et al., 1998; Pallanch, 2011). Finally, hybrid stereophotogrammetry involves the combination of both active and passive types, for example, the 3dMDface System.

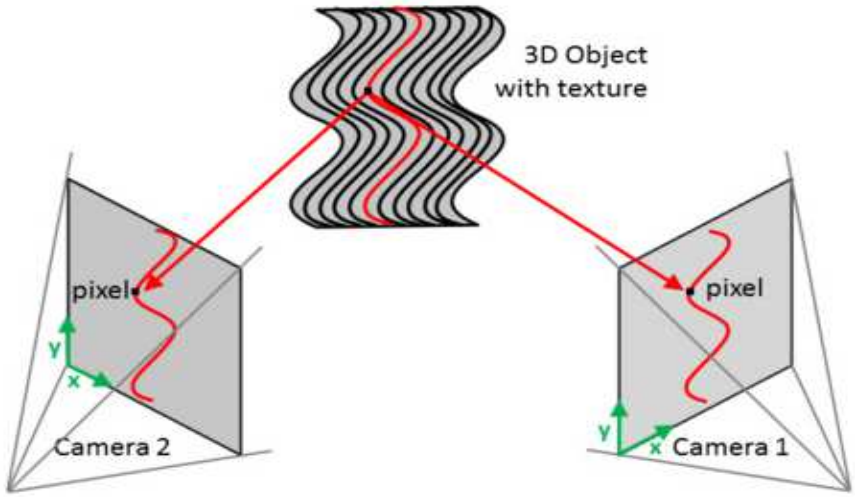

Figure 1.8: Passive stereophotogrammetry. A diagram illustrates how object texture is utilised in the identification of the corresponding pixel using high resolution cameras (Tzou et al., 2014).

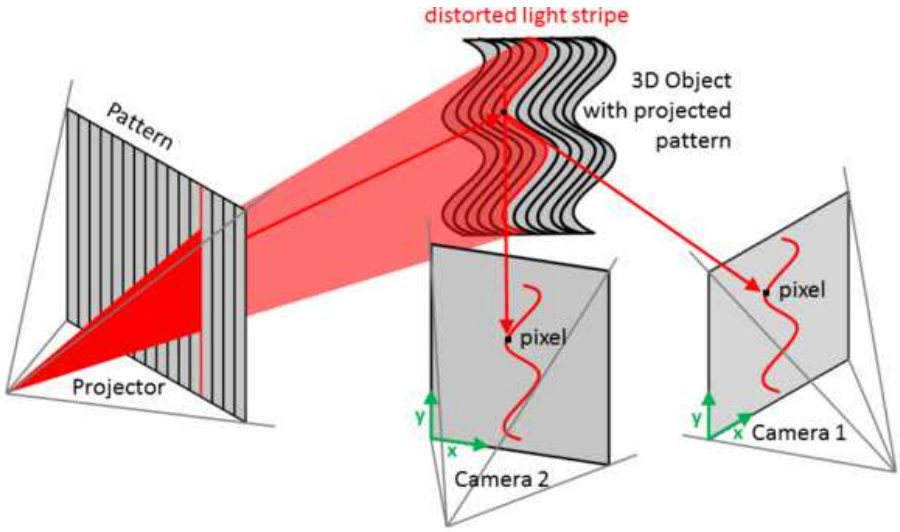

Figure 1.9: Active stereophotogrammetry. A diagram illustrates how the distortion in the projected light pattern helps in the identification of the corresponding pixel (Tzou et al., 2014).

1.2.4.3.1 3dMDface System

The 3dMDface System is a static 3D capturing system that consists of two modular units that capture the face from ear to ear. The modular units consist of six medical machine vision cameras (two stereo pairs of digital geometrical cameras and one stereo pair of texture cameras) and an industrial-grade flash system (Figure 1.10). The cameras are equipped with high-quality sensors that precisely synchronise the capture times of the three-dimensional surface geometry and texture. The images that are captured are with a high accuracy and with ultra-fast speed (1.5 milliseconds).

This system is a hybrid system that combines passive and active stereophotogrammetries. The goal of combining these two types of stereophotogrammetry is to ensure correct geometrical data acquisition, for high accuracy and high-quality of the 3D surface image. Image processing with the 3dMDface System takes less than eight seconds and the calibration time is only 20 seconds. 3D facial geometry is produced as one continuous point cloud, which eliminates the errors associated with stitching of data sets together. Unlike the 3dMDface System, the Di3D System image processing takes 60 seconds and the calibration time is five minutes (Tzou et al., 2014).

Images captured by the 3dMDface System were accurate and repeatable for precise clinical evaluation, with an error of 0.2mm within a range from 0.1 to 0.5mm (Lübbers et al., 2010). Indeed, its accuracy was demonstrated in a clinical environment (Nord et al., 2015). The repeated images, which were captured by this system, were accurate in both short- and long-term follow-up. Maal et al. (2010) assessed image registration errors for repeated images after one minute and after three weeks. Their study indicates that the errors were 0.39mm and 0.52mm, respectively. The linear measurements obtained

from images captured by the system were accurate in comparison to direct anthropometries (Wong et al., 2008).

Figure 1.10: 3D 3dMDface System (Ort et al., 2012).

The 3dMDface System is considered a useful clinical tool for the evaluation of craniofacial abnormalities (Heike et al., 2009). Data collected from images captured by the system for adults and children with craniofacial abnormalities were highly accurate with just sub-millimetre errors (Aldridge et al., 2005).

1.3 Image registration

Image registration is a procedure by which a set of 3D models are spatially aligned, and this enables the comparison between the models. The comparison may be carried out for a cohort group of patients or for the same patient, with 3D images taken at various time intervals to study facial growth, or the changes following orofacial surgery or orthodontic treatment. Image registrations are two types: “point-based registration” and “surface-based registration”, based on the distinct features that characterise the procedure.

1.3.1 Point-based registration

This type of registration relies on corresponding 3D points for alignment. Usually, facial landmarks are utilised for the alignment of 3D facial images, and the registration can be accomplished by one of the following analyses.

1.3.1.1 Procrustes analysis

Procrustes analysis is a shape analysis tool in which point-based registration is applied to minimise the distances between the points of image sets due to the difference in location, rotation and size. Procrustes analysis is either general or partial. In “General Procrustes Analysis” (GPA) the alignment of the set of images is achieved by translating surface points. Thus all the images have the same centroid (geometrical centre of the configuration). The images are then changed to have the same size, and finally the images are rotated, so the distances between the corresponding landmarks are minimised. GPA is applied to compare facial shape differences between the sets of landmarks where size difference is not considered (Ayoub et al., 2011a). In “Partial Procrustes Analysis” (PPA) the sizes of the images are maintained. PPA has been applied in studies of facial asymmetry, where the

set of facial landmarks was mirrored and PPA was applied for the alignment of the original and the mirror sets of facial landmarks to measure facial asymmetry (Hajeer et al., 2004a).

1.3.1.2 Bookstein analysis

Bookstein analysis is another type of landmark-based shape analysis; the idea of this analysis is that the alignment of the images is on certain facial landmarks that are considered fixed or anchor points (not affected by surgery). These landmarks are utilised to establish a baseline for the alignment on which the coordinates system is created. In Bookstein analysis, exocanthion landmarks (right and left) were usually the fixed points for the determination of the horizontal axis. A second axis was created to be orthogonal to the horizontal axis and crossing the nasion landmark, which helped with the orientation of the images. The third axis was a vertical orthogonal axis that was crossing the nasion. This approach helped to align the images and to identify the vertical axis from which the deviations of facial landmarks in the cleft and non-cleft side were measured and compared with the control (Ayoub et al., 2011b).

1.3.1.3 Thin-plate spline analysis

This analysis is a landmark-based graphical analysis that is utilised to demonstrate shape changes between two corresponding images (Chang et al., 2002). In this analysis, a grid is used to locate the landmarks of two images separately. This grid consisted of very small increments called splines. The changing of the shape of one image to correspond with the landmarks on the other image is accomplished by a deformation in the small increments of this grid to match the shape of the other image, while the stability in the shape of the grid means there is no shape difference between the two images (Bookstein, 1989). The differences between “deformation” of the shapes are

quantified by the bending energy of these increments. When there are no differences between the compared facial shapes, the differences will be quantified as zero. In the field of 3D facial imaging, grid deformation was applied to quantify the magnitude and direction of facial soft tissue or facial hard tissue shape changes to evaluate the effect of orthognathic surgery (Soncul and Bamber, 2004), and to evaluate the effect of facial growth (Cevidanes et al., 2005). However, one of the popular applications for grid deformation was the wrapping of facial imaging to achieve a mathematically average face (Hammond, 2007; Guo et al., 2013).

1.3.1.4 Frame-based registration

The frame-based registration method is based on the construction of three orthogonal planes for each 3D facial image. The registration can be achieved by the alignment of the planes of a group of images.

The placement of the planes is achieved by a computed method that itself is based on the digitisation of facial landmarks. Before the creation of the planes, the orientation of the 3D facial image had to be adjusted to a natural position for the canthal-superaurale line to be horizontally positioned. The horizontal plane is the first to be constructed. It passes through the midline point of the nose (usually nasion) and must be parallel to the level of a plane that was 7.5° above the alare-tragus plane (Figure 1.11). The sagittal and coronal planes were established to be orthogonal to the horizontal plane and crossing the nasion landmark (Worasakwutiphong et al., 2015).

Plooij et al. (2009) constructed another frame plane, in which the midline point was the “pupil reconstructed point” that was digitised in the midline of the nose on the line connecting the pupils of the eyes. The horizontal plane was parallel to a plane that was 7° below the canthal-superaurale line. The vertical plane was posterior from the pupil reconstructed point in a constant

distance and perpendicular to the first plane. Furthermore, the median plane runs perpendicular to the vertical and horizontal plane. The intra- and inter-observer reproducibilities of this frame-based registration method were 1.0mm and 1.2mm, respectively (Maal et al., 2010). The main drawback of the latter frame is that it cannot be used to evaluate facial soft tissue growth changes as the vertical plane is placed at a constant distance from the pupil reconstructed point. This frame was modified in 2013 as it was proposed to be used in the assessment of facial growth changes in 3- to 12-month-old infants with and without clefts. In the modified frame, an additional vertical plane was placed at the pretragion point so that it was parallel to the original vertical plane that was placed 12cm behind the pupil reconstructed point. According to Brons et al. (2013) the intra- and inter-observer reproducibilities of the frame were 0.4mm and 0.5mm, respectively.

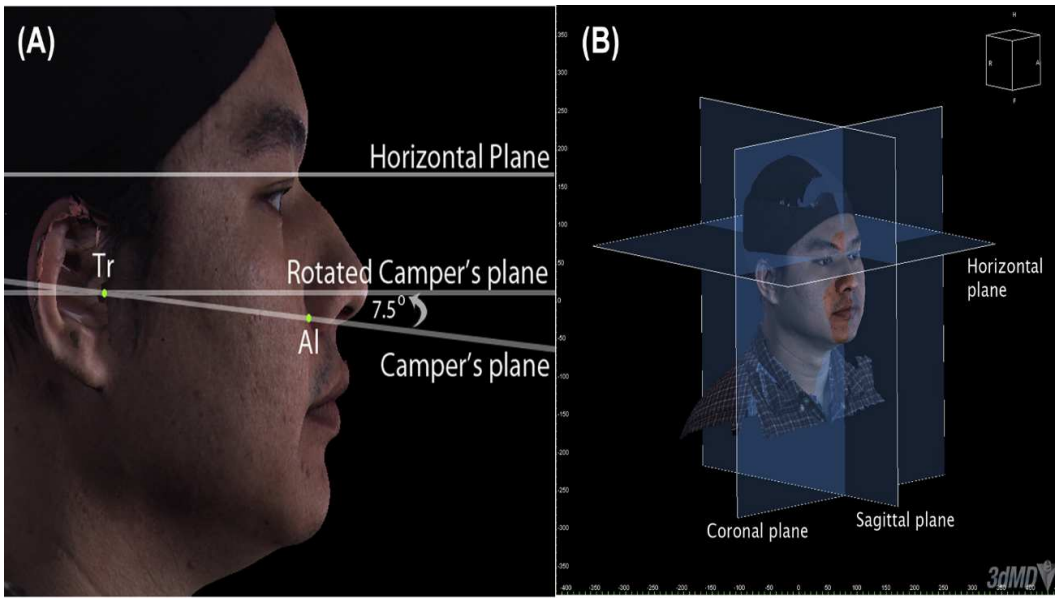

Figure 1.11: Setting of a frame-based for 3D facial image (A) The horizontal plane is parallel to the plane which is 7.5° up rotated from the alare-tragus plane. (B) The three reference planes: horizontal, sagittal and coronal, quoted from Worasakwutiphong et al., 2015.

In terms of visualisation of facial shape changes after primary cleft lip surgery, Schwenzer-Zimmerer et al. (2008a) established a horizontal plane only for the alignment of the 3D image before and after primary lip surgery. The plane was considered to constitute the skull base of facial 3D models, and it was constructed by digitising three landmarks only: the nasion and Right tragus superior point and Left tragus superior point.

However, the use of a frame-based registration method for clinical evaluation of post-operative shape changes have not been popular, and was limited to eliminating image rotation. It had to be followed by another registration method (for example, surface-based) to translation the 3D images (Worasakwutiphong et al., 2015; Meulstee et al., 2017). Furthermore, the method is based on the identification of few landmarks. Errors in locating these key points would affect the accuracy of the method.

1.3.2 Surface-based registration

This registration relies on the similarity of 3D facial surfaces. This method does not depend on landmarks; and the registration of 3D models depends on the distances between the surfaces which are represented by the distances from the points (vertices) of one model to the closest surface of the other model. The registration can be obtained by minimising the total of the distances between the surfaces of the two 3D models. Iterative Closest Point (ICP) is an algorithm which is usually applied to surface-based registration. This algorithm aligns the 3D models by selecting the closest points between the two surfaces until the minimum total distance is achieved (Besl and McKay, 1992). An initial alignment using facial landmarks, is usually required before the iteration process.

1.4 Surface-based analysis

The similarities and differences between the aligned surfaces can be visualised by a colour coded map which represents the differences in different colour, and can be objectively quantified by measuring the mean of distances between the two surfaces, the percentage of surface area and volume (Souccar and Kau, 2012).

Colour coded map is a comprehensive method, whereby the distances between the vertices of the first model to the closest surface in the second model are presented in colours. One of the 3D models is considered the base model and the displacement of the second model in relation to the base model is either positive, negative or zero. If there is no difference between the two vertices, i.e. the distances are zero, the corresponding regions are presented in green. Positive differences (the second model is outward from the base model) are represented in red. Negative differences (the second model is inner to the base model) are presented in blue. A scale, which combines the colour map, clearly identifies the gradual changing scale of numerical values of these colours which evolve between maximum and minimum values (Naudi et al., 2013).

Whilst there was no perfect symmetry in human faces, studies that evaluated facial asymmetry by superimposing the original 3D model on its mirror image copy usually applied ICP registration with allowing tolerance of 0.5mm, (Djordjevic et al., 2013).

The disparity between two 3D models can be objectively determined by measuring the mean of distances between these surfaces. The distances between the vertices of the two surfaces could be positive or negative depending on the direction of the difference between the superimposed surfaces. The mean of distances was quantified using three mathematical

methods: the arithmetic mean (Khambay and Ullah, 2015; Ozsoy et al., 2015), the mean of absolute distance (Alqattan et al., 2013) and the root mean square distances (RMS) (Taylor et al., 2014; Kornreich et al., 2016). However, the arithmetic mean is misleading since the positive values cancel the negative ones (Khambay and Ullah, 2015). With regard to facial asymmetry, a study by Ozsoy (2016) compared the evaluation of the total and regional facial asymmetries of 51 healthy adults using the three sets of measurements (the arithmetic mean, the mean of absolute distances, and the root mean square distances (RMS)). The results of their study showed that the absolute distances and root mean square distances were accurate enough for the objective quantification of facial asymmetry, while the arithmetic mean was inadequate for the quantification of facial asymmetry.

The symmetry was also measured in percentage of surface area. In this situation the percentage of surface areas, where the linear distances between original and mirror shells were below 0.5mm, was calculated (Djordjevic et al., 2014b).

1.4.1 Concepts of measuring the distances between the surfaces of two 3D models

The 3D facial model consists of tens of thousands of vertices (points). Measuring the distances between the corresponding points is required for evaluation the differences between the two 3D surfaces.

The first concept measures the distance between the vertices of the first surface mesh which intersects the surface of the second mesh at a right angle. The distance is recognised as “normal” (Figure 1.12). The “radial method” is the second concept. It forms by tracing the curvature of the human face for selecting the point in the second mesh. The distances measured between the intersecting points of the two meshes by radiating

lines extending from the centre of the first mesh. The third method is the "closest point"; as its name suggests, the distances are measured between the points on the first mesh to the closest surface point on the second mesh (Miller et al., 2007). There is no agreement on the most accurate method of surface measurements. The lack of anatomical correspondence is the main drawback of these methods, as the points (vertices) on the two surfaces may not be anatomically related, (Kau and Richmond, 2010). The dense correspondence analysis provides an alternative method of ensuring the anatomical correspondence of the two surfaces.

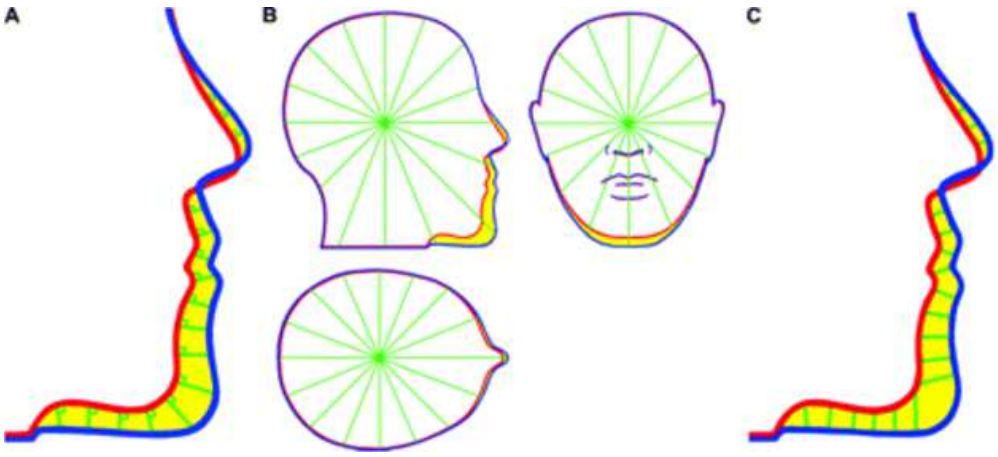

Figure 1.12: A diagram illustrates the types of distances between two surfaces: (A) normal, (B) radial (C) closest point, quoted from (Miller et al., 2007).

1.4.1.1 Dense anatomical correspondence analysis

In this method, a generic mesh, which is a mathematical face mask that consists of a fixed number of vertices, is utilised for representation of the 3D models. This method measures the distances between the corresponding vertices of 3D images, which ensures the anatomical correspondence

between two surfaces of the 3D models. The first introduction of dense correspondence analysis was by Mao et al. in 2006. Although this method is a surface based analysis, it can be considered a comprehensive landmark method as it represents the surfaces by a dense of corresponding mathematical landmarks.

Claes et al. (2012) employed dense correspondence analysis for the assessment of facial shape changes after orthognathic surgery. This helped in the tracking of each point (vertex) before and after surgery. In their study, the facial mask was an anthropometric mask, averaging 400 healthy human faces. Dense correspondence analysis was applied to evaluate the impact of orthognathic surgery on facial expressions using 4D imaging (Figure 1.13) (Al-Hiyali et al., 2015). It can provide an insight into facial shape changes in three directions: X, Y, and Z; It was applied to analyse the direction of facial shape changes after orthognathic surgery (Almukhtar et al., 2016).

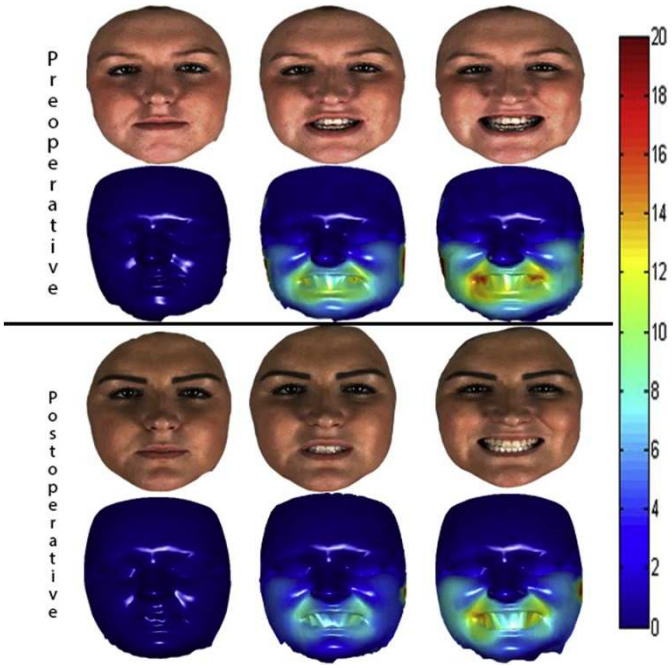

Figure 1.13: The application of generic mesh in the evaluation of the impact of orthognathic surgery on facial asymmetry during smiling expression (Al-Hiyali et al., 2015).

1.4.1.1.1 Generic mesh conformation

The generic facial mesh has the shape of a human face and consists of a fixed number of vertices (points) that can reach to tens of thousands, which was index. This mesh can be conformed on a 3D facial image to represent the shape of the 3D images by tens of thousands of mathematical landmarks (Ju and Siebert, 2001a, 2001b). In this conformation process, the mesh is wrapped and adjusted to fit the 3D facial images in a process called "elastic deformation". The first step in the "conformation process" is the digitisation of facial landmarks on the mesh and 3D image. Thereafter, a thin plate spline process was applied to move the landmarks on the mesh to be in correspondence with matching landmarks on the facial image. In the second step, each local area of the facial mesh is adapted on the 3D image to allow each vertex of the mesh to match its anatomical correspondence, guided by the surface morphology. This conformed mesh represents the 3D facial image in a standard set of thousands of landmarks. This enables the comparison between a set of conformed meshes using dense correspondence analysis of these thousands of points (Mao et al., 2006).

The validity of the generic mesh in representing the underlying surfaces was proved by our research team (Almukhtar et al., 2017). In their study, 3D facial images were captured for a group of volunteers at rest and at maximum smile, facial landmarks had been marked on their faces before image capturing. The images at rest were conformed on their related facial images at maximum smile, and the Euclidean distances between facial landmarks of the conformed meshes and their original images at maximum smile were calculated. The overall error was 1.13mm. The accuracy of the generic mesh in the analysis of facial soft tissue changes has been investigated by our research team (Cheung et al., 2016). 3D Facial images

were captured for 20 volunteers at rest and after different simulated surgical procedures after marking facial landmarks on their faces. A generic mesh was conformed on the images at rest and for the simulated procedures. The Euclidean distances between facial landmarks on the images at rest and simulated procedures were calculated and compared with corresponding landmarks of the conformed meshes. There was no significant difference between simulated surgical movements and the measurements based on generic mesh. The procedure was repeated and showed an error within ±0.4mm.

1.5 Facial averaging

The 3D average face can be obtained by averaging a group of 3D images; it represents the morphological characteristic of facial features belonging to that set of 3D images (Hammond, 2007).

1.5.1 Clinical application of 3D facial averaging

Facial averaging of 3D facial models has been used to compare differences of facial morphologies of various populations (Bozic et al., 2009; Kau et al., 2010; Talbert et al., 2014), and for the assessment of facial gender differences (Kau et al., 2006). The method has also been applied to demonstrate the characteristic facial morphology of Cl III patients before orthognathic surgery (Božič et al., 2010), or to demonstrate facial changes due to facial growth (Koudelová et al., 2015). The latter investigated the changes of facial shape and form during puberty by constructing average faces for 13 girls and 17 boys aged 12 years in a longitudinal study. The 3D facial models for the two groups were captured at one-year intervals in a four-year period.

Facial averaging has a clinical application in the analysis of craniofacial dysmorphology (Islam et al., 2015); it is an important tool for diagnosis of the syndromes, and permits comparisons between syndromic and non-syndromic faces (Hammond, 2007).

The average face of 359 healthy individuals, consisting of approximately of 10,000 points, was utilised as an anthropometric facial mask for evaluating facial asymmetry for patients with facial growth disorders and hemi mandibular hyperplasia (Claes et a., 2011; Walters et al., 2013).

1.5.2 Methods of averaging facial morphology

1.5.2.1 Dense Surface Model (DSM)

In this method, thousands of surface points are utilised to obtain an average of a set of images. Surface points are regarded as mathematical landmarks which overcome the problem of the limited number of anatomical points in specific facial regions. Due to the fact that facial landmarks are utilised in the construction of the average face, this method is also known as the landmarks method.

The manual digitisation of landmarks on a group of 3D surface images is the first step of constructing an average face. This is followed by the application of General Procrustes Analysis (GPA) to obtain the mean positions of these landmarks. Thin-plate spline (TPS) analysis is then applied to maximise the superimposition of the corresponding images. This enables the thousands of corresponding points of each surface to be superimposed in order to produce an average Dense Surface Model (DSM) (Hammond et al., 2004; Hammond, 2007).

The main drawback of this method is that it does not ensure the anatomical correspondence of surface points of the averaged Dense Surface Model. This

means that the correspondences of surface points of a group of 3D images after GPA and TPS application, may not necessarily match the anatomical correspondence of all these points in the original images.

1.5.2.2 Landmark independent approach

3D images averaging in this method requires a construction of a template. This template is achieved by averaging all the points in each 3D image for a group of images. There are two processes employed: point-wise averaging in the 'z' direction or point-wise averaging in the radial direction. The obtained average face is used as a base shell for an image to construct the average model, that is utilised as a base shell for the other images. This step is applied for the entire images using the Iterative Closest Point (ICP) algorithm (Kau and Richmond, 2010). The average face obtained by this technique can be considered as a mathematical average face which lacks anatomical correspondence. This is its main disadvantage.

1.6 Facial asymmetry

In clinical terms, symmetry is defined as the balance, while asymmetry is the imbalance (Bishara et al., 1994). Asymmetry can be classified into three types: “antisymmetry”, “directional” asymmetry and “fluctuating” asymmetry. Antisymmetry means that the dominancy can be on either side of the body, such as, hand dominancy. In directional asymmetry, one side of the body is commonly the dominant, such as, the heart position. Fluctuating asymmetry describes the small random deviations from perfect bilateral symmetry, i.e. traits that are averagely symmetrical. It represents the genetic and environmental pressures experienced by individuals during development (for example, mutation and pollution). It is considered an indicator of developmental stability whereby the higher the fluctuating asymmetry, the less developmental stability (Palmer and Strobeck, 1992; Sforza et al., 2010).

Facial symmetry is the balance and the correspondence of the size, shape and arrangement between the right and left sides of the face. The nature of the human face is bilateral symmetry, so one side of the face mirrors the other around the midsagittal or symmetry plane (Shah and Joshi, 1978). However, perfect facial symmetry almost never exists, and slight facial asymmetry is acceptable and considered normal. Facial symmetry is correlated with attractiveness (Baudouin and Tiberghien, 2004; Sforza et al., 2010), however, the correlation between symmetry and attractiveness might not be constant, whereby symmetry and asymmetry are causes of attractiveness and beauty. Faces regarded as attractive may also display elements of asymmetry (Peck et al., 1991). In a study by Inui et al. (1999) facial symmetry was found to be correlated with TMJ health where patients with internal derangement of the TMJ showed facial asymmetry. Thornhill and Gangestad (2006) proposed a hypothetical correlation between facial symmetry and good health.

1.6.1 Evaluation of facial asymmetry

One of the earlier attempts to utilise photographs for the evaluation of facial asymmetry was made by Ferris, 1927. The method was developed due to the clinical value of photographs for the identification of facial features and documentation of the progress of orthodontic treatment. The concept of this technique was based on bisecting the positive and negative facial photographs of the patient in the midline. Thereafter, two perfectly symmetrical photographs were created by combining each half reverse image with its original one (Figure 1.14). The asymmetry was clarified by comparing the two images. Since then, several studies have evaluated facial asymmetry using 2D facial photographs. However, the application of 2D projection for the evaluation of facial asymmetry has its drawbacks; firstly, the face is three dimensional, and its asymmetry can be vertical, horizontal and anteroposterior, and the 2D photograph is unable to represent the third dimension (the anteroposterior dimension) of the face. Secondly, the 2D projection is greatly affected by the angle formed between the symmetry plane and the recording camera, as this angle increases, the asymmetry also increases (Trpkova et al., 2003; Hartmann et al., 2007). The evolution of 3D imaging is the potential solution to this problem, and it has been the choice for the evaluation of facial asymmetry in many studies (Hajeer et al., 2004a; Huang et al., 2013; Verhoeven et al., 2013; Djordjevic et al., 2014a; Ovsenik et al., 2014).

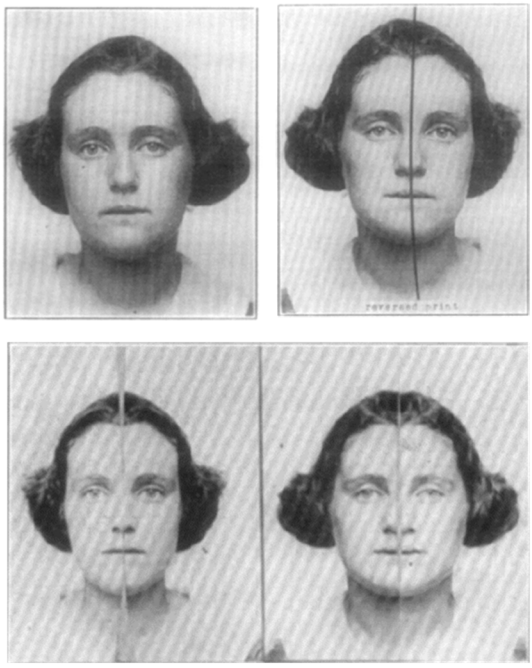

Figure 1.14: The first method for facial asymmetry assessment using 2D photographs. The original and negative photographs (upper left and right images respectively) were bisected in the midline. The difference in measurements between the two perfectly symmetrical photographs (lower left and right images) represented facial asymmetry (Ferris, 1927).

1.6.2 Evaluation of facial asymmetry in the non-patient population

In an attempt to evaluate normal soft tissue asymmetry, Farkas and Cheung (1981) evaluated the facial asymmetry of 308 children (6, 12 and 18 years groups). In their direct anthropometric study, six pairs of measurements on the lateral sides of the face were used to measure the asymmetry. They found that the average difference between the right and the left side was 3mm or 3% and the right side was larger than the left side. The difference

between male and female was not significant. This "normal" asymmetry between the two sides of the face was described as the "laterality of asymmetries".

In 2001, Ferrario et al. assessed the asymmetry of 314 healthy subjects who were divided into three groups according to their age (12-15 years, 18-30 years and 31-56 years), and each group was subdivided into male and female. Facial landmarks were digitised directly on the face and their coordinates were obtained by the 3D computerised electromagnetic digitiser. "Distance From symmetry" (DFS) method was used to calculate the asymmetry. This process involves the construction of a symmetry plane passing through nasion and perpendicular on a plane whilst passing through exocanthi. Having been constructed for each 3D image, the bilateral landmarks' coordinates were used to calculate the right and left gravity central points for each facial side. The right centre of gravity was mirrored on the left side around the symmetry plane. The lateral asymmetry vector DFS_l was calculated by measuring the vector between the left gravity centre and the rotated right gravity centre, which was characterized by magnitude and direction (3 coordinates). The midline vector DFS_m was determined by horizontal coordinates of midline landmarks from the symmetry plane. The total asymmetry DFS_t was the summation of the magnitude of DFS_l+ DFS_m. To eliminate the effect of different facial dimensions, DFS_t% was calculated as the ratio of DFS_t to the mean distance between nasion and centre of gravity left and right. The threshold of maximum normal asymmetry for DFS_t and DFS_t% was calculated as the mean +2SD. Their method helped to identify the direction of dominance in X, Y and Z directions by dividing the DFS_l into three components (X, Y and Z) for each individual and calculating the mean for each group. Their results showed that facial asymmetry was not related to age or gender. The difference between the most symmetrical and most asymmetrical groups was less than 2.5mm. In the three groups, the right side

was larger, inferior, and posterior. However, the adolescent female group showed that the right side was smaller.

Many studies have been identified the right side of the face as more dominant than the left side (Farkas and Cheung, 1981; Ferrario et al., 1994; Ferrario et al., 2001). Whilst other studies have found that the dominancy is to the left side (McIntyre and Mossey, 2002; Ercan et al., 2008).

In a landmark independent method, Kornreich et al. (2016) assessed the normal asymmetry of 350 adult faces using the mirroring technique. The results concluded that the total facial asymmetry was 0.625 ± 0.16mm (0.61mm for females and 0.66mm for males). In the study of Djordjevic et al. (2014b), the entire facial asymmetry for males was 0.61mm, and 0.54mm for females and the differences were not significant.

Facial asymmetry varied according to facial parts. The lower third of the face was reported as the most asymmetrical part of the face (Patel et al., 2015). However, Farkas and Cheung (1981) identified the upper third of the face as the most asymmetrical.

To date, there has been no final agreement regarding the acceptable level of facial asymmetry, beyond which asymmetry is considered abnormal and can affect facial aesthetics.

Newborn babies without craniofacial abnormalities are usually born without noticeable asymmetry of the face and head. Asymmetry of the head might develop during labour. However, this is self-rectifying over a few days and is not permanent. The recumbent position of an infant in its first few months of life encourages the development of head and facial asymmetry. The continuous pressure of the pillow can lead to flatness of the occipital region, usually on the right side. If this condition persists, a corresponding bulging of

the frontal bone will develop on the same side. This will be accompanied by prominence of the cheek due to the prominence of the malar bone and the ear will move forward and the eye will appear more prominent on the affected side. This condition is usually treated by lying the infant in a fixed posture that is opposite to that causing the condition (Greene, 1931).

White (2005) employed 3D stereophotogrammetry in order to assess the longitudinal asymmetry of healthy infants at 4 life stages: three months, six months, one year and two years. Asymmetry scores were obtained by scaling sets of facial landmarks for 3D images into a common size. Each landmark set was reflected into an arbitrary plane to produce a mirror copy. Partial Procrustes Analysis was applied to eliminate the distances between the original and the corresponding reflected landmarks by rotation and translation. From here the average landmark configuration was obtained. The asymmetry score was calculated as the mean squared distance between the average landmarks and the corresponding original landmarks. A slight degree of facial asymmetry was reported, and the mean asymmetry score of 83 infants was 3, and 90% of them had asymmetry score range from 1 to 4 (White et al., 2004). The upper face was the most asymmetrical part of the face, and facial asymmetry generally decreased with age (White, 2005).

1.6.3 3D asymmetry assessment for cleft patients

Facial asymmetry of cleft patients was the topic of investigation in several studies (Bilwatsch et al., 2006; Stauber et al., 2008; Meyer-Marcotty et al., 2011; Bugaighis et al., 2014a; Bell et al., 2014; Djordjevic et al., 2014a; Kuijpers et al., 2015). There are variety of techniques available for the quantitative analysis of 3D facial asymmetry.

1.6.3.1 Location of homologous landmarks in relation to symmetry plane

This is a simple method for the evaluation of facial asymmetry. Whereby homologous facial landmarks are digitised on the face and a symmetry plane is constructed. The 3D position of each facial landmark is identified. The asymmetry is analysed by calculating the difference in 3D positions of two homologous landmarks on the face in relation to the symmetry plane. This method helps to identify the dominant side of the face. Furthermore, the asymmetry of each of the paired landmarks can be analysed in three directions: X, Y and Z. This method was the method of choice for earlier studies for the evaluation of facial asymmetry of cleft patients (Ras et al., 1994)

Describing the asymmetry as the differences between the pair measurements of the two sides of the face using the symmetry plane has been criticised, due to the difficulty in identification of symmetry plane. The identification of the symmetry plane by facial landmarks at the midline of the face is inaccurate. These landmarks might be affected by the asymmetry and might not be located on the middle of the face. The validity of the symmetry plane identified by facial landmarks is questionable due to inaccuracy associated with landmarks digitisation, furthermore the landmarks cannot describe the entire facial surface.

The symmetry plane can also be calculated by measuring the midsagittal plane of the symmetrical face that is obtained by the registering the original and mirror images (Djordjevic et al., 2013; Djordjevic et al., 2014b), or by measuring the centre between the original and the reflected points of the 3D models (Stauber et al., 2008; Hartmann et al., 2007). The latter method is sensitive to the alignment procedure of the original images, which might affect the accuracy of measuring facial asymmetry (Wu et al., 2011).

In an attempt to improve the identification of the symmetry plane in craniofacial patients, Wu et al. (2016) introduced a method for the symmetry plane identification before and after cleft repair that does not rely on the mirror image approach. In this computerised method the midsagittal plane of the 3D facial model was obtained by calculating the geomatical midline of the upper and lower thirds only of the 3D facial model. This method omitted the middle third of the face where a gross asymmetry present due to the cleft that would affect the calculation of the midsagittal plane. The computer considered the upper and lower third only for calculating the midsagittal plane. However, omitting important third of the face might be not practical.

Identification of the symmetry plane was challenging, and, to date, there is no agreement on one method. For these reasons, further methods were developed to quantify the facial asymmetry in cleft cases.

1.6.3.2 Euclidean Distance Matrix Analysis (EDMA)

This analysis was developed by Lele (1991) and Lele and Richtsmeier (1992) for objective comparison of the shape differences of craniofacial structures. In this analysis, all possible distances between the homologous landmarks were calculated and arranged into two individual matrices describing each half of the face. By dividing the values of each matrix by the corresponding

values of the other matrix, the differences described shape differences. If the two shapes, two halves of the face, were symmetrical, all ratios would be equal to 1. If the first shape was larger, the ratios would be more than one. Consequently, the opposite is true, when the ratios would be less than one if the first shape was smaller. The method relies on the measurement between the landmarks and is independent on landmark coordinates. Moreover, it describes each half of the face individually and identifies the local asymmetries. If the two shapes were not symmetrical and all the ratios in the difference matrices had equal values, the difference is in size and not in shape. Otherwise, the difference would be in shape and size (O'Grady and Antonyshyn, 1999).

The application of this method is common in 2D rather than 3D as it does not require to landmark coordinates. It was applied by Seidenstricker-kink et al. (2008) for 3D evaluation of facial soft tissue and hard tissue asymmetry of cleft infants before and after primary lip surgery.

1.6.3.3 Asymmetry scores

Asymmetry Scores is a landmark-based approach for the quantification of facial asymmetry. The first step in this method is based on the digitisation of the facial landmarks of each 3D image. A mirror image is created for each set of facial landmarks; Partial Procrustes Analysis (PPA) minimises the distances between mirror landmarks and corresponding original ones. The distances between original and mirror images' corresponding landmarks are measured in millimetres. This value represents the asymmetry score. In perfect symmetry, the asymmetry score would be zero (Hood et al., 2003; Bugaighis, et al., 2014a). This method helped to overcome the problem associated with symmetry plane identification, as it does not require for symmetry plane construction.

The facial asymmetry of 20 infants with unilateral cleft (10 UCL, 10 UCLP) was assessed longitudinally using this approach. The results were compared to the results of 25 matched control cases (Hood et al., 2003). Stereophotogrammetric images were captured prior and following primary lip repair and at 1-year follow-up. Facial landmarks were digitised on the 3D images to obtain asymmetry scores for the nose, lip and the face. Higher facial asymmetry was noted in the UCLP cases than UCL cases, with a significant improvement in nasal asymmetry following lip repair. In the UCL cases, asymmetry scores of the nose did not show significant improvement after the primary surgery.

This method employs a set of facial landmarks in order to quantify the asymmetry, which does not describe facial surface asymmetry between these landmarks, and does not depict the asymmetry of facial regions where the landmarks are few and difficult to identify. A limited set of facial landmarks would not have described the complex facial morphology adequately.

1.6.3.4 Curve analysis

Curve analysis is a computerised method of facial analysis which describes the characteristics of facial morphology by using curvatures extracted from the facial topology. Human face consists of curvatures that form facial structures such as lips, cheeks, nose and chins. The method relies on the extraction of curvatures that describe the contour of the facial region of interest. These curves can be extracted either by constructing a plane using facial landmarks and the curve is defined by the points of the facial surface that intersect that plane. Alternatively, extracting the curvatures that follow the surface topology offers another method. The latter method is not constrained to a particular plane or landmarks (Higgins, 2009).

Bell et al. (2014) used this method to quantify the residual facial asymmetry of 10-year-old UCLP and UCL children at rest and at maximum smile. Asymmetry scores were obtained from five facial curves describing the contours of the upper lip, nose, between the eye region, the subnasal region, and the facial midline. The method was more informative than facial landmark analysis, and it could be more insightful to adopt this analysis to describe the whole facial surface.

1.6.3.5 Mirroring technique

The first application of this method was in 1999 by O'Grady and Antonyshyn. Clearance vectors were used to display the difference between 3D facial model and the mirror copy. These vectors are coloured lines representing the distances between the vertices of the two model's surfaces. The asymmetry was quantified by measuring the volume of asymmetry, which represents the difference between one half of the face and its contralateral mirror image. It was calculated by computing the average clearance vector length of the clearance vector range (O'Grady and Antonyshyn, 1999).

Mirroring technique is a surface-based approach for the assessment of facial asymmetry, it is the method of choice for the evaluation of the residual asymmetry of cleft patients (Meyer-Marcotty et al., 2011; Djordjevic et al., 2014a ; Kuijpers et al., 2015). This method is a landmark-free method, used to visualise and quantify the asymmetry of facial surfaces where few anatomical landmarks are available.

In this method, a mirror image is created for the 3D facial model, which is then superimposed on the original (Figure 1.15). It permits for direct comparison between the surfaces of the two halves of the face, and also provides a robust description of facial morphological asymmetry rather than depending on a few sets of landmarks.

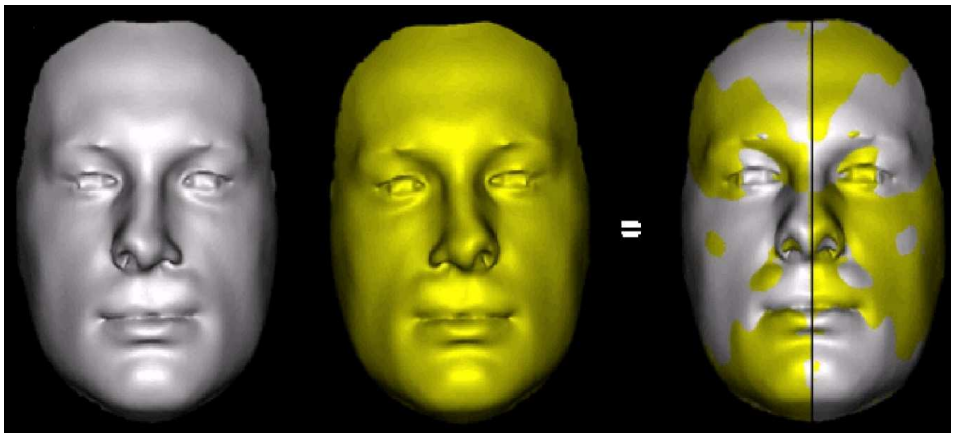

Figure 1.15: Mirror image method for facial asymmetry assessment. Surface registration of the original image of UCLP patients (grey) on its mirror copy (yellow), (Meyer-Marcotty et al., 2011).

The original and mirror images are usually registered with ICP algorithm, and the mean of absolute distances is measured to quantify the asymmetry of the whole face. This method gives further insight into the asymmetry of each anatomical facial region. Djordjevic et al. (2014a) divided the original and mirror images into four horizontal facial regions using three horizontal parallel planes passing through the subnasale, the corners of the mouth and the inner corners of the eyes. Excluding the forehead region, UCLP patients had a significantly higher facial asymmetry compared to those in the control group. In this study, the residual asymmetry was measured for each horizontal facial region. However, it was not clear for which anatomical area this residual asymmetry was quantified. Kuijpers et al. (2015) divided the original and mirror images of the face using five planes into four regions. Three of the five planes were parallel horizontal lines passing through the exocanthions, subnasale and labiale inferius, while the vertical planes were passing through the right and left endocanthion and cheilion (Figure 1.16). This method disclosed the residual asymmetry of the nose, lips, cheeks, and chin. In their study, the nose was the most asymmetrical region in the cleft

groups. While the chin was the most asymmetrical region in the control group. The measured residual asymmetry considered both the upper and lower lips as one anatomical region. The residual asymmetry of the upper lip should have been analysed separately. The rationale is that this was the area which had the highest impact from the surgery and was the site of the cleft itself. Likewise, the residual asymmetry of the nose was included in the cheek regions, and it should have been analysed separately. The authors chose artificial facial planes to conduct the asymmetry analysis which did not follow the anatomical boundaries of facial regions.

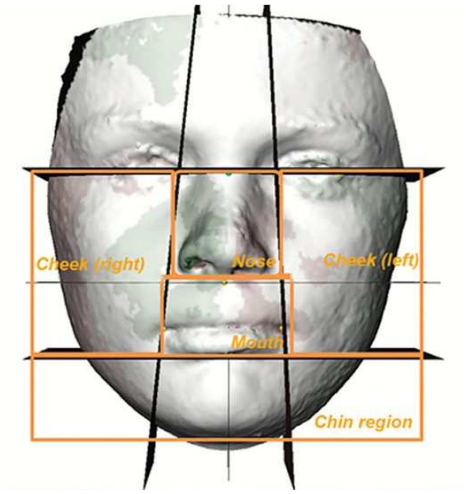

Figure 1.16: : Regional facial asymmetry was quantified by dividing the original and mirror models using facial planes, quoted from (Kuijpers et al., 2015).

The techniques for mirror image creation are independent on the plane that are used for the reflection of the original image to create the mirror copy. In some studies, facial asymmetry was evaluated by mirroring the 3D facial image on a plane positioned outside the face (Kuijpers et al., 2015; Patel et al., 2015; Kornreich et al., 2016). In other studies, this was also achieved by reflecting the original image onto the midsagittal plane (Primozic et al., 2009).

1.6.3.6 Dynamic asymmetry

The development of 4D imaging facilitates the capturing of video stereophotogrammetric for a variety of facial expressions. The video usually consists of 60 images per second, capturing facial movement in sequence. Facial landmarks can be digitised on the first frame and can be tracked automatically or manually in the following frames. This technology was utilised for the evaluation of the facial asymmetry of the smile and the lip pucker expression of 12 unilateral cleft patients with or without cleft palate, and 11 controls. The age of the total sample was from 8 to 18 years old. To quantify the asymmetry, the displacement and the speed of the digitised landmarks were quantified. The Euclidian distance between the position of each landmark in the resting frame and its position on each frame was calculated for the cleft and non-cleft sides. While the Euclidian distance between each landmark position in two successive frames represented the speed of the landmarks' motion, there was significant dynamic asymmetry of cleft patients with maximum asymmetry at the mid-philtral ridge landmark due to lip scarring (Hallac et al., 2017).

The 4D system is capable of producing approximately 60 3D images per second; each image consists of approximately 500,000 points. However, few landmarks quantified the asymmetry of the upper lip and eye regions only. Consequently, the asymmetry of the facial surfaces could not be described comprehensively.

1.7 3D assessment of the treatment outcomes of cleft lip and palate patients

Objective assessment of the residual facial dysmorphology of cleft patients has attracted many investigators; it helps to assess the quality of treatment outcomes and to improve the implemented treatment procedures. Indirect morphometries of 3D facial cleft models are more common methods (Duffy et al., 2000; Ayoub et al., 2011a, 2011b; Zreaqat et al., 2012; Bugaighis et al., 2014b) than direct morphometries (Farkas et al., 1993). Linear and angular measurements and facial ratios of cleft patients were compared to the control group. Some studies considered a surface-based method to demonstrate the residual dysmorphology of cleft patients by constructing mathematical average faces of the cleft groups. The average face of each cleft group was superimposed on the average face of the control group (Figure 1.17) (Duffy et al., 2000; Bugaighis et al., 2014c). Alternatively, each 3D facial image of cleft patients was superimposed on the average face of the controls (Djordjevic et al., 2014a).

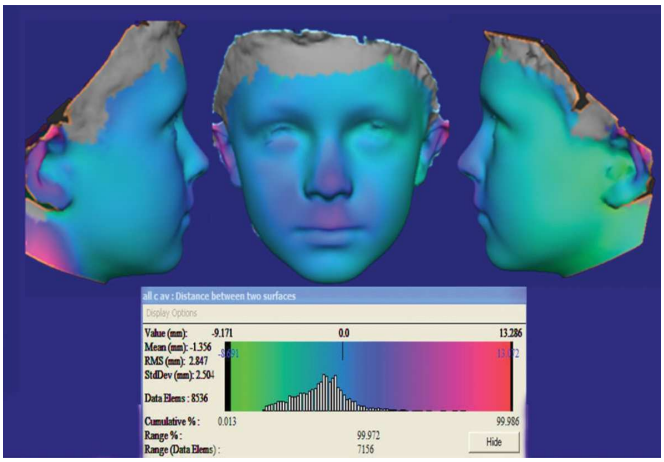

Figure 1.17: Colour coded map and histogram showing the difference between the surfaces of the average faces of UCLP and Control groups, quoted from (Bugaighis et al., 2014c).

In comparison to the controls, the UCLP patients had shorter faces and narrower mid-facial width. These patients had straight profiles, with reduced maxillary prominence. The nasolabial region is the most affected region by the cleft. The nasal bridge is shorter and the nasal base is wider. The columella is shorter, and the alar wing of the cleft side is longer. The upper lip is shorter and the philtrum is wider than the control. Facial dysmorphology is prominent in patients with cleft extending in both primary and secondary cleft palate.

These cross-sectional studies showed a diversity of variations regarding patient age. For example, in some study the age was at three years (Ayoub et al., 2011a, 2011b), while in others the age was at eight to 12 years (Bugaighis et al., 2014a). The number of landmarks used for the analysis also varied widely between 15, as suggested by Duffy et al. (2000), and 50 landmarks, according to Ayoub et al. (2011b).

1.7.1 Evaluation of facial changes of cleft lip infants

There are limited studies on cleft lip and palate patients during the early years of life. In a cross-sectional study of Japanese UCLP patients, Yamada et al. (2002b) investigated the facial morphology of eight patients at four months, 18 patients at one year and a half, and twenty patients at four years. The images were captured before and after surgical correction using an optical surface scanner. The first group had images just before surgery. The postoperative images were taken at two time intervals: two weeks and three months postoperatively. The coordinates of the facial landmarks were extracted automatically in relation to three constructed planes of the 3D images, and angular and linear measurements were compared with the control groups. Their main findings were larger nasal tip angle and alar asymmetry were noted in all cleft groups. In the non-cleft side, the cupid's

bow was longer than the cleft side. At four years, vertical and anteroposterior asymmetry of nostril landmarks were determined.

Singh et al. (2007) analysed images of 37-week unilateral cleft infants. The purpose of their study was to assess the influence of Naso Alveolar Molding (NAM) on nasolabial morphology. Average faces for cleft patients before and after NAM and for 10 matching control groups were constructed. Principle component analysis showed similarities in facial morphology between cleft patients after surgery and the control group. Finite-element scaling analysis (FESA) for the average faces of cleft patients before and after NAM treatment showed a volume reduction of the labial tubercle, the columella and the lower lip, with volume increase in the nasal tip, and under the nares beside the columella.

In 2013, Krimmel et al. compared facial landmarks of 30 cleft children aged 0–6 years, with 344 healthy children aged 0–7 years old. Cleft patients showed widening of the nose in comparison to the controls. However, facial morphology in the vertical and sagittal directions was comparable to normal. It was concluded that surgery and orthodontic treatments of cleft patients could treat the vertical and sagittal deficiencies, but insufficient growth was noted in the transverse direction.

All the above studies were cross-sectional studies that compared the facial morphology of cleft groups with controls. To date, there are no longitudinal studies that comprehensively and precisely monitor facial shape changes of cleft patients over time.

1.8 Cleft severity

The type of primary surgical intervention is influenced by cleft severity. Traditionally, initial cleft severity is assessed subjectively by surgeons. However, objective quantification approaches are necessary for the precise assessment of the magnitude of residual cleft dysmorphology, to provide a better quality of care to cleft patients.

1.8.1 Methods of assessing the severity of cleft lip and palate

Farkas et al. (1993) regarded anthropometry a valuable measure for the assessment of severity of cleft deformities. In their study, direct measurements of the face and nose were obtained from three- to twelve-month-old complete unilateral and bilateral cleft children before and after surgical repair of the cleft lip. Facial indices were the tools used for the classification of the magnitude of the lip dysmorphology as mild, moderate and severe.

Slade et al. (1995) introduced the “rating scale” for assessing the initial cleft severity. The study was carried out on the facial photographs of cleft infants. Staff members with different specialities rated facial severity from 1 to 7, where 7 denoted maximum dysmorphology. The complete cleft was more severe than the incomplete cleft, and the bilateral cleft was more severe than the unilateral cleft.

Dental casts before surgical repair has been utilised to measure the severity of cleft. The cleft defect was usually measured in relation to palate measurements (Suzuki et al., 1993; Johnson et al., 2000; Peltomäki, et al., 2001). The dental cast would be marked, and the measurements could be obtained either by software analysis of the scanned dental casts (Johnson et al., 2000) or directly from the dental cast (Peltomäki, et al., 2001).

Stereophotogrammetry has been used to evaluate cleft severity. Hood (2005) assessed the severity of cleft infants by indirect anthropometry using patients' 3D facial images. In their study, ratios of the measurements of the cleft side of the face to the corresponding measurements of the non-cleft side were obtained using facial landmarks. These ratios were utilised to measure the degree of horizontal and vertical discrepancies of nasal floor and the upper lip. Schwenzer-Zimmerer et al. (2008a) utilised 3D laser-scanned images to apply a formula that helped to objectively quantify the severity of the cleft preoperatively. Their formula was used to guide the surgeon to the most appropriate surgical manoeuvre for cleft cases individually. Their formula was based on calculating the ratios of linear measurements on the cleft side to non-cleft side of eleven cleft patients.

Utilising laser-scanned facial casts, Nakamura et al. (2005) assessed cleft severity by surface area and linear measurements of the nasolabial region. The sample group for this study was composed of 21 UCLA and 20 UCLP Japanese patients with an average age of 133 +4.5 days. A light colour pen was used to mark eleven facial landmarks on the facial casts. After scanning, each landmark coordinates were measured in relation to the reference planes. The differences in linear measurements between the cleft and non-cleft sides were used to measure facial dysmorphology. The surface area of the cleft defect was obtained by subtracting the surface area of the medial and lateral part of the cleft lip from the total surface area of the upper lip.

In 2014, Uchiyama et al. developed a "five-step rating scale" to assess the cleft severity of incomplete unilateral cleft infants at age four months using a paired rating method. The method was applied to rank thirty facial casts, according to their aesthetic, by twenty surgeons and anesthesiologists. Paired rating refers to the comparison between the images of the total sample based on pairs i.e. two images together. It was noticed that the severity of facial cleft was directly related to the rating score.

In 2014, Wu et al. developed an automated computer-based system to measure cleft severity. This method included the automatic application of a grid-patch on the cleft of the infant's face, to separate the region into many patches to measure the symmetry in relation to a mid-facial plane. The identification of the mid-facial plane was crucial in the study and was verified by five different methods. Two were based on manual methods that were accomplished by two experts; the first was by digitising the medial facial landmarks on the eyes and the chin regions, and the second was by manual direct identification of the medial plane. The other methods were based on advanced automatic method. Nevertheless, the manual methods were the gold standards for the verification of the automatic methods.

1.8.2 The relation of cleft severity to the surgical outcome

Variety of factors can affect the treatment outcomes of cleft patients. These include the timing of the primary surgery, magnitude of the distorted dentofacial growth and initial severity of cleft (Johnson et al., 2000).

Preoperative dental casts were utilised to quantify cleft severity, and maxillary growth was recorded from lateral and posterior-anterior radiographs (Chiu and Liao, 2012; Liao et al., 2010; Huang et al., 2015). The main shortcoming of using dental casts to quantify the severity of the cleft is the absence of the landmarks in the edentulous infant palate. Moreover, the reproducibility of landmarks depends on the quality of dental casts and the operator experience in identifying the landmarks accurately (Seckel et al., 1995). The results of quantifying the severity of the cleft based on dental relationship were contradictory to those based on the mid-facial growth (Chiu and Liao, 2012; Wiggman, et al., 2013; Huang et al., 2015). Antonarakis et al. (2015) studied the association between measurements of the cleft in complete UCLP patients before primary lip repair with maxillary growth at eight and a half years. Lateral cephalometric radiographs were taken before

alveolar bone graft and orthodontic treatment. The study concluded that the extent of lateral lip hypoplasia could affect later maxillary growth deficiency.

In terms of soft tissue morphology, Hood (2005) investigated the correlation between asymmetry scores of UCL and UCLP patients before surgery and at two-year follow-up. Their sample was 3D facial images of cleft infants from Cleft Centres at Glasgow and Edinburgh. Most of the cleft infants in their study, had modified Millard Cheiloplasty and McComb primary rhinoplasty procedures which were performed by different surgeons, and without pre-surgical orthopaedics. In this landmark-based study, the asymmetry scores improved after surgery, however, nasal asymmetry scores for columella, nasal base, nasal rim and nostrils showed no significant correlation between asymmetry score (of UCL and UCLP) before surgery and at two-year follow-up.

1.9 Aims

The aim of this study was longitudinal evaluation of facial asymmetry of the surgically managed UCLP patients using advance facial analysis tool, and to compare the postoperative residual asymmetry with a control group.

1.9.1 Objectives

The objectives of the study are:

1. Quantify the improvement of facial asymmetry following primary surgical repair of cleft lip.

2. Compare the postoperative residual asymmetry with age-matched control.

3. Assess the changes of facial asymmetry at four years following surgery.

4. Study the impact of maximum smile on the residual facial dysmorphology following the surgical repair of UCLP.

5. Explore the correlation between the initial severity of cleft lip and the residual asymmetry of UCLP.

1.9.2 Null hypotheses

The null hypotheses to be tested in this study are:

1. There is no significant difference between facial asymmetry before and after the surgical repair of cleft lip of UCLP cases.

2. There is no significant difference between residual postoperative asymmetry of the surgically managed UCLP cases and facial asymmetry of age-matched control group.

3. There is no significant change in facial asymmetry in repaired UCLP due to facial growth during the first 4 years after surgery.

4. There is no significant difference in the magnitude of facial asymmetry in repaired UCLP at rest and at a maximum smile.

5. There is no significant correlation between the initial severity of cleft lip and the residual asymmetry of UCLP.

Chapter two

Methodology

2 Chapter two: Methodology

2.1 Study sample

2.1.1 Cleft patients

The sample of this study consists of 30 non-syndromic complete UCLP cases (eight girls and twenty two boys), all of Caucasian origin and all followed the same treatment protocol. They underwent the same surgical procedure: "modified Millard Cheiloplasty and McComb primary rhinoplasty" between the age range of 3 to 5 months. The surgical procedures were carried out by the same surgeon. The right: left ratio was 6:24. Pre-surgical orthopaedics was not used in any of the cases in this study, and none of the patients had a Simonart's band.

Preoperative 3D facial images were captured for each patient one or two days before the surgery, and postoperative images were captured approximately four months after surgery, and before palatal surgery. The selected images were among those of 39 patients. Poor quality or incomplete images were disregarded. The images were captured at Edinburgh's NHS Lothian Medical Photography Service at the Royal Hospital for Sick Children during the routine clinical treatments. The images were stored in the NHS Lothian network system. The images were captured in the period of time from 2011 to 2016, and the same method of image capturing was applied during this period of time.

Ethical approval has been obtained from NHS Research Ethics Committees (Reference: 15/SW/0095), and research project no. 2015/0205 was allocated by Research and Development, NHS Lothian to conduct this study on facial

images which were already captured for cleft patients before and after surgery

The ethical approval was amended to recall the patients for two additional 3D facial images: one with the face at rest and another with maximum smile. Image sets for 15 patients (four girls and eleven boys) were captured in this prospective part of the study. Unfortunately, images of maximum smile of two patients were omitted for some technical reasons during data transfer, therefore, this part of the study was limited to 13 images of maximum smile.

2.1.2 Control group (non-cleft infants)

The control group of this study was 3D facial images of 70 six-month old healthy infants. The images of the control subjects used in this study were taken from the available historical data of 3D images of a prievous study (White, 2005). These images were captured using the C3D system at the Royal Hospital for Sick Children, Glasgow and at Glasgow Dental Hospital and School. All of the infants were Caucasian in origin, with no craniofacial abnormalities and no perinatal complications.

2.2 Image acquisition of cleft patients

3dMDface System (3dMD Inc., Atlanta, GA, USA) was used to capture the 3D facial images of cleft patients. It is a non-invasive stereophotogrammetric system that consisted of two modular units (Figure 2.1). Each unit had two high-resolution digital stereo cameras, one high-resolution texture camera (2 megapixels) and one infrared light projector. Light flashes were included in the system to illuminate the face during capture.

Figure 2.1: 3dMD Face System.

All images were captured by a professional photographer at the NHS Lothian Medical Photography Service, at Edinburgh Royal Hospital for Sick Children based in Scotland, UK. System calibration was carried out in the morning prior to the image acquisition sessions. The infant was seated on a raised infant seat about one and a half metres from the camera (Figure 2.2, Figure 2.3). The chair position was moved to ensure that the child's face could be seen within a frame of the 3dMDface software on a computer's screen that was connected to the imaging system (Figure 2.4a). The photographs were taken at rest expression, while the infant was looking slightly above the halfway point of the two camera pods. This stance ensured a clear picture of the nose. The imaging system was able to capture the whole face from the right ear to the left ear to generate the 3D facial model.

Figure 2.2: Position of the raised infant seat in front of the 3dMD Face System.

Figure 2.3: Infant's seat used for the proper sitting of a cleft infant during image capturing.

The image capture time was 1.5 ms. The system captured six 2D images simultaneously for the patient's face, three from each side (right and left); Four black-and-white images were captured with structured light patterns projected on the patient face and two additional colour images. These images were processed directly through the connected computer to obtain a dense 3D facial point cloud (Figure 2.4b). Following this step, a polygonal mesh model was reconstructed from the 3D point cloud, and colour facial textures were mapped to produce the 3D realistic facial model (Figure 2.5).

For the follow-up imaging session, the same 3D device, location and capture protocol were utilised in order to maintain homogeneity of the sample. Two facial expressions were captured at the imaging session. The first image was at rest and the second image was at a maximum smile. At the rest position, the images were captured following the same protocol of the original images before and after surgery. For maximum smiling, the children were instructed to smile according to protocol developed by our research team (Garrahy, 2002; Johnston et al., 2003). The children were verbally asked to say 'cheese' and smile as maximum as they can, while biting their teeth together, this procedure helped in the reproducibility of the smiling. The same procedure was repeated during the image capturing as the children

were tilting their head slightly upward above the midpoint of the two camera pods.

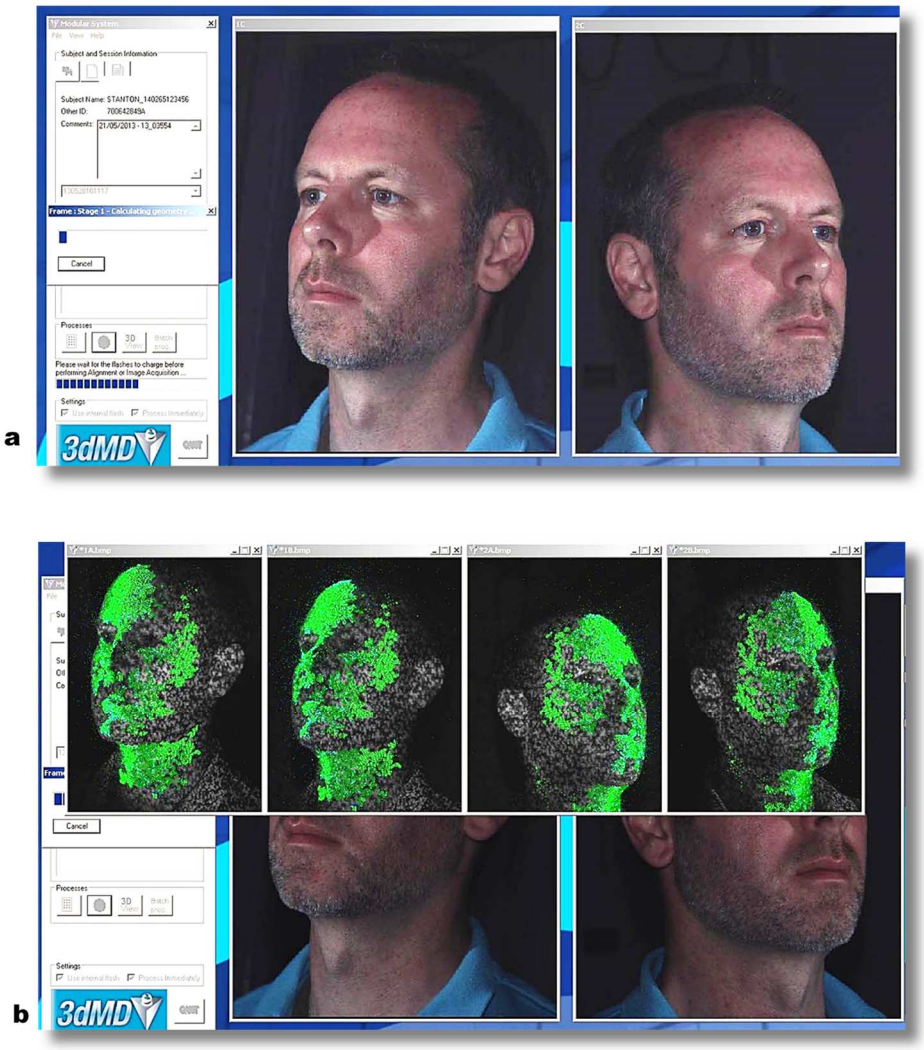

Figure 2.4: a) R and L images of the face seen on the 3dMD frame viewer on the computer screen during image capturing by the system's right and left cameras. (b) Continuous point cloud formed automatically from the four captured images.

Figure 2.5: 3D facial image of a cleft infant, preoperatively (left), postoperatively (middle) and at a 4-year follow-up (right).

2.3 Calibration process

The calibration procedure was carried out each morning before the image capture sessions. During the capture sessions, cautions were taken to avoid any movements of the imaging system, to prevent errors in the 3D images as a result of invalidity of the calibration parameters.

The calibration process was performed with the aid of a calibration board. This board contained dots and a T in the middle. To calibrate the system, two images had to be acquired by holding the calibration board with the "T" letter inverted. In the first image, the board was tilted backwards to 45 degrees, and in the second image, the board was tilted forwards to 45 degrees (Figure 2.6). The subsequent calibration process was performed automatically. The appearance of an error message indicated that the calibration process needed to be performed again.

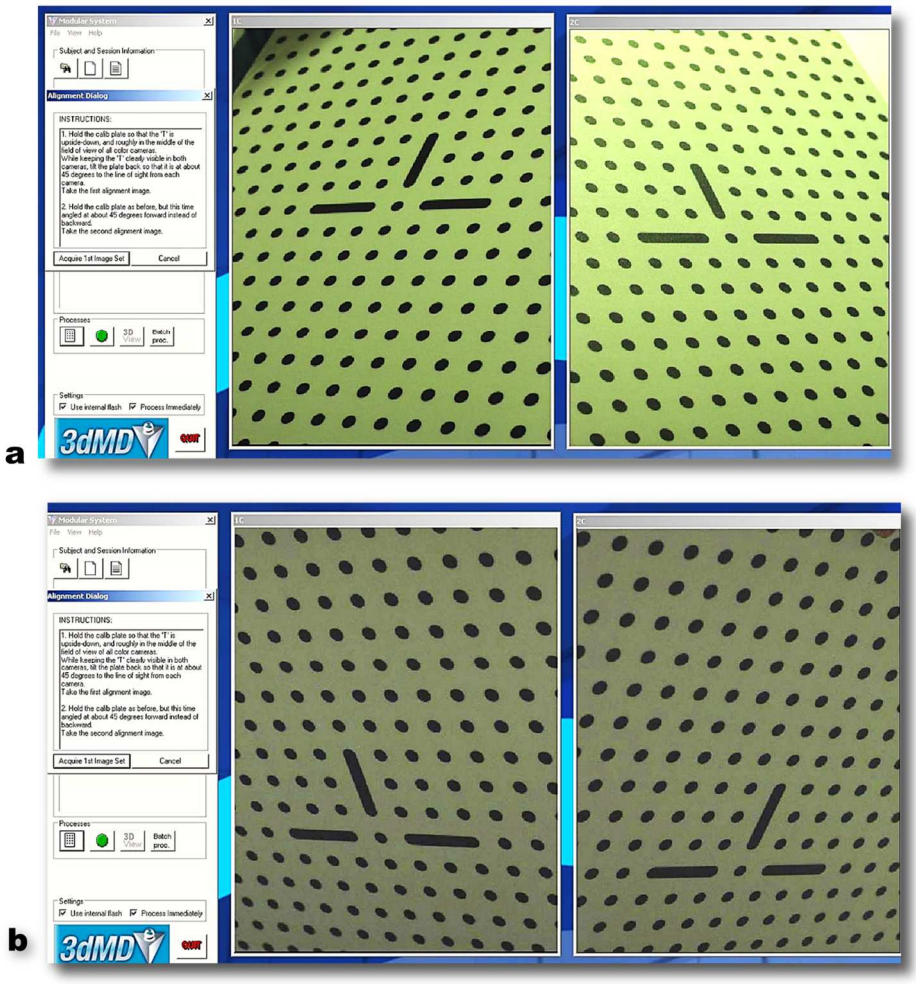

Figure 2.6: Image set of the calibration board by right and left cameras of the system: (a) First image set of tilting board backwards to 45 degrees, (b) Second image set of tilting board forwards to 45 degrees.

2.4 Image transfer

The 3D images were transferred from NHS Lothian network system to Glasgow's Dental School computer using the Secure File Upload "safe haven" (Figure 2.7). An approval was obtained from NHS Lothian to use the "safe haven". An NHS Lothian ID had been created for data access, and an NHS Lothian email and password had been utilised for login to the Secure File Upload web page. Image sets of 30 patients were uploaded to "safe haven", and were downloaded onto a computer at Glasgow Dental School.

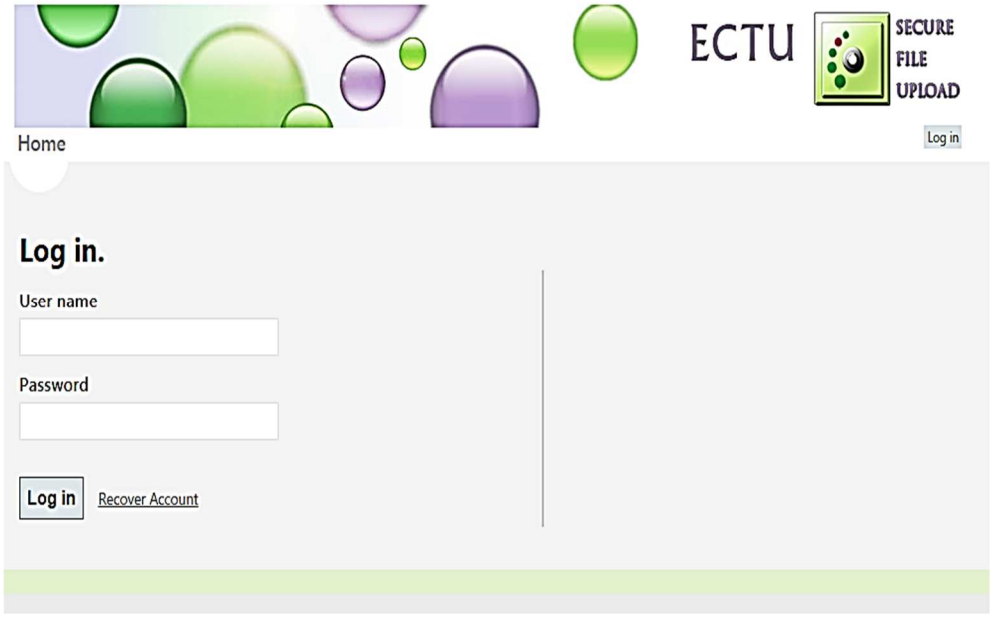

Figure 2.7: Secure File Upload login web page.

2.5 Assessment of facial asymmetry of cleft infants using the Iterative Closest Point (ICP) method

In this part of the study, facial asymmetry of 30 cleft infants before and after surgery was evaluated using ICP algorithm. Each image was imported into the VRMesh software (VirtualGrid, Bellevue City, WA). Image surfaces under the chin region, beyond the anterior border of the ears and hairline, which were of no interest in this study, were removed from the 3D facial image (Figure 2.8) (Mcavinchey,2013).

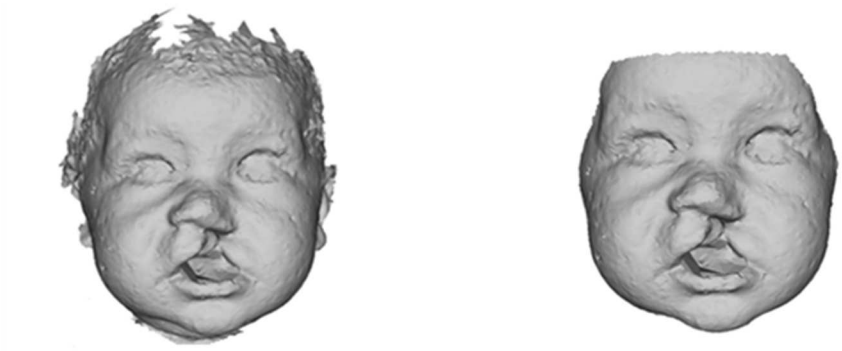

Figure 2.8: Standardised method for trimming unwanted surfaces. Left image: 3D model before trimming unwanted surfaces. Right image: 3D model after the trimming process.

A mirror image of each cropped 3D facial model was created using a lateral reflection plane outside the face (Meyer-Marcotty et al., 2011; Kornreich et al., 2016). In this study, the reflection plane was 150mm away from the centre of the model and perpendicular to the line passing through the right and left exocanthion landmarks of that model (Figure 2.9). Each mirror image was initially superimposed on the original model guided by nine facial

landmarks: R and L exocanthion, R and L endocanthion, pronasale, subnasale, R and L cheilion, sublabialis (Figure 2.10). ICP algorithm was applied to refine the superimposition, and as a perfectly symmetrical face rarely exists in nature, the ICP was set with a 0.5mm tolerance (Primozic et al., 2009; Djordjevic et al., 2013) (Figure 2.11).

A colour map demonstrated the differences in shape between the original and reflected mirror images and identified the discrepancies between the superimposed 3D facial models. The distances between the vertices of the original image to the surface of its mirror model were transferred into an Excel sheet. Facial asymmetry score was measured from the 90th percentile of the absolute distances. These distances would be zero if the face was perfectly symmetrical.

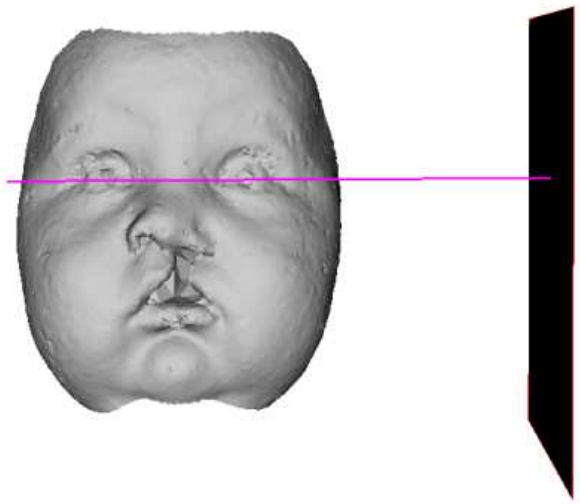

Figure 2.9: Standardisation of the mirroring technique.

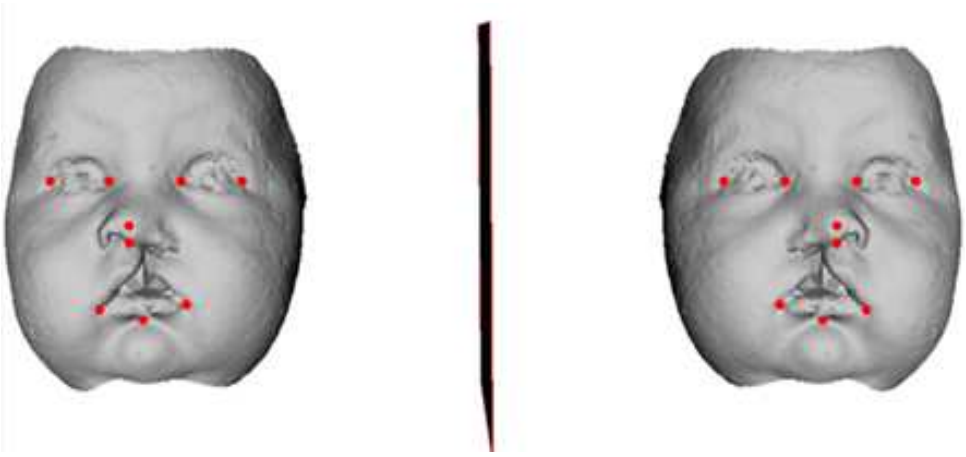

Figure 2.10: Nine facial landmarks for the initial superimposition of the original 3D image (left) and its mirror copy (right).

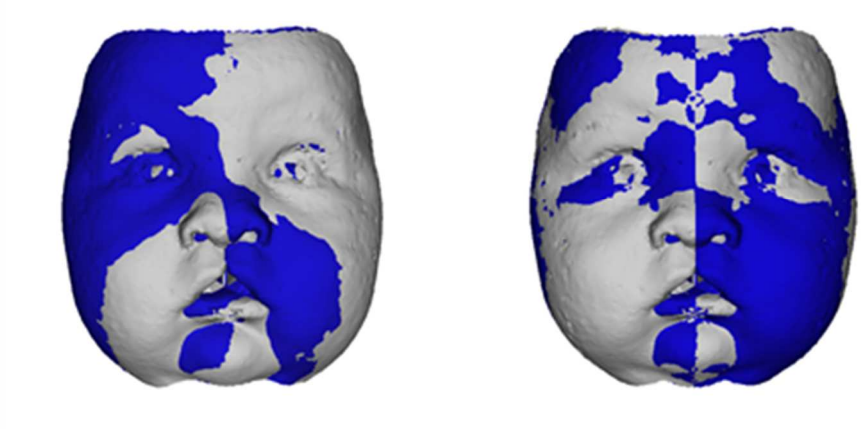

Figure 2.11: Surface-based registration original (grey) and mirror (blue) images. Left image: Initial registration. Right image: ICP registration.

2.5.1 Evaluation of regional facial asymmetry using ICP

The regional facial asymmetry was measured by dividing the original and mirror images into nine anatomical regions (Table 2.1) guided by facial landmarks (Table 2.2) (Farkas, 1994; Kolar and Salter, 1997). The facial regions were: forehead, eyes, nose, upper lip, lower lip, chin and cheeks (Figure 2.12) (Shafi et al. 2013; Naudi et al., 2013; Khambay and Ullah, 2015). A colour map was used to illustrate the magnitude of the 3D asymmetry of the facial regions. The linear distances between the original and mirror images for each facial region were transferred into an Excel sheet. Thereafter, the regional facial asymmetries were measured from the 90^{th} percentile of absolute distances between the superimposed original and mirror images at the respective facial regions.

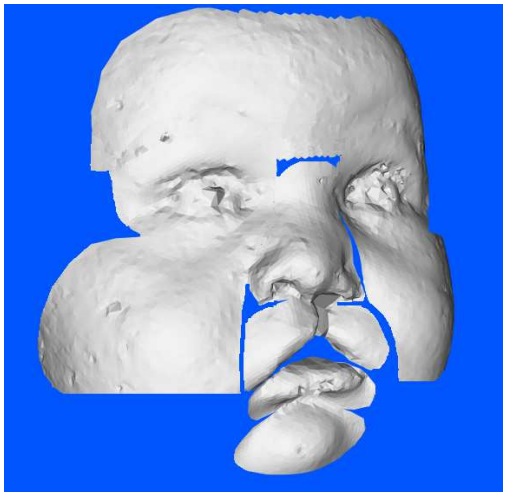

Figure 2.12: Original 3D model divided into facial regions.

2.5.1.1 Errors of asymmetry measurements (reproducibility)

Fifteen 3D facial images were selected randomly from the sample. The same operator re-measured the asymmetry for the complete face and each facial region after two weeks. The 90th percentile of the absolute distances between the original 3D model and the mirror one were calculated for the entire face and for the facial regions.

2.5.1.2 Statistical analysis

The distribution of asymmetry scores was tested for normality. Normality tests (Shapiro-Wilk test and the Kolmogorov-Smirnov test) reject the null hypothesis that the asymmetry scores for each group are derived from a standard normal distribution ($p \leq 0.05$). To detect significant differences between the repeated asymmetry scores, a Wilcoxon Signed-Rank test was utilised. The test was also utilised to detect significant differences between asymmetry scores of the whole face and the facial regions before and after surgery. The significance level was set at 0.05.

Table 2.1: Definitions of divided facial regions guided by facial landmarks, (Farkas, 1994; Kolar and Salter, 1997).

Facial_regions	Definitions of the soft tissue areas
R-cheek	Maxillofrontale(R)_infraorbitale(R)_gonion(R)_cheilion(R)
L-cheek	Maxillofrontale(L)_infraorbitale(L)_gonion(L)_cheilion(L)
Chin	Ch⊥pog(R)_sublabiale_ Ch⊥pog(L)_ gnathion
ULip	Cheilion(R)_subnasale_stomion superioris_cheilion(L)
LLip	Cheilion(R)_stomion inferioris_cheilion(L)_sublabiale
Nose	Alar crest point(R)_subnasale-alar crest point(L)_maxillofrontale(L)_Nasion-maxillofrontale(R)
Forehead	Nasion_superciliare(R)_frontozygomatic(R)_ frontotemporale(R)-trichion-frontotemporale(L)_ frontozygomatic(L)_superciliare (L)
R-eye	Superciliare(R)_maxillofrontale(R)_infraorbitale (R)_frontozygomatic (R)
L-eye	Superciliare (L)_maxillofrontale (L)_infraorbitale (L)-frontozygomatic (L)

Table 2.2: Facial landmarks for dividing the original and mirror images (Farkas, 1994; Kolar and Salter, 1997).

Landmarks	Landmark definition
Nasion(n)	deepest point of the concavity of the bridge of the nose in the midline
Infraorbitale (R and L or)	Point on the lower margin of the orbit at its lowest point
Frontotemporale (R and L ft)	point on the lateral side of the forehead, located lateral to the elevation of the linea temporalis, its position is at the level of the eyebrow end point
Superciliary-(R and L sci)	highest point on the upper margin of the mid portion of the eyebrow
Maxillofrontal-(R and L mf)	Point located at the base of the nasal root. It is close to medial margin of the orbit where the nasofrontal and maxillofrontal sutures meet. It is medial from endocanthion landmark
Frontozygomatic (R and L fz)	most lateral point on the frontozygomatic suture
Gnathion-(gn)	Most inferior point of the chin contour, in midline
Cheilion-(chR and chL)	points at the mouth corner on the labial commissure
Stomion superioris-(stos)	point on the lowermost extent of the vermillion border of the upper lip, in the midline (postoperative only)
Stomion inferioris (stoi)	point on upper margin of vermillion of lower lip, in midline
Cheilion perpendicular at level of pogonion- (R and L Ch⊥pog)	point constructed by intersecting a line that extends from the cheilion perpendicular on a line passing horizontally at the level of the pogonion
Subnasale-(sn)	point of maximum concavity in the midline where the columella base meets the upper lip skin
Gonion-(R and L go)	most lateral point on the mandibular angle close to bony gonion
Trichion-(R and L tr)	point on the hairline on the midline of forehead
Sublabialis-(sl)	point of maximum concavity in the midline between the chin and the lower lip
Alar crest (acR, acL)	most lateral point in the curved baseline of each ala

2.6 Assessment of facial asymmetry using dense correspondence analysis

In this section of the study, a generic mesh was utilised to evaluate facial asymmetry of cleft patients before surgery, after surgery, and at four-year follow-up. It was also utilised to evaluate facial asymmetry of the non-cleft control group.

2.6.1 Generic mesh characteristics

The generic mesh model in this study was a triangular mesh that had a human face shape but without texture (Figure 2.13). Its boundaries extended from the hairline to the submental region vertically and from one ear tragus to the other horizontally. The vertices of the generic mesh were symmetrically distributed, and the sizes of the triangles were uniformly increased from the smallest diameter (0.5mm) in the central zone of the face to approximately 7.5mm at the peripheries. The small triangles accurately illustrated the intricacies of the nasolabial region and gave a clear picture of the corner regions of the mouth and nose. This artificial mesh was precisely constructed by the 3D virtual modality software, DI4D, without defects or holes. The nostril holes, mouth and eyes were filled out. The mesh was in an "obj" file format, and it had to be converted to "wrl" file format to be utilised in the conformation process. This mesh consisted of 7,190 vertices (points), which were indexed.

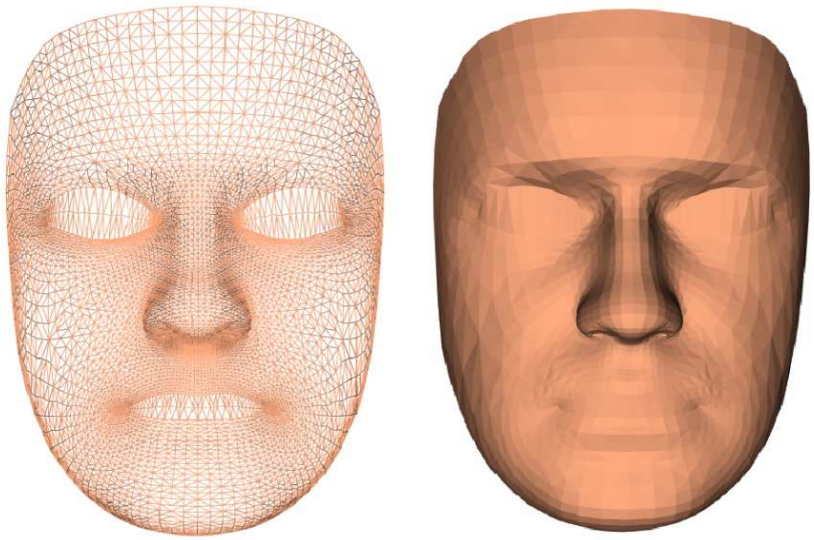

Figure 2.13: Generic facial mesh.

2.6.2 The generic mesh conformation on 3D facial images

The conformation of the generic mesh was performed by an in-house developed software program. This conformation software was developed by Ju and Siebert (2001a, 2001b) and was characterized by multiple 3D imaging tools such as 3D landmarking, 3D image conformation, linear measurements between two 3D surfaces (normal and absolute) as well as providing a colour coded distance map. During the conformation process, the generic mesh is wrapped and fitted on 3D facial images of cleft infants and the control group. This process copied the child's 3D facial shape to the generic mesh (Figure 2.14) and established the anatomical correspondences between the conformed 3D images. Having individually imported the generic mesh and each 3D image into the software, facial landmarks were digitised on the generic mesh and the images and saved in "txt" file format. The sequence of facial landmark digitisation on the image and the mesh was consistent. Subsequently, each postoperative image and the generic mesh were loaded into the software (Figure 2.15), and the landmarks of the postoperative image and the generic mesh were imported from the "txt" files on the image

and the generic mesh. The thin plate spline process was applied on the corresponding landmarks to deform the generic mesh towards the postoperative image. This was followed by an elastic adaptation of the generic mesh surfaces onto the 3D image surfaces. This was a fully automated process which involved a further deformation of the generic mesh onto the surfaces of the 3D image. The final outcome of this step by step process was a conformed mesh that had the shape of the 3D image whilst also maintaining the topology and number of vertices of the original mesh. The postoperative conformed meshes were saved as a "wrl" file. The postoperative meshes were further conformed to the preoperative images. In this procedure, the preoperative image and the postoperative conformed mesh and their landmarks for the same patient were imported into the software (Figure 2.16). The same conformation procedure was repeated and the final preoperative conformed mesh was saved as a "wrl" file.

Figure 2.14: : Postoperative conformed mesh of cleft infant, frontal and 45° lateral views right and left.

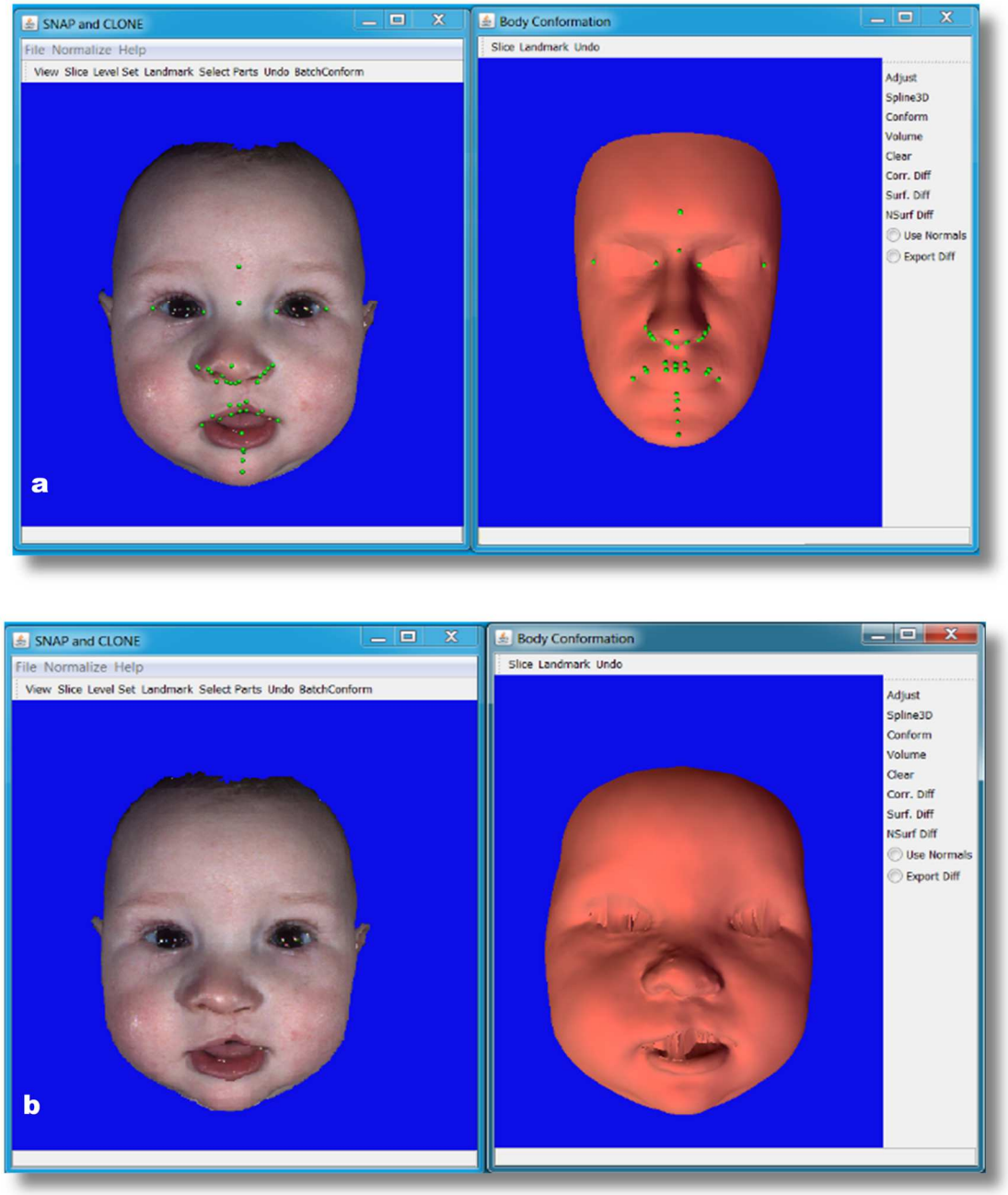

Figure 2.15: Conformation of the postoperative mesh: (a) facial landmarks were imported on the postoperative 3D image and the generic mesh, (b) thin plate spline and conformation processes were applied to obtain the postoperative conformed mesh.

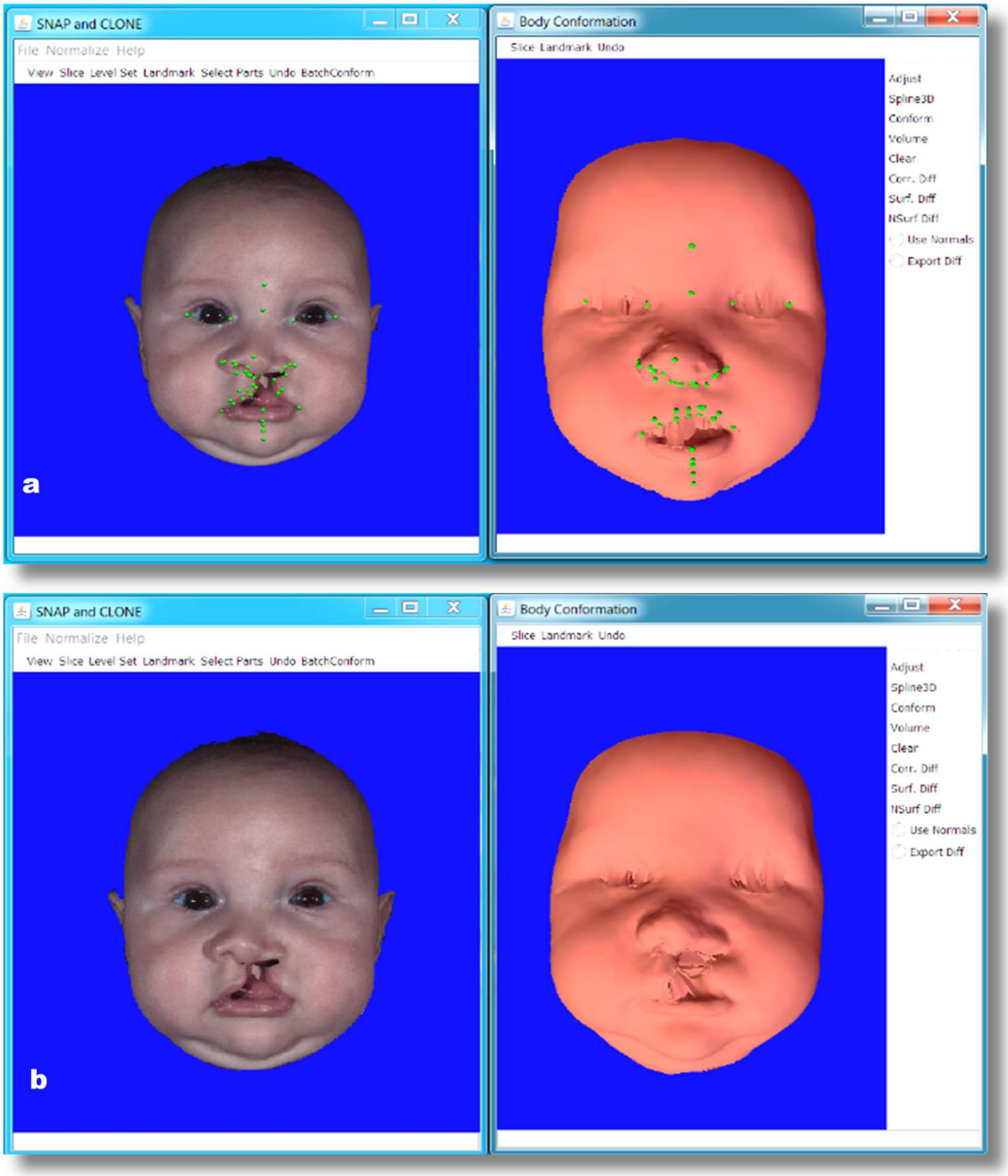

Figure 2.16: Conformation of the preoperative mesh: (a) facial landmarks were imported on the preoperative 3D image and the postoperative conformed mesh, (b) thin plate spline and conformation processes were applied to obtain the preoperative conformed mesh.

2.6.3 Facial landmarks for generic mesh conformation

Table 2.3 and Table 2.4 show the landmarks which were digitised on the generic mesh, preoperative and postoperative images as well as on the facial images of the control group. Thirty-three anatomical facial landmarks (Farkas, 1994; Hood et al., 2004; Hood, 2005; Ayoub et al., 2011a) were digitised. An additional eight facial points were digitised to help the mesh to adapt more on variant morphological features of the upper lip in cleft patients (Table 2.5).

Table 2.6 illustrates additional landmarks and points utilised for the conformation of the preoperative meshes (Hood et al., 2004; Nakamura et al., 2005).

Table 2.3: Facial landmarks of the forehead and mandible used for the conformation of generic mesh (Farkas, 1994; Hood et al., 2004; Hood, 2005; Ayoub et al., 2011a).

	landmark	Landmark definition
Forehead and eyes		
1,2	Exocanthions-(exR, exL)	Point at outer skin junction where the upper lid meets the lower lid, most lateral extent of the lower eyelid
3,4	Endocanthions-(enR, enL)	innermost point at the junction between the upper and lower lids
5	Glabella-(g)	point of maximum convexity in midline of supraorbital ridge.
Chin and mandible		
6	Pogonion-(pg)	most anterior midpoint of the chin
7,8	Gonion-(goR, goL)	most lateral point on the mandibular angle
9	Sublabialis-(sl)	point of maximum concavity in the midline between the lower lip and the chin

Table 2.4: Facial landmarks of the nose and lips used for the conformation of generic mesh (Farkas, 1994; Hood et al., 2004; Hood, 2005; Ayoub et al., 2011a).

	landmark	Landmark definition
Nose		
1	Subnasale-(sn)	point of maximum concavity in the midline where the columella base meets the upper lip skin
2	Pronasale-(prn)	most protruded point of the apex nasi
3,4	Subalare-(sbalR, sbalL)	point at the lower limit of each alar base where it joins the skin of the upper lip
5,6	Alar crest-(acR, acL)	most lateral point in the curved baseline of each ala
7,8	Alare-(alR, alL)	most lateral point on alar contour
9,10	Alare inner-(al0iR, al0iL)	midpoint on the inner margin of the nostrils between the sbal and c
11,12	Alar outer-(al0oR, al0oL)	point on the outer ala, opposite the al0i point
13,14	Columella-(cR, cL)	highest point on the columella where the nostril starts to curve round
15,16	Edge of columellar base-(sn0R,sn0L)	narrowest and lowest point of columella on inner nosrtril margin/ most lateral aspect of columella
17	Nasion-(n)	deepest point of the concavity of the bridge of the nose in the midline
Lips		
18,19	Cheilion-(chR, chL)	points at the corner of the mouth on the labial commissure
20,21	Crista philtri-(cphR, cphL)	points on each elevated margin of the philtrum just above the vermilion line
22	Labiale-superius (ls)	point at maximum concavity of the philtrum; at the junction of the white roll and the vermillion border of the upper lip
23	Stomion-inferioris (stoi)	point on the upper margin of the vermillion of the lower lip in the midline
24	Labiale inferius-(li)	midpoint of lower vermilion border

Table 2.5: Facial points used for the conformation of generic mesh.

	Facial points	Definition
1,2	Upper lip lateral point mlR, mlL	midpoint located on the vermillion of the upper lip between ch and cph. On the preoperative cleft side, it is located between ch and cph"
3,4, 5,6, 7	Vermillion points of the upper lip (v1R, v1L), (v2R, v2L), (v3)	points on the lower margin of the vermillion of the upper lip which are perpendicularly opposing the ml, cph and ls respectively.
8	Midpoint on the chin	midpoint located between sl and pg

Table 2.6: Additional facial landmarks and points used for conformation of the preoperative images (Hood et al., 2004; Nakamura et al., 2005).

	Landmark and points	definition
1	Crista philtri on major segment (cph')	point on vermillion on major segment, same distance from cph-ls on non-cleft side (preoperative only)
2	Crista philtri on minor segment(cph")	point on vermillion on minor segment, adjacent to cleft, same distance from ch-cph on non-cleft side (preoperative only)
3,4	S1 and S2	points located on the scar tissue of the nostril floor, at midpoint between sbal and c (postoperative only)
5	Cleft margin major (CM)	Point on most lateral superior margin of major segment (preoperative only)
6	Cleft margin minor (CM'')	Point on most medial superior margin of minor segment (preoperative only)

2.6.4 Reproducibility of the conformation process

To evaluate the reproducibility of the conformation process, the conformation of 15 randomly selected postoperative images and 15 randomly selected preoperative images were repeated after an interval of one month. The conformed models were saved in "wrl" files. The reproducibility was evaluated by calculating the mean of distances between the corresponding vertices (points) of the repeated preoperative and postoperative conformed meshes. To measure the error in the three directions (X, Y and Z), the mean of absolute differences between the corresponding points of the repeated preoperative and postoperative conformed meshes were calculated in each direction. Colour map, utilising colour ranged from dark blue to red, illustrated the mean of the distances between the corresponding points of the repeated preoperative and postoperative conformed meshes. In a coded scale from zero to 3mm, the colours changed gradually from dark blue, blue and sky blue to green, yellow, orange and red to represent zero, 0.50 (mm), 1.0 (mm), 1.50 (mm), 2.0 (mm), 2.50 (mm) and 3.0 (mm) respectively. A One-Sample Wilcoxon Signed-Rank test was utilised to test the hypothesis that the absolute differences between the corresponding points in the three directions was larger than 0.5mm for the preoperative and postoperative repeated conformation.

2.7 The application of generic mesh for facial asymmetry assessment

The conformed meshes represent the facial morphology of the set of images of UCLP patients and the control group with the same number of vertices. Dense correspondence analysis was applied to evaluate facial asymmetry utilising these conformed meshes and the in-house developed software program. In order to assess facial asymmetry two methods were employed. The first was to evaluate the average total facial asymmetry and the second was to analyse the individual total face and regional facial asymmetries.

2.7.1 Evaluation of the average total facial asymmetry using the generic mesh

In this method, the average facial asymmetry of cleft patients (before surgery, after surgery and at four-year follow-up) and the average facial asymmetry of the control group were evaluated by constructing an average 3D face for each group. The average facial models were created using the conformed meshes related to each group. Partial Procrustes Analysis (PPA) was applied for averaging the conformed meshes of each group utilising the corresponding vertices (points). Five average faces were constructed: (1) average face of cleft infants before surgery, (2) average face of cleft infants after surgery, (3) average face of cleft children in a resting facial position four years after surgery, (4) average face of cleft children four years following surgery in a maximum smiling position and (5) average face of six-month old non-cleft infants. A mirror image was created for each average face by reflecting it on an arbitrary lateral plane. Each original average mesh was superimposed on its mirror copy. Whilst the generic mesh was indexed to identify for each point (vertex) on the original mesh a corresponding point on its mirror one, Partial Procrustes Analysis (PPA) was applied to minimise the

distances between the corresponding vertices of the original average model and the mirror one. The average facial asymmetry was calculated by measuring the distances between the corresponding points of the original average mesh and the mirror copy. The asymmetry was exhibited in a colour map from blue to red. A scale was coded from 0 to 5mm with colour graduation evolving from dark blue, blue and sky blue to green, yellow, orange and red signifying the distances between the corresponding surfaces of the original average mesh and the mirror one which increased from 0 to 5 mm. In perfect symmetry, the asymmetry would be zero and displayed in a dark blue colour.

The asymmetry was also analysed in three directions by measuring the differences between the corresponding points of the original average mesh and the mirror copy in horizontal (X), vertical (Y) and anteroposterior (Z) directions. These were presented in colour maps; The asymmetry to the right side (X direction), in upward (Y) direction or in forward (Z) direction were exhibited by red. Blue highlights signified asymmetry to the left side (X direction), downward (Y) direction or backward (Z) direction. Finally, green indicated minimal asymmetry.

2.7.2 Quantification of the individual total face asymmetry and regional facial asymmetry

Asymmetry scores were calculated for the total face, nose and upper lip regions for each cleft case and for each of the non-cleft control cases. Total face asymmetry was calculated by creating mirror image for each conformed mesh by reflecting it on an arbitrary lateral plane using the in-house developed software. PPA was applied for the alignment of each original mesh and its mirror copy to minimise the distances between the corresponding points. The asymmetry scores were calculated by measuring the mean of distances between the corresponding vertices of the original mesh and the

mirror mesh for each case in millimetres. The asymmetry scores were also calculated in three directions (X, Y and Z) by measuring the mean of absolute differences (in millimetres) between the corresponding vertices of the original mesh and the mirror copy in the three directions.

To quantify the regional asymmetries, the nose and upper lip regions were extracted from the generic mesh (Figure 2.17) by facial landmarks using VRMesh software. Nasion (n), maxillofrontale (fmR, fmL), alar curvature (acR, acL) and subnasale (sn) defined the boundaries of the nose. Cheilion (chR, chL), subalare (sbalR, sbalL) and subnasale (sn) defined the boundaries of the upper lip. Based on the superimposition of the original face and its mirror face, the mean of distances between the corresponding points for each facial region was calculated. The asymmetry scores were also calculated in three directions (X, Y and Z) by measuring the mean of absolute differences between the corresponding vertices of the original and mirror meshes in the three directions.

2.7.2.1 Statistical analysis

The distribution of asymmetry scores among each of the study groups (control and cleft) was tested for normality. The normality tests (Shapiro-Wilk test and the Kolmogorov-Smirnov test) reject the null hypothesis that asymmetry scores for each group derived from a normal distribution ($p \leq 0.05$). A Wilcoxon Signed-Rank test was applied to compare the differences between asymmetry scores of the total face and each facial region before and after surgery, after surgery and at four-year follow-up, and between rest and maximum smile. The same test was employed to compare the differences between asymmetry scores across the groups in the three directions (X, Y and Z). A Wilcoxon Rank-Sum test was utilised to compare the differences between the control group and surgically managed cleft patients, and also to compare the difference in X, Y and Z directions.

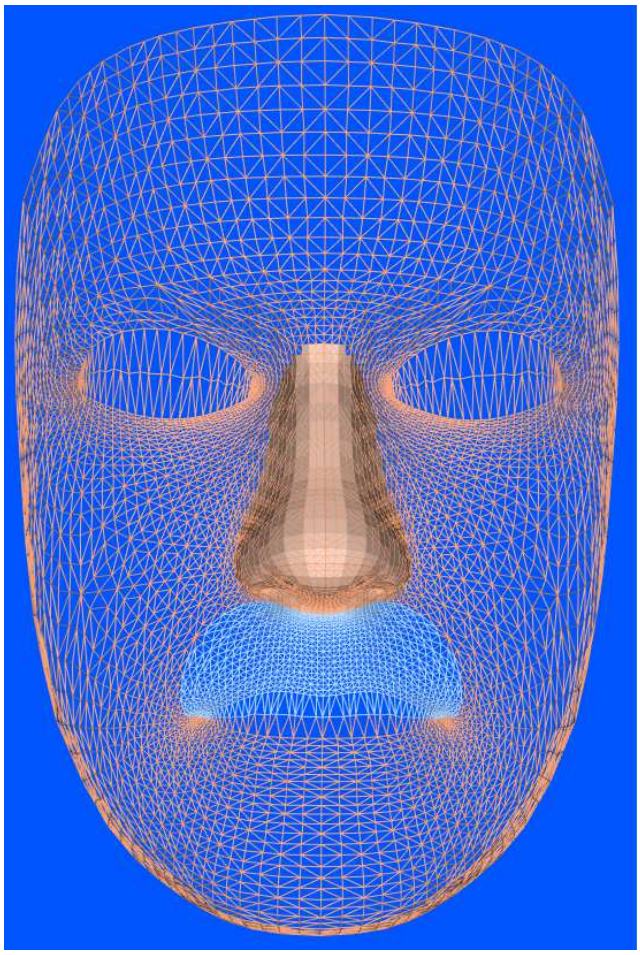

Figure 2.17: The nose and upper lip regions were extracted from the generic mesh.

2.7.2.2 The categorization of asymmetry scores of the control group and the surgically managed cleft patients in relation to perfect symmetry

The asymmetry scores for the nose and upper lip of the control group and surgically managed cleft group were divided into five categories. This was based on the deviations of the asymmetry scores from perfect symmetry (van Loon et al., 2011), which is equal to zero. The first category included these

with asymmetry scores ≤ 0.5; the second category included these with asymmetry scores > 0.5 and ≤ 1; the third category included these with asymmetry scores of > 1 and ≤ 2. The fourth and fifth categories included these with asymmetry scores of > 2 and ≤ 3, and > 3 respectively. The percentage of the cases within each category was calculated.

2.8 Relationship between initial severity of cleft lip and residual postoperative dysmorphology

Four ratios were used to measure the initial severity of cleft lip: nostril base width ratio, nostril length ratio, philtrum height ratio and median cleft width ratio. The ratios of nostril base width, nostril length, philtrum height were obtained from the measurements between the 3D landmarks on the cleft side and non-cleft side (Hood, 2005) (Table 2.7). The median cleft width ratio was obtained by calculating the mean of the superior and inferior cleft width divided by the mouth width (Schwenzer-Zimmerer et al., 2008b) (Table 2.7). These ratios were obtained using Di3Dview software. Each image was imported individually to the software, the landmarks were digitised and the ratios were obtained using the available measurement tool.

In addition to the four ratios, preoperative asymmetry scores of the nose and the upper lip represented the severity of initial dysmorphology of the upper lip and the nose.

In order to measure the postoperative and four-year follow-up residual deformities, postoperative nose and upper lip asymmetry scores were assessed.

Table 2.7: Ratios of cleft severity.

Ratio	Distances
Nostril base width ratio	sbal-sn0 **cleft**/ sbal-sn0 **noncleft**
Nostril length ratio	sbal-c **cleft**/ sbal-c **noncleft**
Philtrum height ratio	sn0-cph' **cleft**/ sn0-cph **noncleft**
Medial cleft width ratio	Mean of superior and inferior cleft width*/ mouth width chR-chL *superior cleft width is the distance between CM and CM'', Inferior cleft width is distance between cph' and cph''

*landmarks' definitions are in Table 2.4 and Table 2.6

The reproducibility of landmarks' digitisation was assessed by re-digitising the landmarks of 15 randomly selected preoperative images after two weeks interval by the same operator. The distances between the repeated digitisation of the same landmarks were measured.

The relationships between asymmetry scores of the total face, nose and upper lip were assessed within and between each study group, before surgery, after surgery and at the four-year follow-up, using Spearman correlation coefficient. The significance level of the correlation test was set at 0.05.

The relationships between the four ratios of initial severity of cleft lip (nostril base width, nostril length, philtrum height and median cleft width) and asymmetry scores before, after surgery and at four-year follow-up were assessed using Spearman correlation coefficient. The significance level of the correlation test was set at 0.05.

Chapter three

Results

3 Chapter three: Results

3.1 Study sample

The mean age of the 30 cleft infants prior to surgery was 3.7 ± 0.8 months, and 8.4 ± 1.8 months after surgery. In terms of long-term follow-up, the mean age of the 15 cleft patients was 4.2 ± 1.1 years.

3.2 Evaluation of facial asymmetry using ICP method

3.2.1 Errors of asymmetry measurements (reproducibility)

Table 3.1 shows there were no statistically significant differences between the repeated measurements of asymmetry scores of the whole face, and for each facial region (p-value >0.05).

3.2.2 Facial asymmetry of the whole face and for each facial region

Table 3.2 shows the descriptive statistics and the p-values from the Wilcoxon Signed rank test of the ninety percentile of absolute distances of the whole face and for each facial region before and after lip repair. The impact of surgery was significant in the regions of the upper lip and nose ($p<0.001$), the analysis of the results indicates that the symmetry of these regions has improved significantly. Likewise, the symmetry of the whole face showed a statistically significant improvement after surgery. Interestingly, the symmetry of the cheeks was also significantly improved ($p<0.05$) following the surgical repair of cleft lip (Figure 3.1, Figure 3.2). The changes in asymmetry scores after lip surgery were not significant in the lower lip, forehead and chin regions.

Table 3.1: Asymmetry measurement errors (in mm) for the whole face and for the anatomical regions.

Facial region	Median difference	Min diff.	Max diff	P-value
Whole face	0.001	-0.040	0.091	0.865
Nose	-0.001	-0.016	0.027	0.394
Upper lip	0.001	-0.029	0.034	0.427
Checks	0.001	-0.022	0.039	0.691
Lower lip	-0.002	-0.040	0.061	0.156
Eye	0.002	-0.051	0.044	0.472
Forehead	-0.006	-0.099	0.060	0.469
Chin	-0.001	-0.013	0.079	0.91

Table 3.2: The ninety percentiles of absolute distances (in mm) between the original and mirror models for the entire face and for the anatomical facial regions.

Facial regions	Before surgery			After surgery			
	Median	Min	Max	Median	Min	Max	P-value*
Whole face	0.63	0.33	1.36	0.55	0.27	0.92	**0.002**
Nose	1.81	0.65	4.06	0.67	0.46	2.75	**0.000**
Upper lip	2.53	0.70	3.13	1.09	0.54	2.44	**0.000**
Lower lip	0.80	0.32	2.57	0.79	0.30	1.18	0.544
Chin	0.69	0.27	1.44	0.57	0.13	1.22	0.185
Forehead	0.59	0.22	1.69	0.53	0.21	1.16	0.254
Cheeks	0.97	0.48	2.24	0.86	0.32	1.89	**0.016**
Eyes	0.65	0.25	1.57	0.56	0.23	1.12	0.614

*bold indicates significant differences.

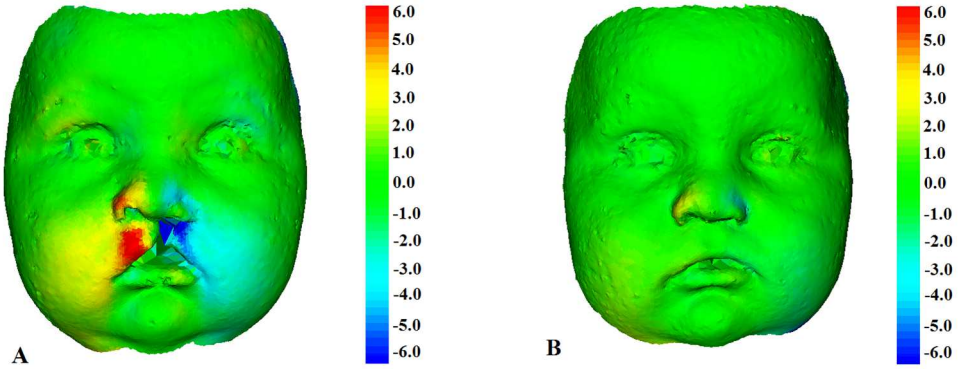

Figure 3.1: Colour maps showing 3D facial asymmetry of UCLP infant (A) preoperatively (B) postoperatively.

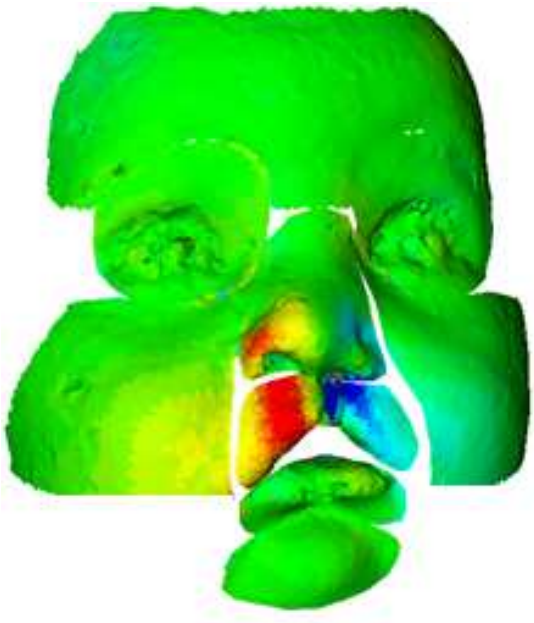

Figure 3.2: Colour map showing the pattern of magnitude of facial asymmetry on facial regions preoperatively.

3.3 Evaluation of facial asymmetry using dense correspondence analysis

3.3.1 Reproducibility of the conformation process

The total error was 0.71mm and 0.60mm for the conformation of the preoperative and postoperative images respectively, with the errors ranging from 0.56mm to 1.00mm for the conformation of preoperative images and from 0.42mm to 0.73mm for the conformation of the postoperative images. Colour maps in Figure 3.3 and Figure 3.4 illustrate the average errors for the conformation process on the preoperative and postoperative images respectively. The nasolabial region exhibited mean error ranging from 0 to 0.5mm, with the peripheries of the mesh registering the highest errors. Table 3.3 shows the median of absolute difference in three directions (X, Y, and Z) of the corresponding vertices of the repeated conformed meshes of the preoperative and postoperative images. The errors for the conformation of the preoperative images were 0.36mm, 0.31mm, and 0.33mm in X, Y and Z directions respectively, and the errors of the conformation of the postoperative images were 0.33mm, 0.28mm, and 0.29mm in the three directions respectively. The errors of the repeated conformation in the three directions were significantly less than the accepted clinically detectable error 0.5mm ($p<0.01$) (Table 3.3).

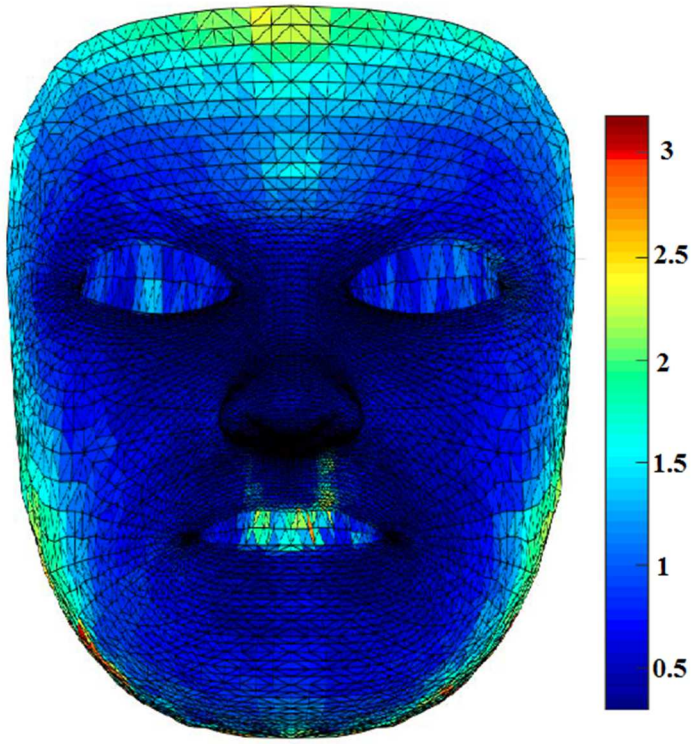

Figure 3.3: Colour map showing the mean errors (in mm) for the conformation process of preoperative meshes.

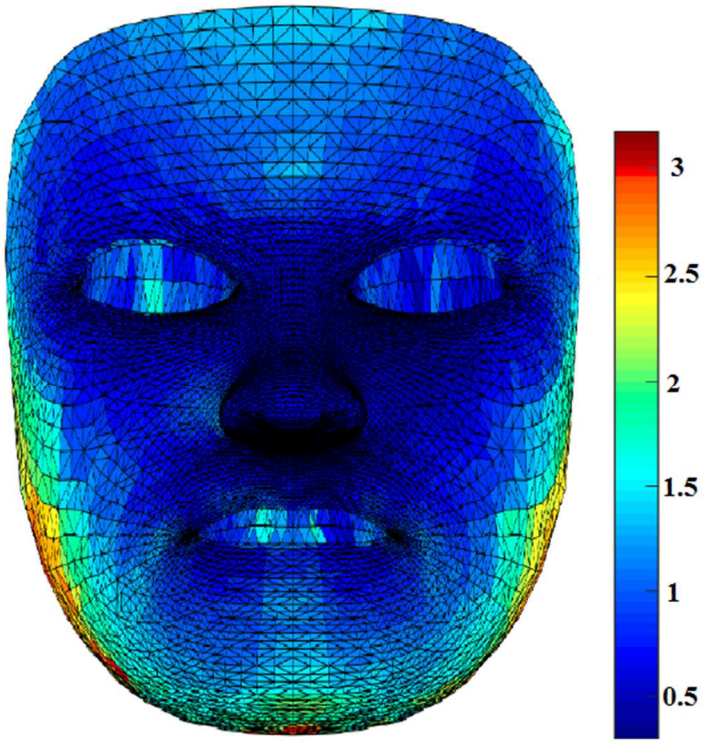

Figure 3.4: Colour map showing the mean errors (in mm) for the conformation process of postoperative meshes.

Table 3.3: Descriptive statistics and p-values of the errors of the conformation process in X, Y and Z directions.

	Preoperatively			*p-value**	Postoperatively			*p-value**
	Median	***Min***	***Max***		***Median***	***Min***	***Max***	
X-direction	0.36	0.26	0.69	**0.003**	0.33	0.20	0.39	**0.000**
Y-direction	0.31	0.27	0.40	**0.000**	0.28	0.19	0.36	**0.000**
Z-direction	0.33	0.26	0.40	**0.000**	0.29	0.20	0.34	**0.000**

*bold indicates significant differences.

3.3.2 Average facial asymmetry

3.3.2.1 The average facial asymmetry before surgery

The average pre-surgical facial asymmetry is illustrated in Figure 3.5. The red colour in the nasolabial region represents the ultimate asymmetry at the upper lip and the nose before primary lip surgery. The maximum asymmetry is demonstrated by the dark red colour at the columella, vermillion and philtrum of the upper lip that was more than 5mm. The intensity of the redness has progressively decreased towards the nostrils and tip of the nose which indicates a decreased in the asymmetry in these regions.

The asymmetries in horizontal, vertical, and anteroposterior directions are demonstrated in Figure 3.6; Figure 3.7; Figure 3.8 respectively. The dark blue colour at the philtrum of the upper lip and the columella indicates the maximum deviation toward the non-cleft side, >5m. This asymmetry gradually decreased toward the alar cartilage (blue to sky blue colours, -3mm to -1mm) (Figure 3.6). Vertically, the maximum asymmetry was recorded at the upper lip on the cleft side. Unlike the lip, the nose did not demonstrate vertical deficiency on the affected side, and the sky-blue colour was noted on the nares of the cleft side, signifying its' downward positioning (Figure 3.7). In the anterior-posterior direction, the upper lip, alar base and paranasal area displayed the highest anteroposterior asymmetry, whereas none was recorded at the columella and the bridge of the nose (Figure 3.8).

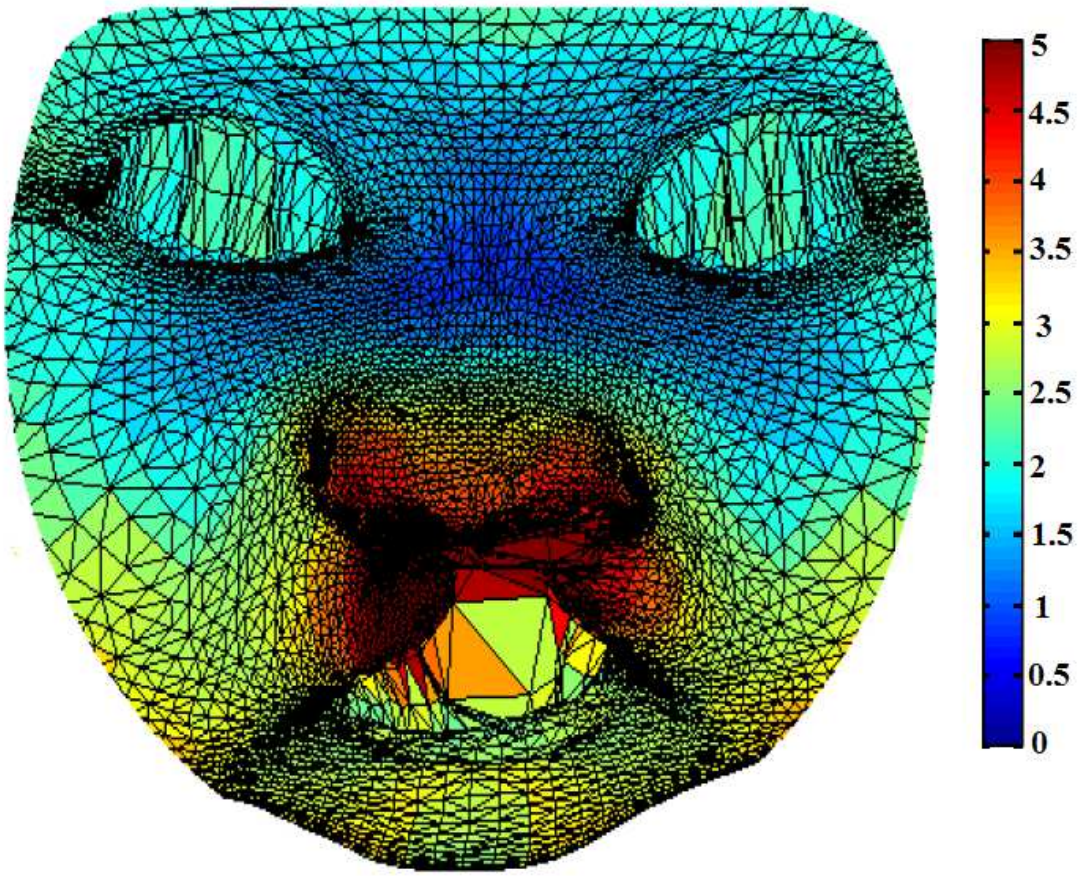

Figure 3.5: Colour map of average asymmetry of cleft patients before surgery. The dark red colour indicates > 5mm distance between the corresponding points (maximum asymmetry). Zero distance between the corresponding points (symmetry) is exhibited in dark blue colour.

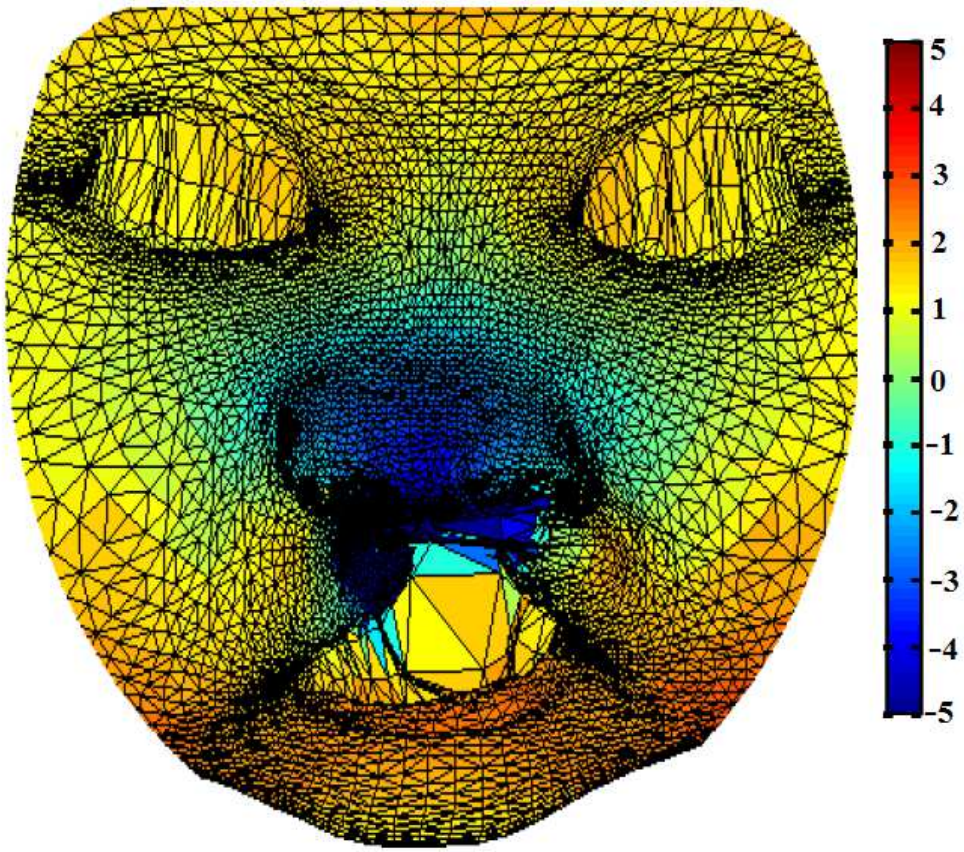

Figure 3.6: Colour map of average mediolateral asymmetry of cleft patients before surgery (X direction). The dark blue colour indicates a maximum shifting to the non-cleft side (> 5mm). The dark red colour indicates maximum shifting to the cleft side. Zero shifting is exhibited in green (symmetry).

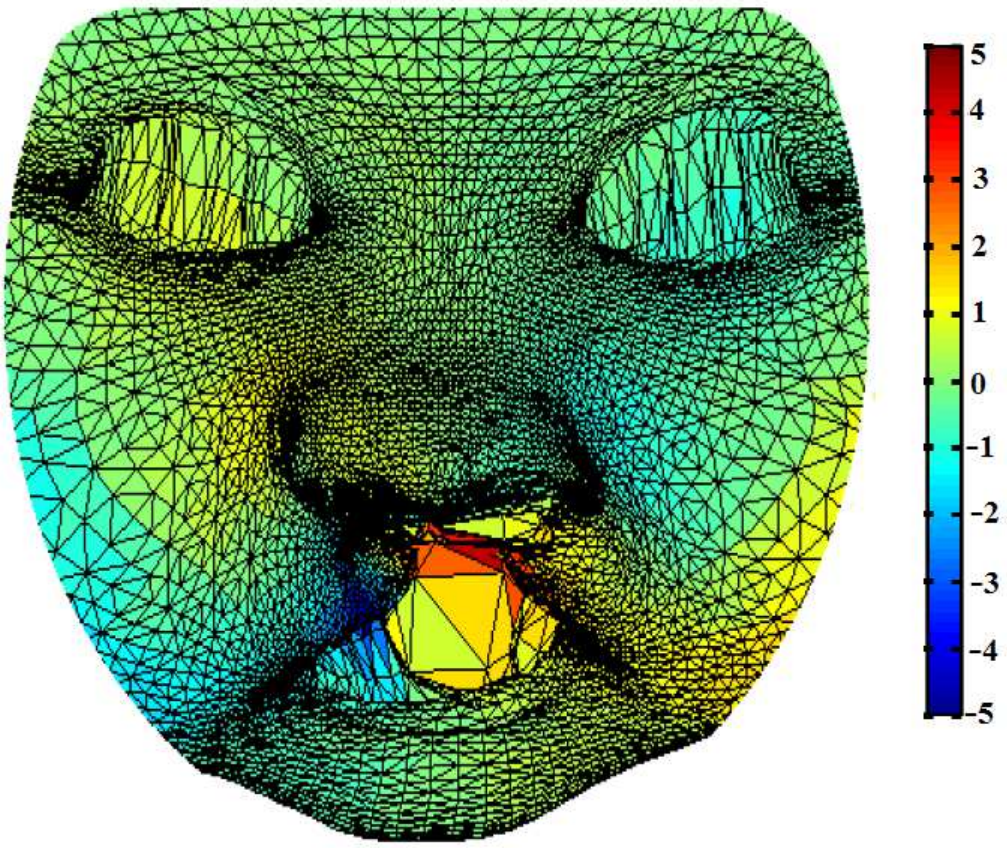

Figure 3.7: Colour map of average vertical asymmetry of cleft patients before surgery (Y direction). The dark blue colour indicates maximum asymmetry in a downward direction. The dark red colour indicates a maximum asymmetry in upward direction (> 5mm). Zero symmetry is represented by green colour (symmetry).

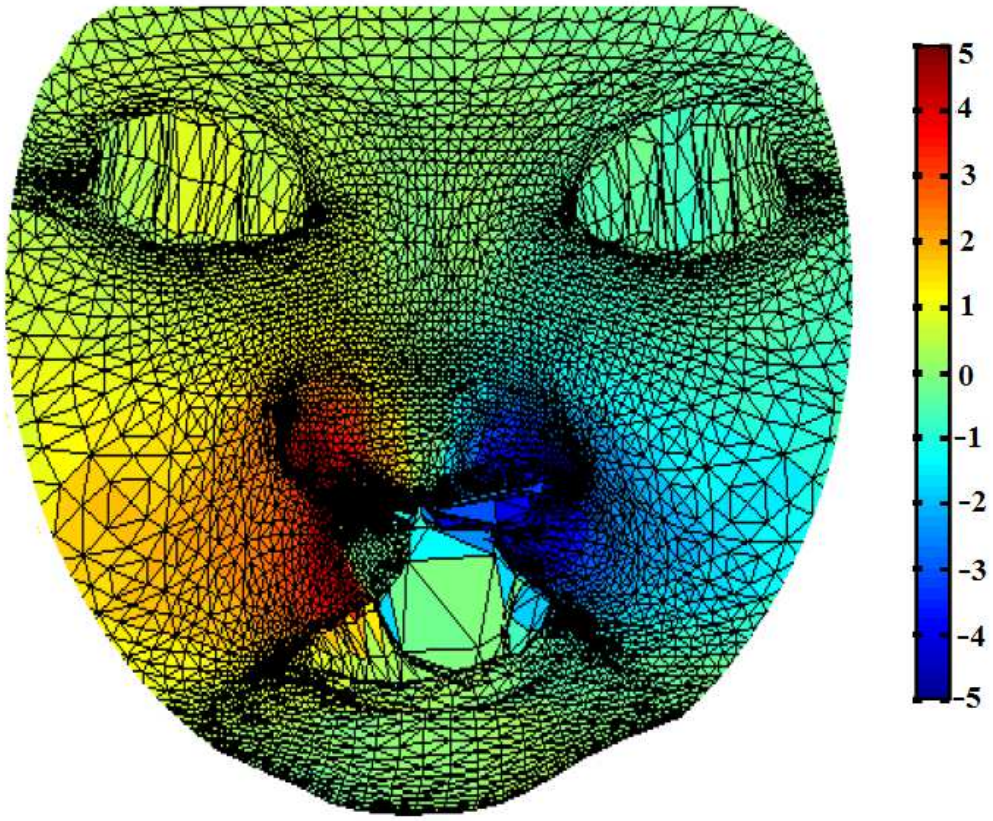

Figure 3.8: Colour map of average anteroposterior asymmetry of cleft patients before surgery (Z direction). The dark blue colour indicates maximum asymmetry in backwards direction. The dark red colour indicates maximum asymmetry in forward direction (> 5mm). Anterioposterior symmetry is indicated by green colour.

3.3.2.2 The average facial asymmetry after surgery

After surgery, significant improvement of facial symmetry was noticed (Figure 3.9). However, residual postoperative asymmetries were recorded at the nasal cartilage and the tip of the nose. Mediolaterally (Figure 3.10), the light blue colour of the nose indicates its shifting towards the non- cleft side (right side) postoperatively. The orange colour of the cupid's bow and the yellow colour of the philtrum of the upper lip denote their shifting towards the cleft side (left side). Vertically, residual asymmetry was noted on the cleft side at the mouth corner (yellow colour) (Figure 3.11). Additionally, the sky-blue colour at the alar cartilage on the cleft side indicates its downward position in comparison to the non-cleft side. The anteroposterior deficiencies were noticed at the alar base, paranasal area and upper lip of the cleft side (Figure 3.12; Figure 3.13)

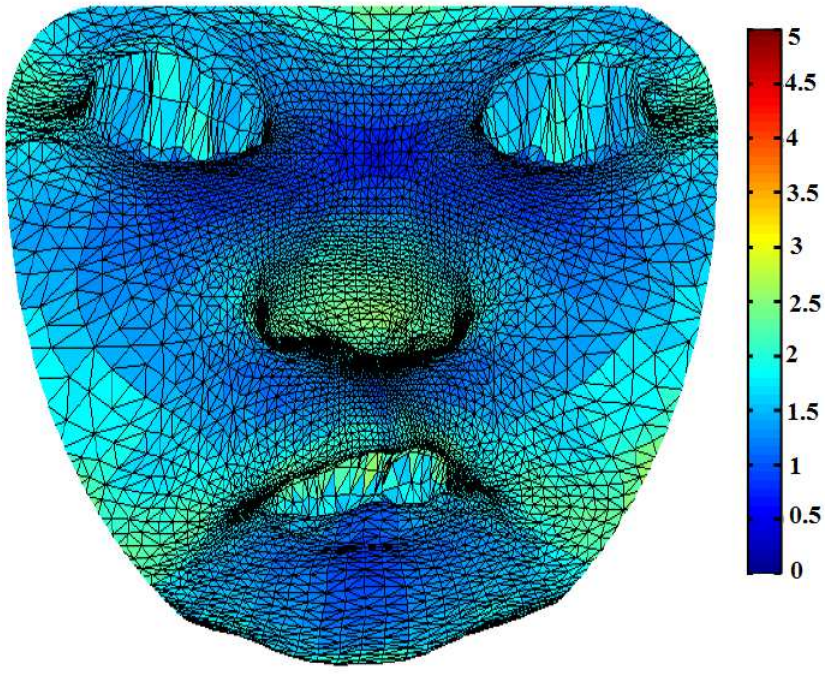

Figure 3.9: Colour map of average asymmetry of cleft patients after surgery.

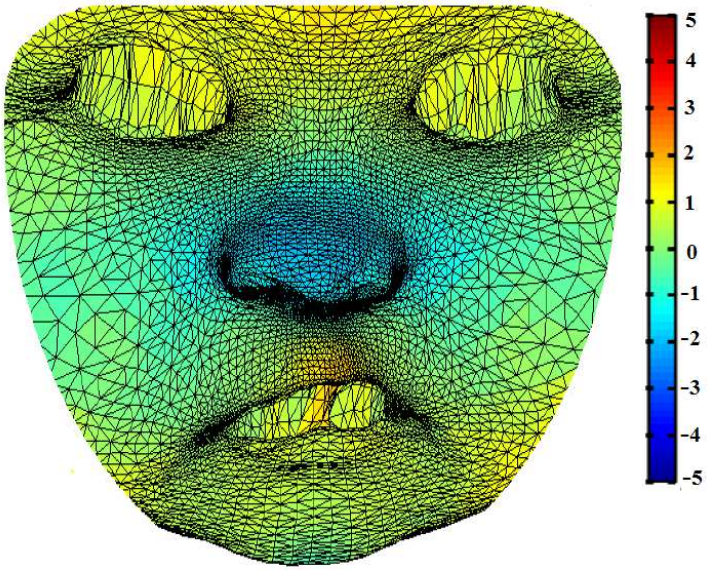

Figure 3.10: Colour map of average mediolateral asymmetry of cleft patients after surgery. The philtrum deviated toward the cleft side (left side) (yellow-orange colour). The blue colour indicates a shifting of the nose to the non-cleft side.

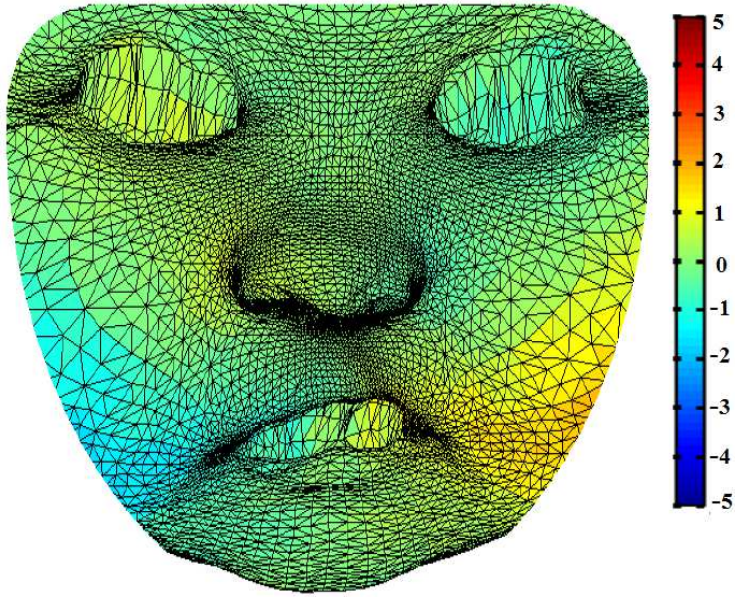

Figure 3.11: Colour map of average vertical asymmetry of cleft patients after surgery (Y direction). Vertical shortening can be noticed on the cleft side at the mouth corner (yellow colour).

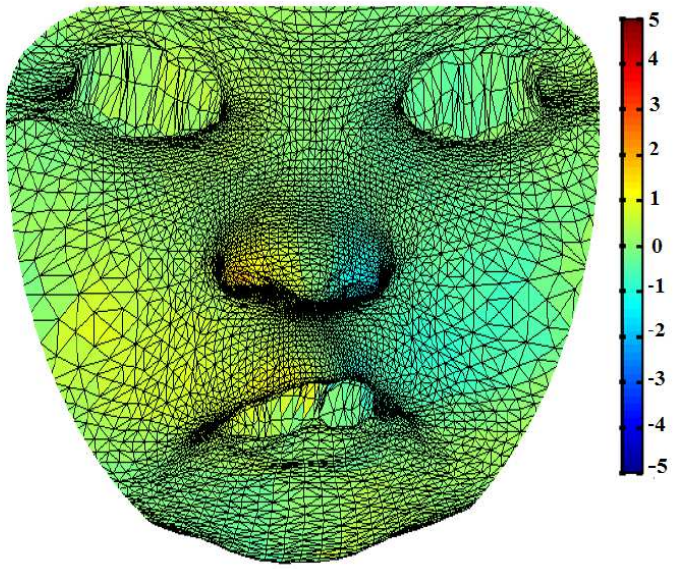

Figure 3.12: Colour map of average anteroposterior asymmetry of cleft patients after surgery (Z direction).

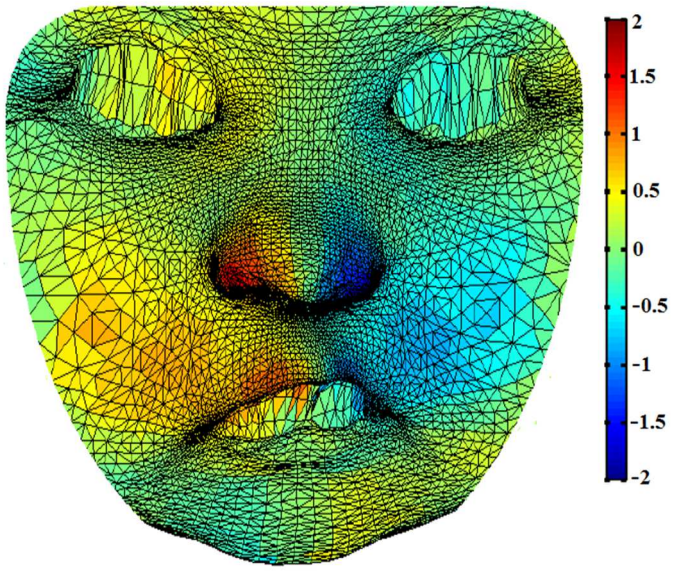

Figure 3.13: Colour map of average anteroposterior asymmetry of cleft patients after surgery (Z direction). The coloured bar is set in a way that the blue colour indicates asymmetry of > 2mm in a backwards direction. The dark red colour indicates asymmetry of > 2mm in a forward direction. Symmetry is exhibited in green colour.

3.3.2.3 Average facial asymmetry for the control group

The average facial asymmetry of the control group is illustrated in Figure 3.14). The facial symmetry trends of non-cleft infants were indicated in blue. The nasolabial region is the most symmetrical region (< 0.5 mm, shown in dark blue). Facial asymmetry increased towards the peripheries. Asymmetry of the face in mediolateral (X) direction is demonstrated in Figure 3.15; the yellow colour at the tip of the nose and the philtrum of the upper lip represents a deviation to the left side of the face. Figure 3.16 illustrates the asymmetry in vertical (Y) direction; the green colour indicates vertical symmetrical regions of the face, the yellow colour of the right alar indicates a vertical deficiency in the right side of approximately 1mm. The anteroposterior (Z) direction was the most symmetrical. The green colour illustrates the symmetry in the control subjects (Figure 3.17).

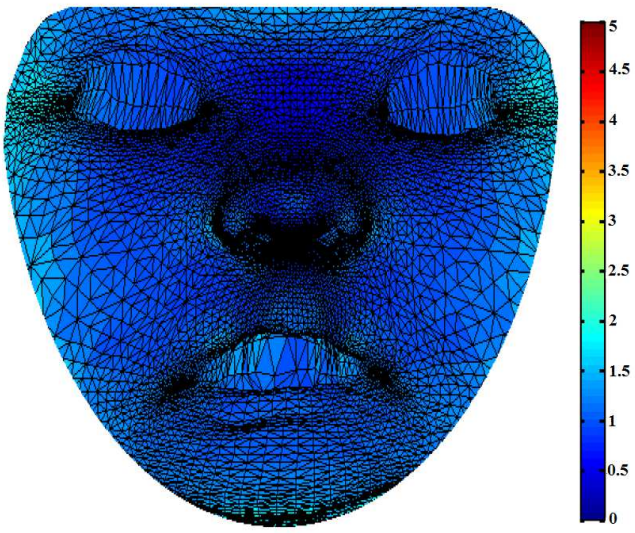

Figure 3.14: Colour map of average asymmetry of the non-cleft control group. The blue colour represents minimum asymmetry (symmetry).

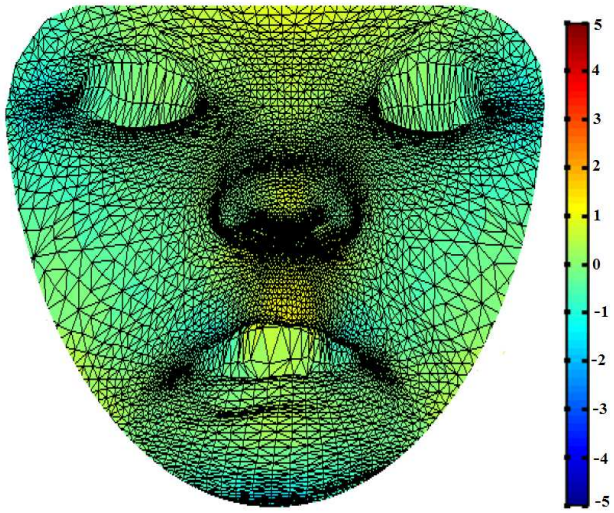

Figure 3.15: Colour map of average asymmetry of the control group in the X direction (mediolateral asymmetry).

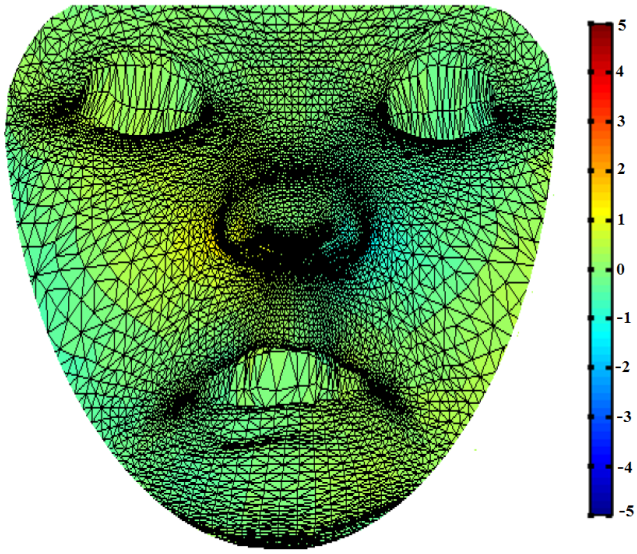

Figure 3.16: Colour map of average asymmetry of the control group in the Y direction.

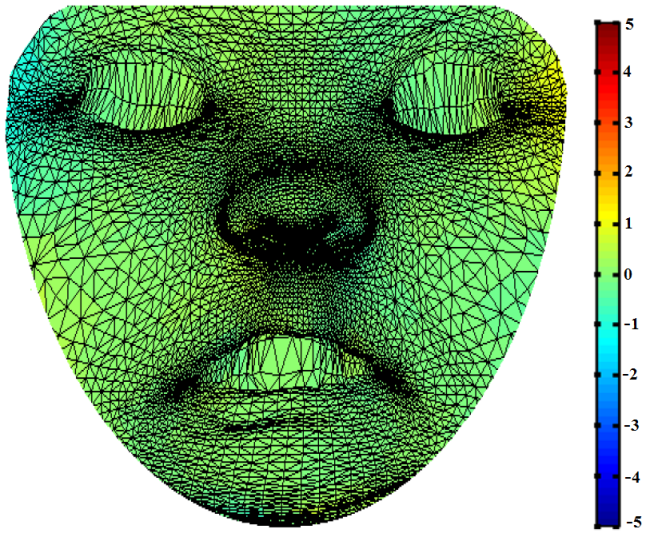

Figure 3.17: Colour map of average anteroposterior asymmetry of the control group in the Z direction. Anteroposterior symmetry is exhibited in green colour.

3.3.2.4 Average facial asymmetry at the four-year follow-up

3.3.2.4.1 At rest position

The average asymmetry at the four-year follow-up is illustrated in Figure 3.18. At this stage, the residual asymmetries were minimum, and were identified at the nares and the vermillion border of the upper lip. Figure 3.19, Figure 3.20 and Figure 3.21 demonstrate the average asymmetry in mediolateral, vertical and anteroposterior directions respectively. Mediolaterally, the nose was shifted towards the non-cleft side (light blue colour) (Figure 3.19). The red colour at the philtrum of the upper lip represents a remarkable shifting towards the scar tissue on the cleft side. The vertical asymmetries (Figure 3.20) were noted at the upper lip, corner of

the mouth, and the cheeks of the cleft side (yellow colour), whereas the sky-blue colour of the nares on the cleft side, that can still be seen in this group, represented the downward position of the alar. Anteroposteriorly, at the four-year follow-up, significant deficiencies in the nares, upper lip and paranasal regions on the cleft side are illustrated in blue (Figure 3.21).

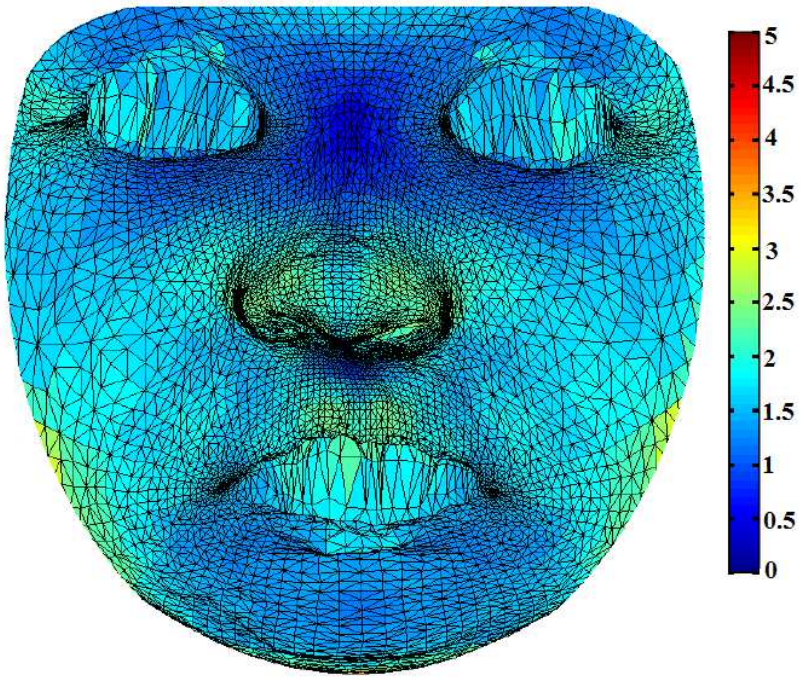

Figure 3.18: Colour map of average asymmetry of cleft patients at the four-year follow-up, at rest position.

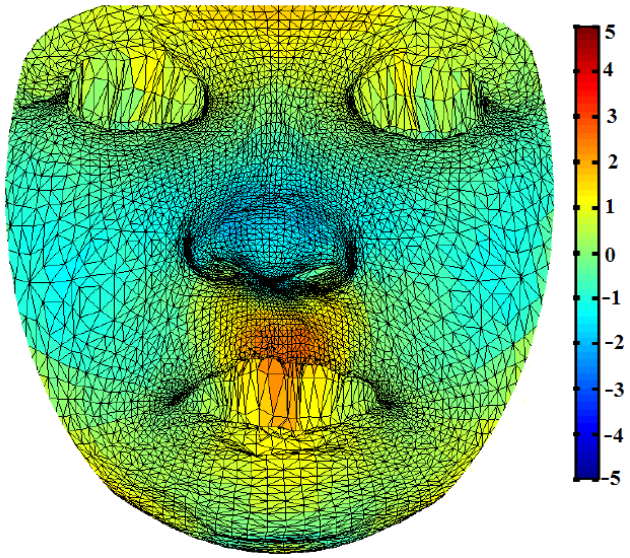

Figure 3.19: Colour map of average mediolateral asymmetry (X direction) at the four-year follow-up, at rest position.

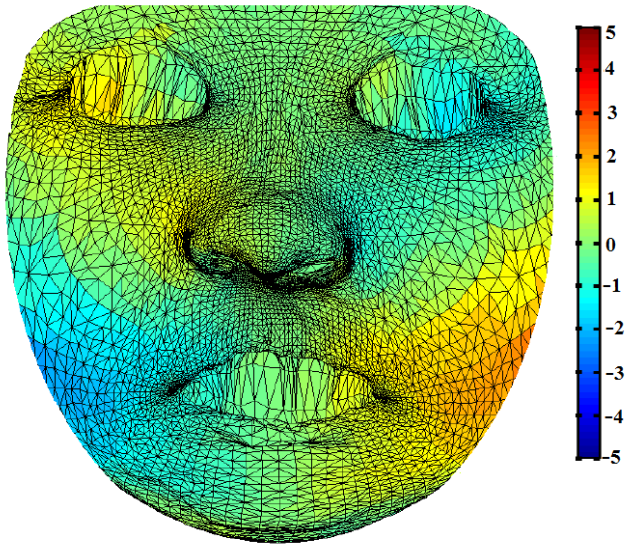

Figure 3.20: Colour map of average vertical asymmetry (Y direction) at the four-year follow-up, at rest position.

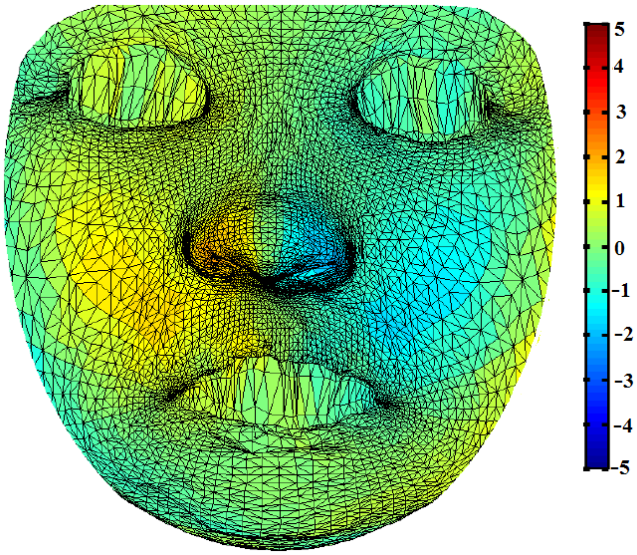

Figure 3.21: Colour map of average anteroposterior asymmetry (Z direction) at the four-year follow-up at rest position.

3.3.2.4.2 At maximum smile expression

During maximum smile, the average asymmetry at the alar base and at the vermillion of the upper lip has increased considerably (Figure 3.22). Mediolaterally (Figure 3.23), the dark red colour at the philtrum of the upper lip showed a considerable shifting towards the scar tissue on the cleft side. Vertical deficiencies were noted at the upper lip and the alar base (shown in yellow) of the cleft side (Figure 3.24). The anteroposterior deficiencies of the upper lip, nares, and paranasal areas substantially increased during maximum smile (Figure 3.25).

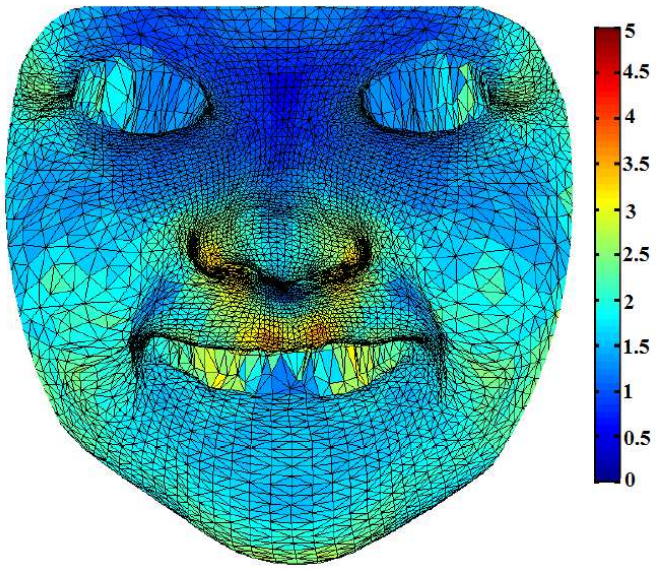

Figure 3.22: Colour map of average asymmetry at the four-year follow-up at maximum smile.

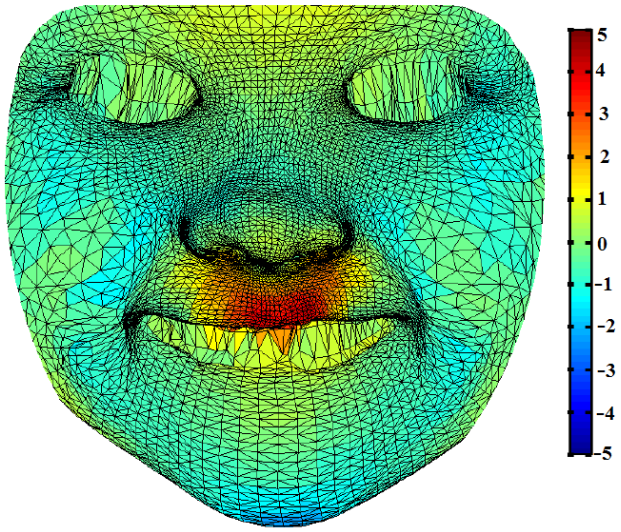

Figure 3.23: Colour map of average mediolateral asymmetry (X direction) at the four-year follow-up at maximum smile.

.

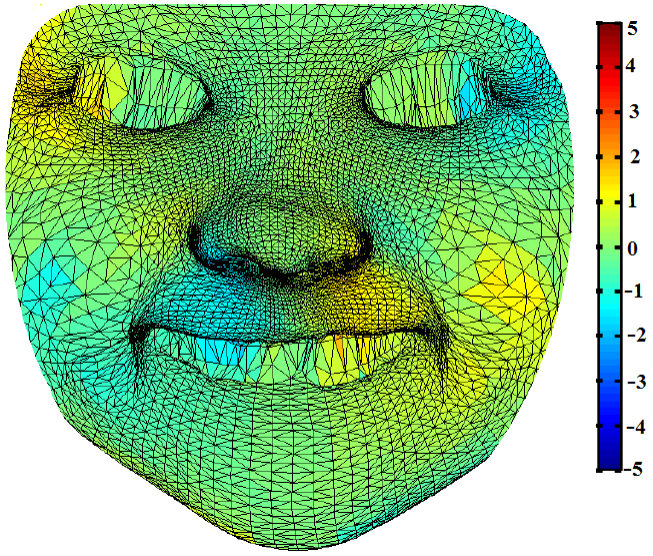

Figure 3.24: Colour map of average vertical asymmetry (Y direction) at the four-year follow-up at maximum smile.

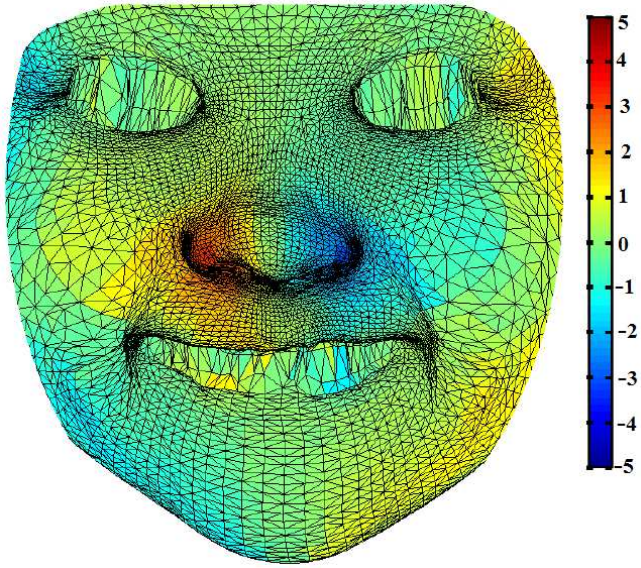

Figure 3.25: Colour map of average anteroposterior asymmetry (Z direction) at the four-year follow-up at maximum smile.

3.3.3 The impact of the lip repair on the total and regional facial asymmetry

Table 3.4 demonstrates the median, minimum and maximum asymmetry scores before and after lip surgery for the entire face, the nose and the upper lip. The asymmetry scores for the face, nose, and upper lip significantly decreased after lip repair ($p<0.001$). The asymmetry scores of the upper lip were higher than those of nose pre- and post-surgery, with the asymmetry scores of the upper lip being 30.59 preoperatively, and 2.28 postoperatively, whereas the asymmetry scores for the nose before and after surgery were 9.97 and 1.52 respectively.

The median, minimum and maximum asymmetry scores of the total face, upper lip and the nose in X, Y and Z directions for cleft patients before and after surgery are presented in Table 3.5. All the asymmetry scores significantly decreased following surgery ($p<0.001$) in the three directions.

Table 3.4: Descriptive statistics and p-values of Wilcoxson Signed ranked test for asymmetry scores of cleft patients before and after surgery.

Asymmetry scores	Preoperatively			Postoperatively			*p-value**
	Median	*Min*	*Max*	*Median*	*Min*	*Max*	
Total Face	22.03	7.2	44.72	6.25	3.114	13.45	**0.000**
Nose	9.97	1.95	33.44	1.52	0.5	3.73	**0.000**
Upper Lip	30.59	7.48	81.15	2.28	0.71	5.52	**0.000**

*bold indicates significant differences.

Table 3.5: Descriptive statistics and p-values of Wilcoxson Signed ranked test for asymmetry scores of cleft patients before and after surgery in X, Y and Z directions.

	Direction of asymmetry	Preoperatively			Postoperatively			p-value*
		Median	*Min*	*Max*	*Median*	*Min*	*Max*	
Total face	***X***	2.60	1.43	4.40	1.35	0.82	2.17	**0.000**
	Y	1.21	0.72	1.96	0.78	0.41	1.34	**0.000**
	Z	1.47	0.87	2.54	0.82	0.53	1.33	**0.000**
Nose	***X***	3.30	1.23	5.97	1.62	0.53	3.51	**0.000**
	Y	1.69	0.49	3.00	0.57	0.33	1.57	**0.000**
	Z	1.34	0.43	2.35	0.52	0.24	1.42	**0.000**
Upper lip	***X***	3.78	1.37	7.32	1.18	0.34	2.45	**0.000**
	Y	1.21	0.51	2.27	0.58	0.21	1.28	**0.000**
	Z	2.87	1.12	4.95	1.00	0.29	2.43	**0.000**

*bold indicates significant differences.

3.3.4 The residual postoperative asymmetry in comparison with control group

The median, minimum and maximum asymmetry scores of the total face, upper lip and nose for the control and surgically managed UCLP cases are illustrated in boxplots in Figure 3.26. As indicated in Table 3.6, the surgically managed UCLP cases showed significantly higher asymmetry scores for the total face, nose and upper lip than were recorded in the control group ($p<0.001$).

Table 3.7 shows the median, minimum and maximum asymmetry scores in X, Y and Z directions for the total face, nose and upper lip for both the cleft group and the control group. The asymmetry scores of the cleft group after surgery were significantly higher in the three directions (X, Y and Z) in comparison with the control group.

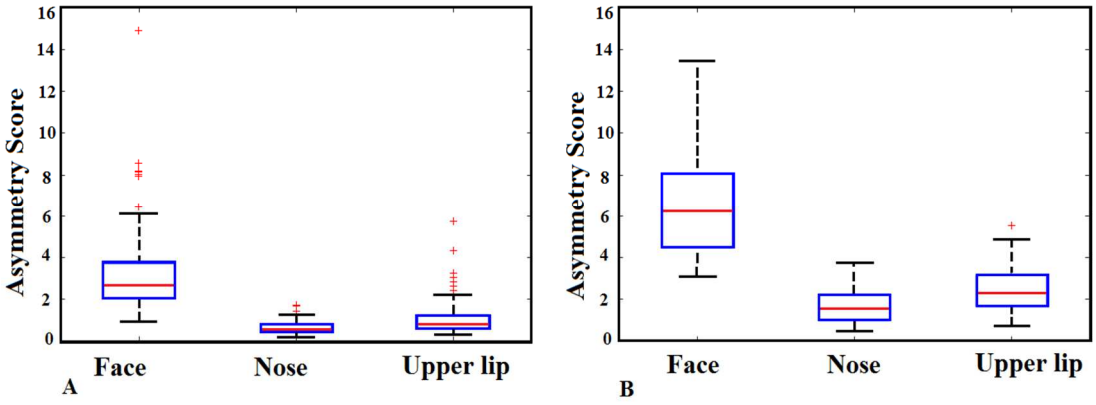

Figure 3.26: Boxplots of the asymmetry scores of the total face, upper lip and nose for (A) the non-cleft control group and (B) surgically manged cleft cases. Median, three quartiles, minimum, and maximum are shown.

Table 3.6: Descriptive statistics and p-values of the Wilcoxson rank-sum test for the asymmetry scores of the control group and surgically managed cleft cases.

Asymmetry scores	Control group			Surgically managed UCLP			*p-value**
	Median	***Min***	***Max***	***Median***	***Min***	***Max***	
Total face	2.70	0.95	14.88	6.25	3.11	13.45	**0.000**
Nose	0.54	0.20	1.72	1.52	0.50	3.73	**0.000**
Upper lip	0.82	0.32	5.74	2.28	0.71	5.52	**0.000**

*bold indicates significant differences.

Table 3.7: Descriptive statistics and p-values of the Wilcoxson rank-sum test for asymmetry scores of the control group and surgically managed cleft cases in three directions (X, Y and Z).

Facial regions	Direction	Control group			Surgically managed UCLP			*p-value**
		Median	*Min*	*Max*	*Median*	*Min*	*Max*	
Total face	***X***	0.83	0.45	1.99	1.35	0.34	2.45	**0.000**
	Y	0.56	0.32	1.10	0.78	0.21	1.28	**0.000**
	Z	0.53	0.33	1.46	0.82	0.29	2.43	**0.000**
Nose	***X***	0.59	0.25	2.89	1.62	0.82	2.17	**0.000**
	Y	0.45	0.18	0.83	0.57	0.41	1.34	**0.000**
	Z	0.31	0.15	0.96	0.52	0.53	1.33	**0.000**
Up lip	***X***	0.85	0.27	2.44	1.18	0.53	3.51	**0.001**
	Y	0.46	0.19	1.08	0.58	0.33	1.57	**0.024**
	Z	0.35	0.16	1.06	1.00	0.24	1.42	**0.000**

*bold indicates significant differences.

Table 3.8 and Figure 3.27 show the distribution of the asymmetry scores of the control group and the surgically managed UCLP cases according to their deviation from the perfect symmetry. Results of the asymmetry scores for the control group indicate that approximately 81% were close to a perfectly symmetrical nose (<1mm), and approximately 65% were close to a perfectly symmetrical lip. In the surgically managed UCLP group, the asymmetry scores were 26% and 6% for the nose and the upper lip respectively. About one third of the cleft cases showed asymmetry of the lip more than 3mm in comparison to 6% in the control group. Likewise, two thirds of the cleft cases showed more than 1mm asymmetry of the nose, this was limited to 20% of the control group. Notably, in the control group, asymmetry of the nose was the least affected in comparison to the lip, the asymmetry scores of the nose were less than 2mm, while approximately 14% had asymmetry scores of the lip of >2mm.

Table 3.8: Distribution of asymmetry scores for the control group and the surgically managed UCLP cases. The control group and the UCLP patients were distributed according to the asymmetry scores of the nose and upper lip over five categories (from 0 to >3mm).

	Control group (N=70)					**Surgically managed *UCLP (N=30)***				
	≤0.5	**>0.5and≤ 1**	**>1and≤ 2**	**>2and≤3**	**> 3**	**≤0.5**	**>0.5and≤ 1**	**>1and≤ 2**	**>2and ≤3**	**> 3**
Nose	28	29	13	0	0	1	7	12	8	2
Upper lip	9	37	14	6	4	0	2	9	9	10

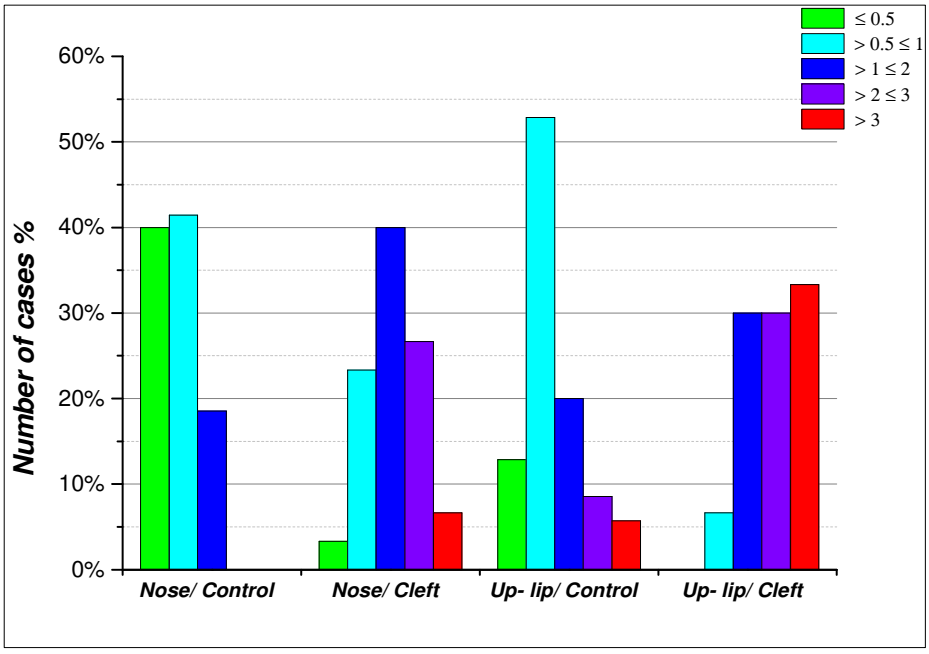

Figure 3.27: The distribution of the magnitude of asymmetry of the control group and surgically managed UCLP cases.

3.3.5 Evaluation of the changes in facial asymmetry scores at four-year follow-up

The asymmetry scores for the face, nose, and upper lip postoperatively, and at four-year follow-up for the 15 cases are presented in Table 3.9. At four-year follow-up, the asymmetry score of the nose had increased significantly, $p<0.01$. The asymmetry scores of the nose at four-year follow-up increased in the three directions, with significant increase in the anteroposterior direction ($p<0.001$) (Table 3.10).

Table 3.9: Descriptive statistics and p-values of Wilcoxson Signed ranked test for the asymmetry scores of cleft patients after surgery and at the four-year follow-up.

Asymmetry scores	After surgery			4 years follow-up			*p-value**
	Median	*Min*	*Max*	*Median*	*Min*	*Max*	
Total face	6.46	3.11	13.45	5.66	3.69	9.36	0.454
Nose	1.39	0.50	3.73	2.23	1.16	4.06	**0.008**
Upper lip	2.76	1.12	5.52	2.13	1.41	3.87	0.303

* bold indicates significant differences.

Table 3.10: Descriptive statistics and p-values of Wilcoxson Signed ranked test for the asymmetry scores of the nose for the UCLP patients after surgery and at four-year follow-up in three directions (X, Y and Z).

Asymmetry scores of the nose	After surgery			4 years follow-up			p-value*
	Median	*Min*	*Max*	*Median*	*Min*	*Max*	
X-direction	1.66	0.75	3.51	1.70	0.40	3.30	0.064
Y-direction	0.61	0.33	1.57	0.88	0.43	1.19	0.095
Z-direction	0.52	0.25	0.93	0.86	0.38	1.46	**0.000**

* bold indicates significant differences.

3.3.6 Evaluation of the changes in facial asymmetry scores at maximum smile

The asymmetry scores of the face, upper lip and nose during rest and at maximum smile at the four-year follow-up are presented in Table 3.11. All the asymmetry scores increased during smiling, with the face and upper lip significantly increased. The asymmetry score of the upper lip during smiling (4.0) was more pronounced than that of the nose (2.6). Table 3.12 shows the asymmetry scores for the total face, nose and upper lip in three directions. The asymmetry scores in the anteroposterior direction (Z) clearly increased significantly during maximum smiling in the face, nose and upper lip. Mediolaterally (X direction) the asymmetry scores increased significantly in the upper lip only, $p<0.001$. Vertically, the asymmetry scores decreased during smiling, however, the changes were not significant in this direction.

Table 3.11: Descriptive statistics and p-values for asymmetry scores at rest and at maximum smile at the four-year follow-up.

Asymmetry scores	At rest			At maximum smile			*p-value**
	Median	*Min*	*Max*	*Median*	*Min*	*Max*	
Total face	5.66	3.69	8.58	7.14	3.37	12.60	**0.047**
Nose	2.23	1.18	4.05	2.63	1.31	4.88	0.216
Upper lip	1.96	1.41	3.87	4.00	1.19	9.98	**0.000**

*bold indicates significant differences

Table 3.12: Descriptive statistics and p-values of Wilcoxson Signed ranked test for the asymmetry scores of UCLP patients at rest position and at maximum smile in three directions (X, Y and Z).

	Direction of asymmetry	At rest			At maximum smile			*p-value**
		Median	*Min*	*Max*	*Median*	*Min*	*Max*	
Total face	***X***	1.29	0.78	1.72	1.35	0.82	1.75	0.191
	Y	0.89	0.68	1.29	0.75	0.41	1.37	0.376
	Z	0.96	0.58	1.28	1.09	0.82	1.68	**0.002**
Nose	***X***	1.04	0.40	2.36	1.22	0.69	2.33	0.685
	Y	0.88	0.43	1.09	0.80	0.20	1.14	0.273
	Z	0.87	0.38	1.46	1.06	0.67	2.22	**0.000**
Up lip	***X***	1.14	0.66	2.51	1.75	1.09	2.75	**0.000**
	Y	0.61	0.30	1.02	0.48	0.32	0.92	0.068
	Z	0.85	0.37	1.74	1.39	0.67	2.45	**0.006**

*bold indicates significant differences

3.4 Relationship between initial severity of the cleft lip and the residual postoperative dysmorphology

3.4.1 Study errors

The mean distance and standard deviation for landmark digitisation error for the 13 landmarks used for the ratios of initial severity of cleft lip are shown in Table 3.13. The overall error was 0.26mm ±0.04.

Table 3.13: The mean and standard deviation of landmark digitisation error.

landmarks		Average error	SD
1	sbalR	0.22	0.07
2	sablL	0.24	0.10
3	sn0R	0.23	0.22
4	sn0L	0.24	0.19
5	cR	0.20	0.09
6	cL	0.28	0.17
7	chR	0.25	0.09
8	chL	0.28	0.15
9	cph''	0.30	0.12
10	cph'	0.29	0.11
11	cph	0.20	0.1
12	CM	0.30	0.13
13	CM''	0.29	0.14
Mean		**0.26**	**0.04**

3.4.2 Relationship between the asymmetry scores of the total face and asymmetry scores of the nose and upper lip in the cleft group

There was a strong correlation between the asymmetry scores of the face, and asymmetry scores of the upper lip and the nose before surgery, $p<0.001$, Table 3.14.

Table 3.14: Correlation between asymmetry scores of the face, nose, and upper lip before surgery.

Asymmetry scores	Nose-Pre		ULip-Pre	
	Correl. Coeffi.	*p-value**	*Correl. Coeffi.*	*p-value**
Face-Pre	0.785	**0.000**	0.856	**0.000**
Nose-Pre			0.913	**0.000**

*bold indicates significant correlation.

Following the primary lip repair, the asymmetry scores of the face were significantly and strongly correlated with the asymmetry scores of the upper lip and the nose, $p<0.01$. Whilst, the asymmetry scores of the upper lip and the nose were not correlated (Table 3.15).

Table 3.15: Correlation between the asymmetry scores of the face, upper lip and nose after surgery.

Asymmetry scores	Nose-Post		ULip-Post	
	Correl. Coeffi.	*p-value**	*Correl. Coeffi.*	*p-value**
Face-Post	0.504	**0.005**	0.468	**0.009**
Nose-Post			0.299	0.108

*bold indicates significant correlation

At four-year follow-up, there was a strong correlation between the asymmetry scores of the face and the nose, p<0.01. However, there was no correlation identified between the asymmetry scores of the lip and the nose, or the lip and the face (Table 3.16)

Table 3.16: Correlation between the asymmetry scores of the face, upper lip and nose four years following lip repair.

Asymmetry scores	Nose at 4 years		ULip at 4 years	
	Correl. Coeffi.	*p-value**	*Correl. Coeffi.*	*p-value*
Face at 4 years	0.711	**0.003**	-0.036	0.898
Nose at 4 years			-0.010	0.972

*bold indicates significant correlation.

3.4.3 Relationship between the asymmetry scores before and after lip surgery

There was no correlation found between the asymmetry scores before surgery and these detected after surgery. With exception of the correlation determined between asymmetry score of the nose after surgery and asymmetry score of the face before surgery, however, this correlation was weak, Table 3.17.

Table 3.17: Correlation between preoperative and postoperative asymmetry scores.

Asymmetry scores	Face-Post		Nose-Post		ULip-Post	
	Correl. Coeffi.	p-value	Correl. Coeffi.	p-value*	Correl. Coeffi.	p-value
Face-Pre	0.285	0.127	0.382	**0.037**	0.195	0.301
Nose-Pre	0.209	0.268	0.254	0.175	0.074	0.697
ULip-Pre	0.184	0.436	0.274	0.143	0.185	0.328

*bold indicates significant correlation.

Table 3.18 shows the correlation between the asymmetry scores after surgery and those detected at the four-year follow-up. Both the asymmetry scores of the face and the nose at the four-year follow-up had a significant correlation with the asymmetry scores of the nose after surgery ($p<0.05$). The correlations of the asymmetry scores of the upper lip after surgery and asymmetry scores at four-years follow-up were not significant.

Table 3.18: Correlation between the asymmetry scores after surgery and the at four-year follow-up.

Asymmetry scores	Face-at 4 years		Nose- at 4 years		Ulip-at 4 years	
	Correl. Coeffi.	*p-value**	*Correl. Coeffi.*	*p-value**	*Correl. Coeffi.*	*p-value**
Face-Post	0.115	0.581	0.260	0.394	0.060	0.832
Nose-Post	0.545	**0.036**	0.674	**0.006**	0.005	0.986
ULip-Post	0.305	0.270	0.460	0.085	-0.174	0.535

*bold indicates significant correlation.

Table 3.19 shows the correlation between asymmetry scores of the face, upper lip and nose before surgery and at four years following lip repair. There was a strong correlation between asymmetry scores of the nose at four-year follow-up with asymmetry scores of the nose before surgery. The asymmetry scores of the upper lip and the face at the long-term follow-up were not significant with asymmetry scores before surgery.

Table 3.19: Correlation between the asymmetry scores before surgery and the at four-year follow-up.

Asymmetry scores	Face- at 4 years		Nose- at 4 years		Ulip- at 4 years	
	Correl. Coeffi.	*p-value*	*Correl. Coeffi.*	*p-value**	*Correl. Coeffi.*	*p-value*
Face-Pre	0.449	0.093	0.368	0.177	0.340	0.216
Nose-Pre	0.373	0.171	0.527	**0.044**	0.286	0.302
ULip-Pre	0.333	0.225	0.334	0.224	0.410	0.129

*bold indicates significant correlation.

3.4.4 Relationship between the ratios of initial severity of cleft lip and the asymmetry scores before surgery, after surgery and at four-year follow-up.

The four ratios describing the initial severity of cleft showed significant correlation with the asymmetry scores of the total face, nose and upper lip before surgery, $p<0.05$, (Table 3.20). However, the correlations of these ratios with the asymmetry scores after surgery (Table 3.21) and at four-year follow-up were not found to be significant (Table 3.22). Cleft asymmetry can be addressed with primary surgical repair which can eliminate most of the facial asymmetry.

Table 3.20: Correlation between the asymmetry scores before surgery and the ratios of initial cleft severity.

Ratios		Face_Pre	Nose_Pre	ULip_Pre
Nostril base width ratio	correl. Coeffi.	0.427	0.703	0.593
	p-value*	**0.019**	**0.000**	**0.001**
Nostril length ratio	correl. Coeffi.	0.444	0.579	0.552
	p-value*	**0.014**	**0.001**	**0.002**
Philtrum height ratio	correl. Coeffi.	-0.424	-0.430	-0.447
	p-value*	**0.012**	**0.018**	**0.013**
Median cleft width ratio	correl. Coeffi.	0.629	0.778	0.735
	p-value*	**0.012**	**0.001**	**0.002**

*bold indicates significant correlation.

Table 3.21: Correlation between 4 ratios describing the severity of cleft and the asymmetry scores after surgery.

Cleft severity ratios		Face-Post	Nose-Post	ULip-Post
Nostril base width ratio	correl. Coeffi.	0.034	0.094	0.156
	p-value	0.860	0.620	0.410
Nostril length ratio	correl. Coeffi.	0.112	0.104	0.213
	p-value	0.554	0.585	0.257
Philtrum height ratio	correl. Coeffi.	0.266	0.251	-0.042
	p-value	0.155	0.182	0.824
Median cleft width ratio	correl. Coeffi.	0.167	0.023	0.213
	p-value	0.379	0.904	0.258

Table 3.22: Correlation between the ratios describing the severity of the cleft and the asymmetry score at the four-year follow-up.

Cleft severity ratios		Face_ at 4 years	Nose_ at 4 years	ULip_ at 4 years
Nostril base width ratio	***correl. Coeffi.***	0.097	0.537	0.162
	p-value	0.353	0.237	0.595
Nostril length ratio	***correl. Coeffi.***	-0.093	0.244	0.032
	p-value	0.742	0.381	0.910
Philtrum height ratio	***correl. Coeffi.***	0.337	0.382	0.029
	p-value	0.832	0.071	0.284
Median cleft width ratio	***correl. Coeffi.***	-0.075	0.149	0.161
	p-value	0.791	0.597	0.566

Chapter four

Discussion

4 Chapter four: Discussion

4.1 Study design

This study investigated the facial asymmetry of UCLP patients before primary lip surgery, after lip surgery, and at four years following lip repair using 3D stereophotogrammetric images. It was designed as a longitudinal cohort study to detect individual variations in data influenced by time, such as growth, which might not be detected by cross-sectional studies (Bishara et al., 1985).

This study consisted of two parts: prospective and retrospective. In the retrospective part, the 3D images were captured routinely before and after primary lip surgery. In the prospective part, 3D images were captured from the same patients four years after primary lip repair. We also had the opportunity to analyse historical data of 3D images of age-matched non-cleft cases that were captured 15 years ago.

4.2 Study sample

4.2.1 Cleft patients

The sample of this study consisted of 3D images of 30 UCLP patients, of whom 15 had completed long-term follow-up. Most of the patients who did not complete the follow-up were those whose parents/guardians did not respond to the invitation emails. In a few other cases, the parents could not attend the follow-up because of the long distance they would have to travel. Patients who underwent surgery at the Royal Hospital for Sick Children, Edinburgh, came from different parts of Scotland (e.g. Shetland, Orkney) and it was difficult for the children and their parent/s to travel the long distance back to the hospital. In the long-term follow-up, two images were captured

for each child: one at rest and one at a maximum smile. Unfortunately, the images of two patients at maximum smile expression were omitted due to technical errors during image transfer. Therefore, the total number of images for the 15 cases was 15 images at rest and 13 images at maximum smile. This study can help to design a future study with suffcient power by measuring the effective size from the parameters obtained by this study.

Compared with previous studies, this study had the highest number of participants. The sample in the longitudinal study by Hood et al. (2003) was 10 UCLP and 10 UCL 3D stereophotogrammetric images. In the study by Seidenstricker-kink et al. (2008), 3D facial computed tomographic images were captured for 26 patients preoperatively and for 19 patients postoperatively. Singh et al. (2007) utilised the pre- and postoperative 3D facial images of 15 UCLP patients, who had Naso Alveolar Molding (NAM) treatment to construct average faces before and after surgery and evaluated shape changes after treatment.

In terms of smiling expression, the sample size of this study was larger than that of Trotman et al. (2000) and Hallac et al. (2017), which was 4 UCLP and 12 UCL(P), respectively, with ages ranging from 14 to 16 years old for the former study and 8 to 18 years for the latter one. However, our sample size was smaller than that of Offerman et al. (1964) and Bell et al. (2014) who recruited 24 unilateral cleft lip patients (age range of 7 to 15 years) and 51 UCLP cases (mean age, 10 years), respectively. Of note, all the above studies were cross-sectional studies that compared the cleft group to a control group and were not longitudinal in nature. Consequently, they had a larger sample size.

This study aimed to investigate the improvements in facial asymmetry after primary lip surgery and the effect of growth on the residual postoperative asymmetry. The preoperative images were captured one or two days before

surgery to eliminate the effect of growth on the preoperative assessment. The postoperative images were taken four months after surgery for two reasons. Firstly, that is usually how long it takes for post-surgical swelling to subside. In the literature, there is variation in the period of postoperative evaluation of cleft patients ranging from one week in the study conducted by Liou et al. (2004) to one month in the study by Pai et al. (2005), and 11 months in that of Seidenstricker-kink et al. (2008). It was indicated that at least three months was required for studies examining post-surgical soft-tissue changes (Ryckman et al., 2010). However, for orthognathic and bone grafting studies the postoperative assessment extends to six months to allow for postoperative swelling to settle. Secondly, the postoperative facial images in this study were captured a few days before palate surgery. The pre- and postoperative mean ages in this study were 3.7 months and 8.4 months, respectively. These time intervals were similar to the mean ages in the study by Hood (2005), where the mean ages were 3.9 months before surgery and 7.1 months after surgery. In studies involving children, the longer the period after surgery, the more the impact of facial growth on facial appearance, which would not serve the aim of this study.

The long-term follow-up was carried out four years following surgery. The mean age of the patients was 4.2± 1.1 years. It is well documented that 82.2% to 92% of total facial development is completed by the age of 5 years (Farkas et al., 1992a). Their study was based on measuring the development of facial shape using direct anthropometry of the face. The width, height and depth of the face were directly obtained from the children's heads. The width was measured at the level of the zygomatic arch and at the gonion angles, the height of the face was measured from nasion to gnathion, and the depth was measured from tragion to subnsasale and gnathion for maxilla and mandible respectively. Hood's (2005) study completed long-term follow-up after two years, while that of Liou et al. (2004) was carried out after three years. This study managed to cover a longer follow-up period than other 3D

facial analysis studies, which provided us with an excellent and unprecedented opportunity to study facial asymmetry.

In this sample, the number of boys (22) was higher than that of girls (8). The number of right cleft cases was six, while that of the left side was 24 cases cleft. This is consistent with the literature, in which boys were shown to be at a higher risk of CL(P) than girls, and the cleft mostly affecting the left rather than the right side of the face (Mossey and Modell, 2012).

All the data in this study were obtained using stereophotogrammetric images. In addition to the accuracy of stereophotogrammetry (Lübbers et al., 2010), it is a safe 3D imaging technique for infants as it does not expose the patients to laser or ionising radiation. Furthermore, its acquisition time is about 1.5 ms, thus reducing the likelihood of image distortion due to the involuntary movement of the babies. It was found to be the method of choice in most cleft studies (Hood et al., 2003; Devlin et al., 2007; van Loon et al., 2010; Ayoub et al., 2011a; Bugaighis et al., 2014a; Bell et al., 2014). In this study, all cleft images (prospective and retrospective parts) were captured using the same 3D device and by the same professional photographer to ensure the homogeneity of the sample and to reduce human errors.

The sample was selected on the basis of the degree of homogeneity of the cases and treatment protocol. The participants were Caucasian in origin, with no history of orthopaedic treatment and were treated by the same surgeon who followed the same surgical technique with each patient. This reduced the impact of variation in surgical techniques on the outcomes (Yamada et al., 2002a; Reddy et al., 2008; Hoffman and Dyleram, 2011).

Assessing facial asymmetry during facial expressions is important. Gross asymmetry during the performance of these expressions will draw the attention of the family and friends to the lip and subsequently to the residual

cleft dysmorphology (Offerman et al., 1964). In this study, the expression of smile was chosen to evaluate the impact of facial expressions on the residual asymmetry for two reasons. Firstly, the reproducibility of this expression has been proven for adults (Johnston et al., 2003) and for children (cleft and non-cleft) (Garrahy, 2002). Secondly, smiling plays a vital role in social interactions and daily communication (Thompson et al., 2004; Van der Geld et al., 2007).

4.2.2 Control (non-cleft patients)

The 3D facial images of the control group in this study had previously been captured by another study (White, 2005). This control group was also used by Hood (2005) to compare the asymmetry of the facial landmarks of the cleft patients with those of the control group. In this study, the data of the same previous study were used because these were already available for a group of children of similar age group to the cleft group following surgery. Regarding the ethical dimension, none of patient's identity was revealed in this study, and only mathematical measurements of the face were used without identifying facial characteristics. Volunteers were happy for the data to be used for research when it was first collected about 15 years ago.

In this study, the historical data of the 3D facial images of the control group was used to compare the residual postoperative asymmetry of cleft with normal population aged six months using dense correspondence analysis. The images of the control group were captured using C3D imaging system, while the images of cleft group were captured using (3dMDface). The accuracy and reliability of the C3D system has already been proven by our research team (Ayoub et al., 2003). Both systems are accurate, reliable and provide 3D facial images using the same philosophy of stereoimaging.

4.3 The application of generic mesh

Dense correspondence analysis was utilised in this study to assess facial asymmetry of the cleft groups and the control group. The generic mesh was utilised to establish the relationship between the anatomical structure and dense correspondence analysis. In this study, the mesh consisted of 7,190 vertices that comprehensively described facial surfaces. This mesh was developed by our research team at the Glasgow Dental School, and it was applied to evaluate the asymmetry of facial expressions before and after orthognathic surgery using 4D imaging (Al-Hiyali et al., 2015). However, in their study the generic mesh was still under development and consisted of 1,982 vertices only, and their study did not analyse asymmetry in three directions. In 2016, it was further developed to analyse facial shape changes after orthognathic surgery in three directions (X, Y and Z), and the mesh consisted of approximately 1,000 vertices (Almukhtar et al., 2016). In this study, the generic mesh was upgraded to contain 7,190 vertices which helped to capture more detail around the area of cleft lip which was considered necessary for this study. In the study of Almukhtar et al. (2016), a generic mesh containing 1000 vertices was enough to provide information on charateristics of facial morpholgy after orthognathic surgery. While in this study, increasing the number of vertices was necesseary to provide details of the nasolabial region. The most condensed available mesh was used in this study. Increasing the number of vertices beyond 7,190 vertices would have made the conformation process slow and susceptible to errors, as the index would be heavy, and it would be difficult for the software to cope with it. Increasing the number of vertices provided more refined analysis, however, there are no studies which identify the optimal number of vertices.

4.4 Errors in the conformation process

The errors in the conformation process of cleft cases preoperatively and postoperatively were evaluated. The errors of the repeated conformation in the X, Y and Z directions, both preoperatively and postoperatively, were significantly less than 0.5mm. The mean errors in the nasolabial region range from 0 to 0.5mm. The errors increased towards the peripheries as fewer landmarks were digitised in the cheek and forehead regions. The accuracy of the conformation process in representing the underlying tissue morphology was investigated at rest and during facial expressions by our research team. The mean error of the conformation process was 1.13 ±0.26mm, and it ranged between 0.73mm to 1.74mm. The minimum error was at the philtral crest landmark, and the maximum was at the gonion. The mean error at maximum smile expression was 1.46 ±0.51mm (Almukhtar et al., 2017). The accuracy of generic mesh in representing the underlying facial morphology, at rest and at maximum smile, was within the clinically acceptable level. The use of generic mesh has also been shown to be valid in representing facial morphological changes (Cheung et al., 2016). The accuracy was from 0.2mm ±0.2 to 0.7mm ±0.5. The higher accuracy was in the centre of the face, and it decreased toward the peripheries. The upper lip showed minimal error.

4.5 Methods for facial asymmetry assessment

4.5.1 ICP method

This study presented a new approach to assessing regional facial asymmetry whereby a 3D model that is divided into anatomical regions using facial landmarks. Previous investigations explored the asymmetry by dividing the face into non-anatomical sections using a set of horizontal and vertical planes (Djordjevic et al., 2014a; Kuijpers et al., 2015). However, their method did

not provide an anatomical understanding of the impact of the surgical repair of the cleft lip on specific anatomical structures. Furthermore, it did not consider the anatomical boundaries of facial regions and confused the understanding of the impact of surgery on facial symmetry. This study attempted to address these deficiencies by subdividing the face into recognised anatomical regions. There was no significant difference between asymmetry scores of repeated measurements for the whole face and facial regions. The errors were comparable to the study by Kuijpers et al. (2015).

The results in this section showed that the ICP method could not provide thorough and comprehensive results in comparison with those provided using the dense correspondence analysis method. In addition to the lack of anatomical correspondence achieved using ICP, the method does not analyse the asymmetry in three directions, which is necessary to detect the underlying source of facial dysmorphology.

4.5.2 Dense correspondence analysis method

Dense correspondence analysis has been reported in the literature to evaluate facial asymmetry of patients with disordered growth and those with hemi mandibular hyperplasia (Claes et al., 2011; Claes et al., 2012; Walters et al., 2013). In these studies, the asymmetry was evaluated in a few selected cases only (three cases in each study). Total facial asymmetry was disclosed using colour map for each case. However, the direction of facial asymmetry was not considered. In 2015, Al-Hiyali et al. applied dense correspondence analysis to the assessment of facial asymmetry in orthognathic patients. In their study, the results were demonstrated objectively to show the impact of orthognathic surgery on facial expressions. However, the direction of asymmetry was not analysed. The application of dense correspondence analysis for the evaluation of facial asymmetry of

UCLP patients before and after primary surgery has not been reported in the literature yet.

In this study, the conformation of generic mesh helped to present the results in two different ways: the “average asymmetry” and “total and regional facial asymmetry”.

In the average asymmetry, colour-coded maps demonstrated the average asymmetry of the total sample. The asymmetry scores of all facial surfaces were illustrated using colour-coded maps, i.e. each colour on the map represents a mean asymmetry score for the total sample. This method of presentation is considered to be both quantitative and qualitative, whereby a qualitative visual method displays the quantity of facial surface asymmetry scores, facilitating the comparison between facial regions. Colour maps enabled the visualisation of the patterns of facial asymmetry for cleft patients and discriminated between the asymmetry patterns of cleft groups and the non-cleft children. The application of this method is not limited to the presentation of asymmetry for a group of patients; it can be used to evaluate facial asymmetry in individual cases. In this situation, the asymmetry would be calculated by measuring the distances between the corresponding points of the original and mirrored models for each individual case and the source of the residual asymmetry can be investigated by analysing the asymmetry in each of the three directions.

The results highlight the indispensable contribution made by the colour map as it helps to identify the pattern of asymmetry. For instance, mediolateral asymmetry was identified in the nose and the upper lip in cleft and non-cleft groups; however, in the control group, the asymmetry was in the same direction, while in cleft patients it was present in different directions. One can argue that using the arithmetic mean can help identify the direction of asymmetry whereby the positive and negative signs indicate the right and left

directions respectively. In this case, the negative signs will cancel out the positive ones, providing an artificially small mean value. It has been proven that the arithmetic mean is not sufficient for the evaluation of facial asymmetry (Ozsoy, 2016).

On the other hand, the total and regional facial asymmetry method helped quantify the mean of asymmetry scores for each facial region by extracting (cutting) the region of interest from the conformed mesh in each case, and calculating the mean of asymmetry scores for the total sample. The regions of interest in this study were the upper lip and the nose, which represented the sites of the cleft and were thus where the impact of surgery was maximised. This method displayed the significant changes in asymmetry scores (due to the effect of surgery, growth, and facial expression) using statistical tests.

The postoperative conformed meshes were utilised for the conformation of the preoperative images. This helped to stabilise the mesh index during the conformation process and facilitated the measurement of morphology variations in the preoperative images.

4.6 Advantages and limitations of the applied methodology

The evaluation of residual facial asymmetry of UCLP has been reported in the literature by using either landmark-based or surface-based method. The former cannot describe whole facial surfaces using a few set of facial landmarks. Each 3D image consists of about 40,000 vertices, and using facial landmarks will not represent facial surfaces in regions where only a few landmarks can be digitised, such as the cheek region. When using the landmark-based method, the morphology of the surfaces between the landmarks is ignored. In contrast, a surface-based method is more

informative as it reveals the disparity between the right and left sides of the face by superimposing the 3D facial model on its mirror image. Nevertheless, the disadvantage of the surface-based method is that superimposing of the original and mirror models is usually accomplished using the Iterative Closest Points (ICP) algorithm. This algorithm minimises the distance between the two 3D models by searching the closest point-to-point relation of the two surfaces irrespective of the anatomical correspondence between these points thus underestimating the facial asymmetry (Verhoeven et al., 2016). For instance, by using ICP to evaluate facial asymmetry of unilateral cleft patients, the maximum asymmetry of the nasolabial region will be levelled out over the facial surfaces, and the asymmetry will be minimised. In fact, the problem with the ICP algorithm lies not only with the facial asymmetry of craniofacial abnormality but also with asymmetry in a normal individual. Human faces are not perfectly symmetrical and thus the ICP is given a tolerance of 0.5mm. Unfortunately, this tolerance was established arbitrarily (Djordjevic et al., 2013), and results in unrealistic measurements. Furthermore, following the registration process, the asymmetry was measured by calculating the minimum distances between the points of the two 3D surfaces irrespective of the anatomical correspondence between the points and thus diminishing facial asymmetry.

This study overcomes the problem of the two above methods (landmark-based and surface-based) by representing the 3D facial surfaces using dense of facial mathematical landmarks (points) that allow for a comprehensive description of all facial surfaces. Furthermore, this study applied Partial Procrustes (PP) analysis to superimpose the original and mirrored images and eliminate the use of the ICP algorithm, so the anatomical correspondence with the registered surfaces (dense of mathematical points) could be considered, and asymmetry was measured by calculating the absolute distances between corresponding points, giving actual and realistic measurements of facial asymmetry.

Another advantage of this method is that it does not rely on the plane of symmetry to quantify asymmetry. The asymmetry scores were calculated by measuring the absolute distances between the corresponding points, irrespective of the symmetry plane. In previous research, a plane of symmetry was established to measure the degree of facial dysmorphology (Bilwatsch et al., 2006; Stauber et al., 2008). The plane of symmetry is usually identified either by the facial landmarks method or surface-based method, and each method has its limitations. Establishing a symmetry plane using facial landmarks is affected by the accuracy of landmark digitisation, and any error in landmark placement will affect the accuracy of the measurements. Furthermore, landmarks do not represent the whole face, and their validity is thus questionable, especially if they are located in asymmetrical areas (Stauber et al., 2008; Xiong et al., 2016). The plane of symmetry was also established by superimposing the original and mirror images of the 3D models of the face. This procedure is associated with methodological error as the plane of symmetry is an artificial plane and based on superimposing images and does not reflect the true anatomical plane to assess asymmetry. Therefore, in this study, this error is avoided by measuring the asymmetry score, which is independent to the plane of asymmetry.

Moreover, this study allowed, for the first time, further analysis of asymmetry in three directions (mediolateral, vertical and anteroposterior). General asymmetry produces limited information about the underlying source of asymmetry. This method of analysis is essential to identify the exact anatomical component responsible for dysmorphology. Furthermore, this study succeeded in objectively quantifying the asymmetry scores in three directions, which is an unprecedented innovation.

This study offered realistic measurements of the degree of asymmetry of facial surfaces at rest and maximum smile. Trotman et al. (2000) evaluated

the magnitude of residual facial asymmetry in the facial expressions of cleft patients by measuring the absolute difference in displacements for a set of anatomical landmarks on the cleft and the non-cleft sides. A wide range of variations was recorded in their study for cleft patients when they smile. These variations were due to the compensatory actions of the lower lip to overcome the restricted movements on the cleft side, which were related to the presence of the scar tissue. Another drawback of their study was that it could not determine whether the asymmetry was present on the cleft or non-cleft side. Furthermore, their study sample was limited to just five BCLP patients and four UCLP patients.

However, the limitation of this study is that the analysis of maximum smile was static and not dynamic. This study considered the magnitude of facial asymmetry, while the movements of facial muscles were not considered. The pattern of these movements and their speed can be attributed to the asymmetry of the nasolabial region of cleft patients. Better understanding of facial asymmetry can be achieved by using 4D imaging to record and analyse the dynamics of facial muscle movements.

The limitation of using the generic mesh in the evaluation of facial asymmetry is that it requires sophisticated mathematical calculations. The in-house developed software was utilised to represent the vertices of the generic mesh mathematically using a specific index. Then, this software was used to conform the mesh and to analyse the asymmetry. This software was developed at the Glasgow Dental School, and high-level programming ability would be needed to develop such software.

This study was an objective study and it did not include patients' opinions. According to psychological studies there is no correlation between the extent of facial dysmorphology and how significantly the patient views this asymmetry. Patients with large defects may not have a major problem with

how they look, and some patients with a very small defect have significant concerns with how they look (Chatrath et al., 2007; Kürkçüoğlu et al., 2016).

4.7 Longitudinal evaluation of the facial asymmetry of UCLP patients

The maximum asymmetry before surgery was observed at the upper lip and the nose. This is not surprising given that the upper lip and the nose represent the sites where the cleft is present. This result is in agreement with that presented by Hood et al. (2003) and Seidenstricker-kink et al. (2008). However, in their studies, a landmark-based method was applied to assess facial asymmetry that could not comprehensively describe the characteristics of the morphology for the nasolabial surfaces between the landmarks.

After surgery, facial asymmetry had significantly improved, and residual asymmetry was noted at the nose, mainly at the tip. The perfect repair of nasal dysmorphology is challenging owing to the complex anatomical structure of the nose. Contradictions exist in the literature regarding the site of residual asymmetry after surgery. The postoperative residual asymmetry was mainly at nasal landmarks in the study by Seidenstricker-kink et al. (2008), while in the study by Hood et al. (2003), the postoperative asymmetry was identified mostly at the upper lip landmarks, with the nose showing significant improvement after surgery. In these studies, the presentation of asymmetry as measurements of individual points leads to contradictory results owing to the lack of detail in the analysis.

Four years following surgery, the asymmetry scores of the nose significantly deteriorated, and the asymmetry showed a different pattern than that after surgery. The asymmetry was identified at the nares and philtrum of the upper lip, while the postoperative asymmetry at the tip of the nose could not

be identified. It was reported that one-third of cleft patients treated with the rotational advancement technique required alar base revision surgery (Mulliken and Martínez-Pérez, 1999). The results of this study are in contradiction to this stated by the study of Hood et al. (2003) who found that the improvement of asymmetry at two years following surgery was significant at the landmarks of the lip rather than the nose. Their study was based on limited landmarks which did not allow the adequate description of nasolabial surfaces.

At maximum smile, the residual asymmetries at the nares and the philtrum of the upper lip increased secondarily to the distorted function of the levator labii superioris alaeque nasi and orbicularis oris muscles in cleft patients which accentuated asymmetry. The asymmetry scores of the total face and the upper lip were significantly accentuated at maximum smile. Impairment of the maximum force capacity of the lip muscles and mechanical limitations in maximum movements because of lip scarring, specifically during smiling, are responsible for the functioning abnormalities of these muscles (Trotman et al., 2000; Trotman et al., 2007b).

Unlike the nose, the asymmetry of the upper lip significantly increased during smiling, probably because of the vital role that the upper lip plays in this facial expression. All the perioral lifting muscles pull the upper lip directly in an upward force, while the complex structure of the nose, which contains bones, cartilage and muscles, support the nose to resist the muscular force imbalance during smiling. The low elasticity of the upper lip caused by scarring is another factor that contributed to the asymmetry observed (Susami et al., 1993). A theoretical concept suggested lip scarring can be reduced by early cleft lip repair in the first or second month because in younger babies lip motion is minimal than in older ones (Tamada and Nakajima, 2010). However, the age of patients at the time of surgery should

be considered, especially the ability of infants to withstand the stress of surgery and cope with the risks posed by general anaesthesia.

Before surgery, the tip of the nose, columella and philtrum of the upper lip shifted to the non-cleft side. The perioral and perinasal muscles lack to the caudal-anterior attachment to the nasal septum (Figure 4.1), which pull philtrum of the upper lip and the nose towards the non-cleft side owing to unequal muscular balance forces related to the presence of the cleft (Campbell et al., 2010).

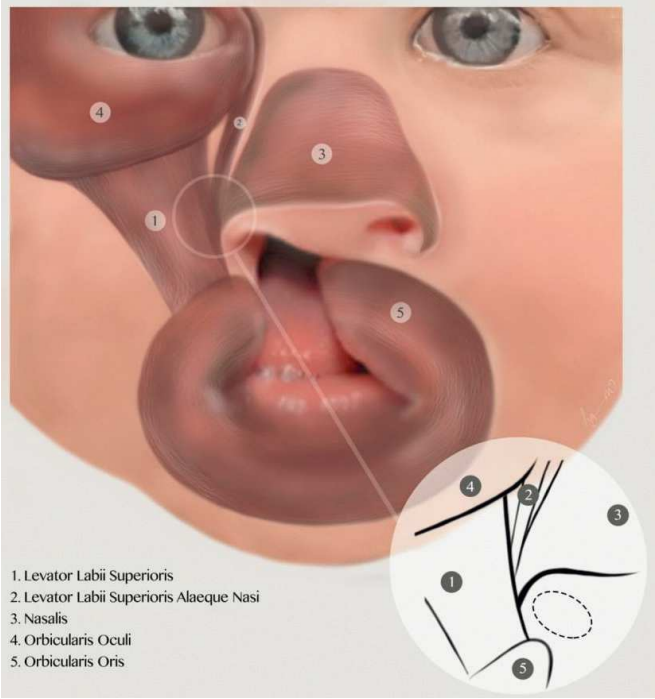

Figure 4.1: Nasolabial muscles in UCLP infant. The presence of a cleft affects the balance forces in the muscles (Drake and Colbert, 2017).

After surgery, the maximum mediolateral asymmetry of the face, nose and upper lip significantly decreased. However, there was minimum lateral

displacement of the nose to the non-cleft side. This could be attributed to the incomplete mobilisation of the lateral alaeque nasi muscle, as this muscle has superior and inferior bundles: the superior bundle inserts on the lateral alar cartilage while the inferior bundle inserts on the orbicularis muscle. Both bundles have to be adequately immobilised and crossed over to be sutured to the matching muscles fibres on the non-cleft side. In landmark studies of 3D facial models of cleft infants by Yamada et al. (1999), lateral deviation of the subalar landmarks of the cleft side of operated cleft infants was observed. However, this study used only a few landmarks and it thus was unable to measure the effect of the cleft on surrounding surfaces. Furthermore, after surgery, the philtrum of the upper lip showed a minor shift towards the scar tissue of the cleft side owing to insufficient approximation of the orbicularis oris muscle fibres during primary cheiloplasty and scar tissue formation.

At the four-year follow-up, the residual deviation of the nose towards the non-cleft side after surgery was still noted. The mediolateral correction of the nose obtained in the primary surgery was retained four years after surgery owing to the adequate support achieved by the repositioning of the lower border of the nasal septum to its correct position at the anterior nasal spine. McComb and Coghlan (1996) noted that uncorrected lateral deviation of the nasal septum during primary surgery persisted until adulthood.

Unlike the nose, the lip showed a significant shift of the philtrum towards the scar tissue of the cleft side. This shift in the growth of the upper lip was due to the inadequate approximation of the orbicularis oris muscle fibres during primary surgery. The superficial fibres of this muscle pass from one side and insert on the skin of the philtral ridge of the other side (Figure 4.2) crossing in the midline and forming the philtral dimple where no muscle fibres insert on the skin (Latham and Deaton, 1976). Tension forces on the skin of the upper lip develop because of inadequate proximation of the orbicularis

muscle fibres in the primary surgery. Hence, during the healing process, scar tissue develops that can pull the lip towards it. It could be argued that this asymmetry is caused by the surgical repair of the cleft palate. However, the pattern of asymmetry noticed did not affect the lateral side of the lip or the cheek do not support this claim, drawing attention to the role of lip scarring on the asymmetry.

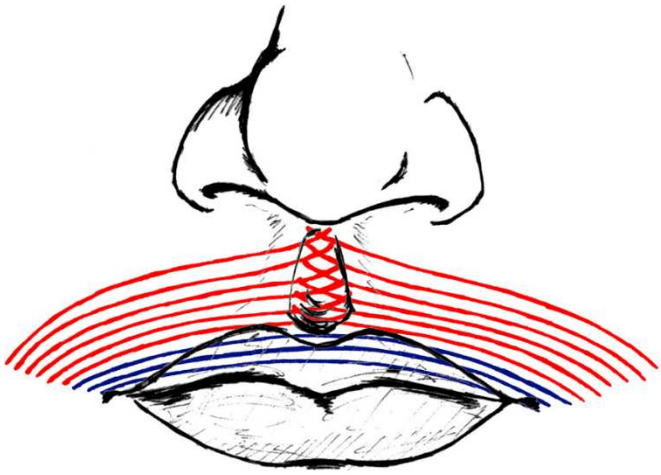

Figure 4.2: The orbicularis oris muscle consists of deep fibres (blue) and superficial fibres (red) (Rogers et al., 2014).

During smiling, a considerable shift of the upper lip towards the scar tissue of the affected side was noted. Offerman et al. (1964) recorded a pronounced displacement of the lip's landmarks laterally on the cleft side in comparison with the non-cleft side. Typically, during smiling, the zygomaticus major muscle contraction is responsible for pulling the corner of the mouth and upper lip upward and laterally (Peck et al., 1992). An impairment in the

lateral movement of the orbicularis muscle was recorded in cleft patients. This impairment was due to the altered anatomy of the upper lip after primary lip surgery and lip scarring. The scar tissue is devoid of muscle fibres and extends vertically in the upper lip, restricting the lateral movement of the lip (Trotman et al., 2007a).

Anatomically, the orbicularis oris muscle consists of two parts, each with different function: the pars peripheralis (superficial/external) and the pars marginalis (deep/intrinsic) (Figure 4.2). The deep part extends horizontally from one modiolus to the other and acts as a constrictor that seals the mouth, whereas the external component runs in the oblique direction and merges with the facial muscles of facial expressions, e.g. the levator labii superioris and zygomaticus minor (Figure 4.3). The superficial part acts as a retractor of the upper lip. During primary lip surgery, the muscle fibres of both parts have to be accurately repaired, considering the muscles fibres' direction. (Park and Ha, 1995; Rogers et al., 2014).

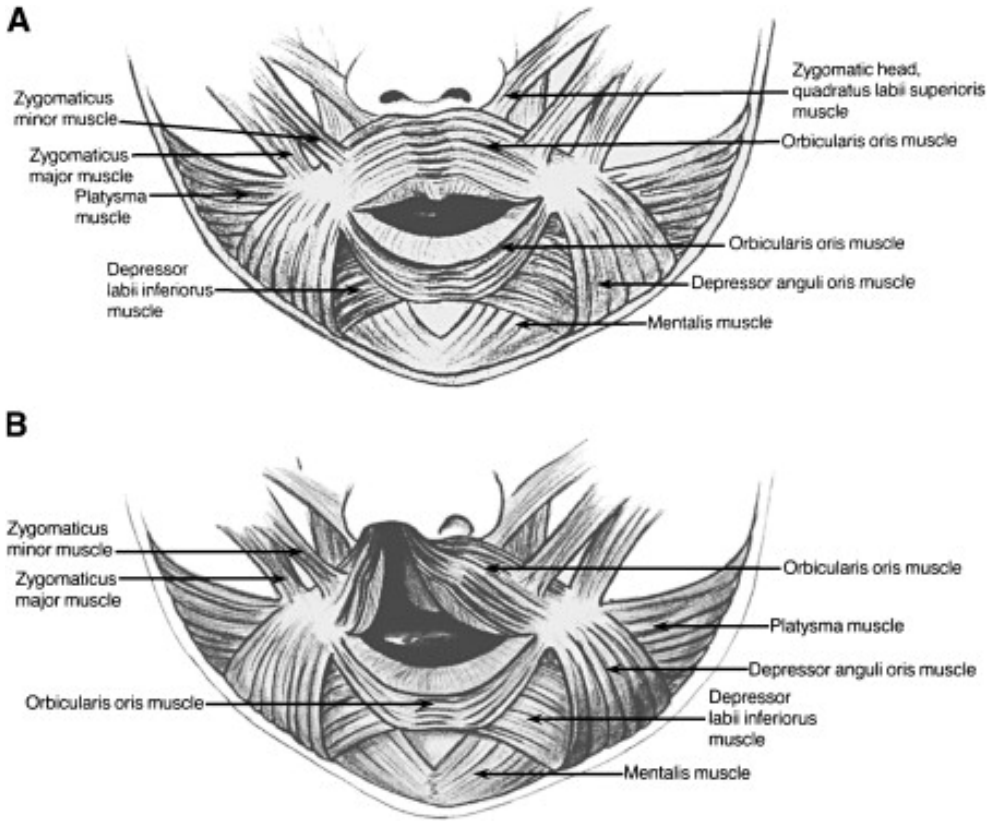

Figure 4.3: Diagram illustrates the anatomy of facial muscles, A: without cleft, B: with cleft, (Arosarena, 2007).

Before surgery, the upper lip and corner of the mouth showed a shortening at the cleft side due to the vertical running of the orbicularis oris muscle from its origin in the modiolus up towards its abnormal insertion in the piriform aperture and the nostril. In comparison with non-cleft side, the alar base was inferiorly positioned on the cleft side. This was attributed to the loss of the perioral and perinasal muscles to their anterior-caudal attachment with the nasal septum. The musculoaponeurotic system was inferoposteriorly, and laterally pulled by the zygomatic muscles. Furthermore, the superfacial musculoaponeurotic was inferiorly displaced by the oblique course of the orbicularis muscle on the cleft side (Anastassov and Joos, 2001).

After surgery, the vertical asymmetry of the total face, upper lip and nose were significantly improved. The vertical deficiency of the upper lip has improved by modified Millard cheiloplasty. Nevertheless, residual asymmetry was noted at the corner of the mouth and the alar base of the nose. This vertical deficiency at the corner of the mouth could be due to the inadequate mobilisation of the orbicularis muscle during the primary surgery. Another reason for this vertical deficiency could be the scar tissue formed after primary lip repair. An incision anterior to the inferior turbinate that extends superiorly along the pyriform rim could be considered to avoid this problem. The inferiorly malposed alar base present on the cleft side before surgery was not completely restored after surgery. During primary surgery, the normal attachment of the muscles of the nose and upper lip (the levator labii superioris alaeque nasi, the levator anguli oris and the oblique fibres of the orbicularis oris) should be restored (Anastassov and Joos, 2001).

At the four-year follow-up, the vertical residual asymmetry at the corner of the mouth and the alar base, which was noted postoperatively, was still present. Adequate compensation by primary surgery is important as it would be maintained four years after surgery.

During maximum smile, the asymmetry scores of the total face, upper lip and nose decreased in the vertical direction. However, the decrease was not significant. It appears that, to some extent, maximum smiling masks facial asymmetry in a vertical direction. This could be due to the balanced upward forces produced by the zygomatic muscles during smiling, as these muscles were not affected by the cleft. The vertical deficiency of the upper lip on the cleft side extended upwards to include the alar base. Inadequate mobilisation and suturing of the bundles of the levator labii superioris alaeque nasi muscle with corresponding muscles on the non-cleft side is the main cause of this deficiency. This muscle has two muscle fibres: one inserted in the lateral alar cartilage and the other in the orbicularis oris muscle. The contraction of this muscle during smiling pulls the nares and the upper lip upwards.

Before surgery, deficiency in the anteroposterior direction was identified at the nares, upper lip, and paranasal area of the affected side, which is caused by the unequal balance forces produced by the zygomaticus muscles on the sides of the face. This was owing to insufficient bony support by the underlying cleft maxilla on the side where the cleft was present (Markus et al., 1992).

Unlike the mediolateral and vertical asymmetries, the anteroposterior asymmetry was managed to some extent by surgery. The backward deficiency of the cleft side could be related to two main factors: the genetic growth deficiency and the iatrogenic factor caused by primary surgery. The paranasal muscles were insufficiently dissected and elevated up to the zygomatic prominence on the cleft side. The effects of both factors cannot be separated. Though the impact of growth is uncontrollable, the effect of surgery can be refined and improved. Complete dissection of the lateral alaeque nasi muscle and subperiosteal undermining around the pyriform fossa

and nasal bone up to the infraorbital foramen and maxillary-zygomatic suture are necessary.

At the four-year follow-up, the anteroposterior deficiency at the nares, paranasal area, and upper lip increased. This deficiency, which increased with age, could be due to two factors: the iatrogenic factor produced by the palatal surgery and the genetically-programmed growth deficiency. Palatal surgery inhibits the growth of the maxilla due to the exposer of the palatal bone and subsequent scar tissue formation (Ross, 1987; Kuijpers-Jagtman and Long, 2000). Intrinsic factors responsible for cleft formation and development are responsible for the deficiency in growth potential (Liao and Mars, 2005). The programmed growth deficiency in cleft patients is one of the phenotypic characteristics of cleft deformities. Another factor that needs to be considered is the impact of scar tissue of the lip after primary surgery. Both lip scarring and palatal cleft repair contribute to anteroposterior deficiency of the nasolabial growth of the cleft side (Naqvi et al., 2015). Radiographic assessment would be required to separate the effect of the lip surgery from the palatal surgery, which was not possible in this study.

During smiling, the anteroposterior asymmetry of the upper lip, nose and the face significantly increased. The insufficient bony support in complete UCLP, which is related to the cleft maxilla, accentuated the imbalanced muscle forces during smiling.

In summary, facial asymmetry dramatically improved after lip repair. However, residual asymmetry can be identified specifically at the nasal tip. The residual asymmetry was more pronounced after growth and showed a different pattern from that seen after surgery, where it was more pronounced at the nares. Facial asymmetry increased during smiling with the major impact on the lip morphology, which showed a lateral shift towards the scar tissue of the cleft side.

The residual anteroposterior asymmetry was more pronounced than the mediolateral and vertical asymmetry at the specific time intervals of this study for two reasons: lip and palatal scaring and the inadequate underlying bony support of the cleft maxilla.

4.8 Comparison with the control group

The control group was characterised by a generally symmetrical pattern of the face. Unlike the cleft group, the nasolabial region was the most symmetrical region in the control group. The upper third of the face is usually the most asymmetrical region in non-cleft children (Farkas and Cheung, 1981). The asymmetry scores of the nose, upper lip and the total face for cleft patients were significantly more than those in the control group.

In terms of the mediolateral direction, there was a significant difference between surgically manged cleft patients at eight months and the control group for the total face, nose and upper lip. In the control subjects, the tip of the nose and the philtrum of the upper lip deviated towards the left side. The finding is in agreement with the results of Farkas and Cheung (1981) who found that the right side of the face was larger in healthy children. In comparison to the control subjects, the noses of surgically managed cleft patients shifted towards the non-cleft side, while the philtrum shifted towards the scar tissue of the cleft side. The preoperative shifting of the nose towards the non-cleft side was not completely restored after surgery. In comparison to the control subjects, the surgically managed cleft cases displayed a different pattern of asymmetry in the nasolabial region. Mainly, the nose and the philtrum shift towards one side. However, in surgically managed cleft patients, the nose and upper lip shift in opposite directions, aggravating the asymmetry.

Vertically, the difference between the control group and surgically managed cleft patients was significant in this direction. The alae of the nose were the least symmetrical facial region in the control subjects. Vertical shortening was evident in the right alar. In surgically managed cleft patients, residual vertical deficiency was noted on the cleft side at the corner of the mouth, while the alar base was inferiorly positioned. The primary surgery did not completely restore the vertical asymmetry of the upper lip and the nose on the cleft side. However, the vertical asymmetry at the alar base could be accepted as the control group showed vertical deficiency of the right alar of the nose.

In the anteroposterior direction, the face of healthy infants was entirely symmetrical in this direction. The asymmetry of the total face, upper lip, and nose of surgically managed cleft patients was higher significantly than that of the non-cleft control group. This symmetry of the control group could be attributed to the anteroposterior bony support provided by the intact maxilla that is not the case in cleft patients. Improvements in the nasal asymmetry of cleft patients have been demonstrated after alveolar bone grafting (Devlin et al., 2007).

White (2005) studied the asymmetry of this control group at the age of three months, six months, one year, and two years. The results showed that the asymmetry scores of the face slightly decreased with time and the changes were not significant between the successive age groups. The changes in the asymmetry scores of the nares and nasal rim were not consistent, while the asymmetry scores of the upper lip decreased with time.

The changes in the asymmetry scores of the control group were different from the changes observed in this study that showed an increase in the asymmetry scores of UCLP over time.

4.8.1 Deviation from perfect symmetry

About 81% of the control group and only 26% of the cleft patients were close to a perfectly symmetrical nose. The figures for the lip were 66% and 6% for the control group and cleft children, respectively. Previous studies showed significant differences in facial asymmetry between cleft and controls and have concluded that achieving normal symmetry among cleft patients is challenging (Hood et al., 2003; Bilwatsch et al., 2006). Van Loon et al. (2011) found that only 18% of cleft patients in their study were close to having a perfectly symmetrical nose. They concluded that the Afroze technique, which they applied in their study, was not able to achieve near-normal symmetry.

It is clear from the results that the asymmetry scores of the nose for all the non-cleft babies were less than 2mm, while the asymmetry scores of the upper lip showed more variations and about 14% of the non-cleft babies had asymmetry scores of >2mm. Therefore, any asymmetry following surgery would be notable clearly in the nose.

4.9 Clinical rationale behind dense correspondence analysis in facial asymmetry assessment

This method gives surgeons a realistic tool for measuring facial asymmetry before surgery, after surgery, at rest and during various functions. It has a clear impact on the decision of surgical technique required and additional revision surgeries to correct the postsurgical residual asymmetry. Furthermore, it can guide surgeons to modify their surgical techniques where necessary to overcome residual asymmetry in the future. It represents an advanced step towards overcoming subjectivity in assessing the asymmetry, and it goes further by introducing a realistic visualisation aid for facial

asymmetry assessment that can be used as an educational tool for the patients and their parents. Furthermore, 3D colour-coded maps can demonstrate the residual asymmetry in the nasolabial region and explain the goals of corrective surgery to patients. It can help avoid over expectations and get a valid consent form.

The unprecedented innovation of the present study was that it analysed facial asymmetry in three directions. This analysis provided an indication of the muscle responsible for residual asymmetry, and can help refine surgery where necessary.

4.10 Correlation between initial severity of cleft lip and residual asymmetry

In this study, different patterns of correlations were noted between asymmetry scores of the nose, face and upper lip at specific time intervals. Before surgery, the asymmetry scores of the nose, face and upper lip were strongly correlated as both the nose and the upper lip were affected by the presence of the cleft. After surgery, the correlation between the asymmetry scores of the upper lip and nose did not exist, but the asymmetry scores of the upper lip and nose were correlated with total facial asymmetry. During the surgery, the upper lip and nose were reconstructed as two individual units. So, the associated asymmetry ceased to exist, and was related to the asymmetry of the total face as two separate anatomical units. At the four-year follow-up, only the asymmetry scores of the nose were correlated with the asymmetry scores of the face. The residual asymmetry of the nose had a significant impact on facial asymmetry. It has been reported that improvement in nasal asymmetry after rhinoplasty improves the total face symmetry, the influential role of the nose on facial asymmetry is attributed

to both the position of the nose at the centre of the face and its protrusion (Carvalho et al., 2013).

The correlations between asymmetry scores before surgery and asymmetry scores after surgery were not significant. We noted only a weak correlation between the asymmetry score of the nose after surgery and that of the total face before surgery. However, a significant correlation was identified between the asymmetry scores of the nose at the four-year follow-up and both the asymmetry scores of the nose after surgery and before surgery. This indicates the residual asymmetry of the nose at four years following primary surgery was related to the residual postoperative nasal asymmetry and the preoperative asymmetry. Therefore, the magnitude of postoperative nasal asymmetry is crucial. McComb and Coghlan (1996) demonstrated the potential effect of primary rhinoplasty, where improper placement of the alar base in primary rhinoplasty did not correct itself until alveolar bone grafting (McComb and Coghlan, 1996). It was noted that quality of primary repair of the cleft nose is important for growth and long-term aesthetic outcomes (Berkeley, 1959; Salyer, 1986). The deterioration of nasal asymmetry with age was due to lack of normal growth potential in cleft patients, an intrinsic factor responsible for developmental deficiency leading to the development of a cleft and potential growth deficiency (Liao and Mars, 2005). It was stated that nasal dysmorphology in most cleft patients was related to the primary dysmorphology of nasal soft tissue (Lindsay and Farkas, 1972). It was noticed that some of the corrected nasal dysmorphology returned to its original, preoperative deformed status (Uchida, 1971).

Unlike the nose, this correlation was not present for the lip, probably because of the earlier rapid growth of the lip in comparison with the nose. Thus, the lip retains the quality of surgical repair, while the impact of growth is more pronounced on the nose. The vertical growth of the skin part of the lip is rapid in the first year of a child's life, and it reaches to 80.2% of its

adult size for both sexes. The rapid growth in nose width and height occur between three to four and one to four years, respectively. By the age of five years, the nose height and width has reached 79% and 87.1% of their adult size, respectively (Farkas et al., 1992b).

The initial severity of cleft was measured using four ratios. Nostril base width ratio and median cleft width ratio measured the horizontal cleft severity; while nostril length ratio and philtrum height ratio measured the vertical cleft severity. There was no significant correlation between the initial severity ratios, residual asymmetries after surgery and at four-year follow-up.

Hood (2005) found no correlation between initial cleft severity and residual asymmetry scores at the age of two years. It was suggested that ultimate surgical outcomes were not affected by initial cleft severity. Another explanation was that in less severe cases, the underlying defect was more severe and affected the outcomes (Hood, 2005). This observation was based on the 3D appearance of the soft tissue morphology of the nasolabial region. Perhaps a different conclusion may be obtained if 3D skeletal analysis was conducted.

Mortier et al. (1997) found a moderate correlation between rating scores of initial cleft severity and residual dysmorphology. In their study, the scores were based on subjective measuring using a rating grid. Hurwitz et al. (1999) found a weak correlation between initial cleft severity and residual nasolabial deformities. The analysis in their study was based on 2D photographs guided by a rating grid.

The agreement between these results and those reported by Hood (2005) can be attributed to the fact that the data were stereophotogrammetric images in both studies and the method used for measuring the severity was based on

calculating the ratios between the distances of the cleft and non-cleft side for the nose and the lip.

It is clear that the ratios of the nasal morphology before surgery did not reflect the significant correlations that were identified between the asymmetry scores before surgery and those at the four-year follow-up. This is a new piece of information which is our research adds to the existing literature. This finding should be taken into consideration at the early stage of primary repair of the cleft lip and palate. The need for future surgical correction including rhinoplasty should be made clear to the children and their families. It is worth noting that before surgery, the asymmetry scores and the ratios showed significant correlations, confirming the validity of the asymmetry scores in representing the initial dysmorphology before surgery.

Chapter five

Conclusions & suggestions

5 Chapter five: Conclusions and suggestions

5.1 Conclusions and translational value of the study

Residual facial asymmetries were detected and identified after primary lip repair. The residual asymmetry was mostly at the tip of the nose. Primary lip repair requires further refinement to reduce residual asymmetry. UCLP patients may require further surgical intervention to deal with the residual asymmetry.

At 4 years follow-up the residual asymmetry was more pronounced and showed different pattern. The residual asymmetry was mostly at the philtrum of the upper lip and nares. Patients/parents should be informed of the likelihood of asymmetry occurring after lip repair and the deterioration of asymmetry in the nasolabial region during growth. The timing of revision surgery should be delayed until growth is completed (after prepubertal growth spurt).

Facial expressions accentuate the residual asymmetry, with greatest impact being on the upper lip. Before lip revision surgery, it is necessary to evaluate and consider the residual asymmetry when the face is static and during facial expressions.

We are able, for the first time, to identify the residual asymmetries in each of the three directions (x, y, z). That has clinical impact by disclosing the potential cause of asymmetry. The residual asymmetries after primary lip repair were higher among cleft infants than non-cleft infants in the three directions. The anteroposterior asymmetry of the nasolabial region of UCLP was pronounced at all time intervals. This was due to the inadequate bony support of cleft maxilla and genetic deficiency of maxillary growth. Dramatic shifting of the upper lip towards the scar tissue of the affected side during

smiling was recorded. The conformed generic mesh is a reliable and innovative tool for comprehensive facial analysis.

Residual asymmetry of the nose at four-year follow-up was correlated to the initial nasal asymmetry and postoperative residual nasal asymmetry. This should be considered in the early stage of primary lip repair. Parents/patients should be informed of the likelihood of the need for rhinoplasty in the future.

During the surgical repair, the orbicularis oris muscle has to be adequately dissected and rotated in the downward direction to eliminate the residual vertical deficiency at the corner of the mouth on the affected side. An incision in the internal lateral side of the nose should be considered to reduce this deficiency.

To avoid the shifting of the philtrum of the upper lip toward the scar tissue on the affected side, the superficial and deep fibres of the orbicularis muscle have to be accurately repaired according to the direction of the muscle fibres. The shifting of the philtrum was due to incomplete approximation of the muscle fibres during surgery.

The levator labii superioris alaeque nasi muscle of the cleft side has to be reflected and sutured to the corresponding muscle fibres on the other side. This will help to avoid the residual shifting of the nose to the non-cleft side, and to eliminate the residual vertical deficiency of the alar base on the cleft side during smiling.

Subperiosteal undermining in the paranasal area is necessary to reduce the anteroposterior deficiency on the cleft side. Scar tissue is the main reason for transverse, vertical and anteroposterior asymmetry.

5.2 Suggestions for future studies

1. Long-term follow up of the same cohort to assess facial asymmetry after the pubertal growth spurt, and comparing the results with an age-matched control group.
2. Application of the generic facial mesh to assess the impact of facial expressions on the residual facial asymmetry of surgically managed cleft patients using 4D dynamic imaging.
3. Application of generic facial mesh to evaluate the residual asymmetry of UCLP patients that have undergone different treatment protocols
4. Evaluate of the facial asymmetry of different cleft groups (UCL, CP) and compare the residual asymmetry with the UCLP group, using generic facial mesh.
5. Develop a mathematical scoring index for asymmetry assessment of cleft patients and patients with abnormal facial muscles movement.
6. Application of generic facial mesh to investigate the impact of nasoalveolar moulding treatment on the dysmorphology, or residual dysmorphology. Nasoalveolar moulding is very controversial, it is expensive and there is a significant burden of care on the patient/ parent. There is no evidence that it helps significantly at the moment. The application of generic mesh to look at the cases where nasoalveolar moulding has been used can help to resolve this debate.
7. Using Magnetic Resonance Imaging to provide better visualisation of muscle asymmetry and extent of lip scaring.

8. Consider patients' attitudes to facial asymmetry and include subjective evaluation of residual facial asymmetry by exploring patients' opinions.

Chapter six

References

6 Chapter six: References

Agrawal, K., Panda, K., 2011. A Modified Surgical Schedule for Primary Management of Cleft Lip and Palate in Developing Countries. Cleft Palate-Craniofacial J. 48, 1–8. doi:10.1597/09-226

Agrawal, K., Panda, K.N., 2006. Use of Vomer Flap in Palatoplasty: Revisited. Cleft Palate-Craniofacial J. 43, 30–37. doi:10.1597/04-034.1

Al-Hiyali, A., Ayoub, A., Ju, X., Almuzian, M., Al-Anezi, T., 2015. The Impact of Orthognathic Surgery on Facial Expressions. J. Oral Maxillofac. Surg. 73, 2380–2390. doi:10.1016/j.joms.2015.05.008

Al-Omari, I., Millett, D.T., Ayoub, A.F., 2005. Methods of Assessment of Cleft-Related Facial Deformity: A Review. Cleft Palate-Craniofacial J. 42, 145–156. doi:10.1597/02-149.1

Aldridge, K., Boyadjiev, S.A., Capone, G.T., DeLeon, V.B., Richtsmeier, J.T., 2005. Precision and error of three-dimensional phenotypic measures acquired from 3dMD photogrammetric images. Am. J. Med. Genet. Part A 138A, 247–253. doi:10.1002/ajmg.a.30959

Almukhtar, A., Ayoub, A., Khambay, B., McDonald, J., Ju, X., 2016. State-of-the-art three-dimensional analysis of soft tissue changes following Le Fort I maxillary advancement. Br. J. Oral Maxillofac. Surg. 54, 812–817. doi:10.1016/j.bjoms.2016.05.023

Almukhtar, A., Khambay, B., Ju, X., McDonald, J., Ayoub, A., 2017. Accuracy of generic mesh conformation: The future of facial morphological analysis. JPRAS Open 14, 39–48. doi:10.1016/j.jpra.2017.08.003

Alqattan, M., Djordjevic, J., Zhurov, A.I., Richmond, S., 2013. Comparison between landmark and surface-based three-dimensional analyses of facial asymmetry in adults. Eur. J. Orthod. 37, 1–12. doi:10.1093/ejo/cjt075

Anastassov, G.E., Joos, U., 2001. Comprehensive management of cleft lip and palate deformities. J. Oral Maxillofac. Surg. 59, 1062–1075. doi:10.1053/joms.2001.25852

Anderl, H., Hussl, H., Ninkovic, M., 2008. Primary Simultaneous Lip and Nose Repair in the Unilateral Cleft Lip and Palate. Plast. Reconstr. Surg. 121, 959–970. doi:10.1097/01.prs.0000299942.84302.16

Antonarakis, G.S., Tompson, B.D., Fisher, D.M., 2015. Preoperative Cleft Lip Measurements and Maxillary Growth in Patients With Unilateral Cleft Lip and Palate. Cleft Palate-Craniofacial J. 52, 150204130143000. doi:10.1597/14-274R1

Arosarena, O.A., 2007. Cleft Lip and Palate. Otolaryngol. Clin. North Am. 40, 27–60. doi:10.1016/j.otc.2006.10.011

Ayoub, A., Garrahy, A., Millett, D., Bowman, A., Siebert, J.P., Miller, J., Ray, A., 2011a. Three-Dimensional Assessment of Early Surgical Outcome in Repaired Unilateral Cleft Lip and Palate: Part 1. Nasal Changes. Cleft Palate-Craniofacial J. 48, 571–577. doi:10.1597/09-147

Ayoub, A., Garrahy, A., Millett, D., Bowman, A., Siebert, J.P., Miller, J., Ray, A., 2011b. Three-dimensional assessment of early surgical outcome in repaired unilateral cleft lip and palate: part 2. Lip changes. Cleft Palate. Craniofac. J. 48, 578–83. doi:10.1597/09-148

Ayoub, A.F., Garrahy, A., Hood, C., White, J., Bock, M., Siebert, J.P., Spencer, R., Ray, A., 2003. Validation of a vision-based, three-dimensional facial

imaging system. Cleft Palate-Craniofacial J. 40, 523–529. doi:10.1597/02-067

Balaji, S., 2013. Textbook of Oral & Maxillofacial Surgery., 2nd ed. Elsevier India.

Batlle, J., Mouaddib, E., Salvi, J., 1998. Recent progress in coded structured light as a technique to solve the correspondence problem. Pattern Recognit. 31, 963–982. doi:10.1016/S0031-3203(97)00074-5

Baudouin, J.-Y., Tiberghien, G., 2004. Symmetry, averageness, and feature size in the facial attractiveness of women. Acta Psychol. (Amst). 117, 313–332. doi:10.1016/j.actpsy.2004.07.002

Bell, A., Lo, T.-W.R., Brown, D., Bowman, A.W., Siebert, J.P., Simmons, D.R., Millett, D.T., Ayoub, A.F., 2014. Three-Dimensional Assessment of Facial Appearance Following Surgical Repair of Unilateral Cleft Lip and Palate. Cleft Palate-Craniofacial J. 51, 462–471. doi:10.1597/12-140

Berkeley, W.T., 1959. The Cleft-Llip nose. Plast. Reconstr. Surg. 23, 567–575. doi:10.1097/00006534-195906000-00001

Berkowitz, S., 2013. Cleft Lip and Palate, Third Edit. ed, Cleft lip and palate. Springer Berlin Heidelberg, Berlin, Heidelberg. doi:10.1007/978-3-642-30770-6

Besl, P.J., McKay, N.D., 1992. A method for registration of 3-D shapes. IEEE Trans. Pattern Anal. Mach. Intell. 14, 239–256. doi:10.1109/34.121791

Bilwatsch, S., Kramer, M., Haeusler, G., Schuster, M., Wurm, J., Vairaktaris, E., Neukam, F.W., Nkenke, E., 2006. Nasolabial symmetry following Tennison – Randall lip repair : A three-dimensional approach in 10-year-old patients

with unilateral clefts of lip , alveolus and palate. J. Cranio-Maxillofacial Surg. 34, 253–262. doi:10.1016/j.jcms.2006.03.001

Bishara, S.E., Burkey, P.S., Kharouf, J.G., 1994. Dental and facial asymmetries: a review. Angle Orthod. 64, 89–98. doi:10.1043/0003-3219(1994)064<0089:DAFAAR>2.0.CO;2

Bishara, S.E., Ortho, D., Jakobsen, J.R., 1985. Longitudinal changes in three normal facial types. Am. J. Orthod. 88, 466–502. doi:10.1016/S0002-9416(85)80046-4

Boo-Chai, K., 1966. An ancient Chinese text on a cleft lip. Plast. Reconstr. Surg. 38, 89–91.

Bookstein, F.L., 1989. Principal warps: thin-plate splines and the decomposition of deformations. IEEE Trans. Pattern Anal. Mach. Intell. 11, 567–585. doi:10.1109/34.24792

Bozic, M., Kau, C.H., Richmond, S., Ihan Hren, N., Zhurov, A., Udovič, M., Melink, S., Ovsenik, M., 2009. Facial Morphology of Slovenian and Welsh White Populations Using 3-Dimensional Imaging. Angle Orthod. 79, 640–645. doi:10.2319/081608-432.1

Božič, M., Kau, C.H., Richmond, S., Ovsenik, M., Hren, N.I., 2010. Novel method of 3-dimensional soft-tissue analysis for Class III patients. Am. J. Orthod. Dentofac. Orthop. 138, 758–769. doi:10.1016/j.ajodo.2009.01.033

Brody, A.S., Frush, D.P., Huda, W., Brent, R.L., 2007. Radiation Risk to Children From Computed Tomography. Pediatrics 120, 677–682. doi:10.1542/peds.2007-1910

Brons, S., van Beusichem, M.E., Maal, T.J.J., Plooij, J.M., Bronkhorst, E.M.,

Bergé, S.J., Kuijpers-Jagtman, a M., 2013. Development and reproducibility of a 3D stereophotogrammetric reference frame for facial soft tissue growth of babies and young children with and without orofacial clefts. Int. J. Oral Maxillofac. Surg. 42, 2–8. doi:1016/j.ijom.2012.07.006

Bugaighis, I., Mattick, C.R., Tiddeman, B., Hobson, R., 2014a. 3D asymmetry of operated children with oral clefts. Orthod. Craniofac. Res. 17, 27–37. doi:10.1111/ocr.12026

Bugaighis, I., Mattick, C.R., Tiddeman, B., Hobson, R., 2014b. 3D Facial Morphometry in Children With Oral Clefts. Cleft Palate-Craniofacial J. 51, 452–461. doi:10.1597/12-217

Bugaighis, I., Tiddeman, B., Mattick, C.R., Hobson, R., 2014c. 3D comparison of average faces in subjects with oral clefts. Eur. J. Orthod. 36, 365–372. doi:10.1093/ejo/cjs060

Burke, P.H., Beard, L.F.H., 1967. Stereophotogrammetry of the face. Am. J. Orthod. 53, 769–782. doi:10.1016/0002-9416(67)90121-2

Burt, J.D., Byrd, H.S., 2000. Cleft Lip: Unilateral Primary Deformities. Plast. Reconstr. Surg. 105, 1043–1055. doi:10.1097/00006534-200003000-00032

Campbell, A., Costello, B.J., Ruiz, R.L., 2010. Cleft Lip and Palate Surgery: An Update of Clinical Outcomes for Primary Repair. Oral Maxillofac. Surg. Clin. North Am. 22, 43–58. doi:10.1016/j.coms.2009.11.003

Carlson, D.S., 2005. Theories of Craniofacial Growth in the Postgenomic Era. Semin. Orthod. 11, 172–183. doi:10.1053/j.sodo.2005.07.002

Carvalho, B., Ballin, A., Becker, R., Berger, C., Hurtado, J., Mocellin, M., 2013. Rhinoplasty and facial asymmetry: Analysis of subjective and

anthropometric factors in the Caucasian nose. Int. Arch. Otorhinolaryngol. 16, 445–451. doi:10.7162/S1809-97772012000400004

Cevidanes, L.H.S., Franco, A.A., Gerig, G., Proffit, W.R., Slice, D.E., Enlow, D.H., Yamashita, H.K., Kim, Y.J., Scanavini, M.A., Vigorito, J.W., 2005. Assessment of mandibular growth and response to orthopedic treatment with 3-dimensional magnetic resonance images. Am. J. Orthod. Dentofac. Orthop. 128, 16–26. doi:10.1016/j.ajodo.2004.03.032

Chang, H.P., Liu, P.H., Chang, H.F., Chang, C.H., 2002. Thin-plate spline (TPS) graphical analysis of the mandible on cephalometric radiographs. Dentomaxillofacial Radiol. 31, 137–141. doi:10.1038/sj.dmfr.4600681

Chapman, K.L., Hardin-Jones, M.A., Goldstein, J.A., Halter, K.A., Havlik, R.J., Schulte, J., 2008. Timing of Palatal Surgery and Speech Outcome. Cleft Palate-Craniofacial J. 45, 297–308. doi:10.1597/06-244

Chatrath, P., De Cordova, J., Nouraei, S.A.R., Ahmed, J., Saleh, H.A., 2007. Objective Assessment of Facial Asymmetry in Rhinoplasty Patients. Arch. Facial Plast. Surg. 9, 184–187. doi:10.1001/archfaci.9.3.184

Cheung, M.Y., Almukhtar, A., Keeling, A., Hsung, T.-C., Ju, X., McDonald, J., Ayoub, A., Khambay, B.S., 2016. The Accuracy of Conformation of a Generic Surface Mesh for the Analysis of Facial Soft Tissue Changes. PLoS One 11, e0152381. doi:10.1371/journal.pone.0152381

Chiu, Y.-T., Liao, Y.-F., 2012. Is Cleft Severity Related to Maxillary Growth in Patients With Unilateral Cleft Lip and Palate? Cleft Palate-Craniofacial J. 49, 535–540. doi:10.1597/10-044

Claes, P., Walters, M., Clement, J., 2012. Improved facial outcome assessment using a 3D anthropometric mask. Int. J. Oral Maxillofac. Surg. 41, 324–330.

doi:10.1016/j.ijom.2011.10.019

Claes, P., Walters, M., Vandermeulen, D., Clement, J.G., 2011. Spatially-dense 3D facial asymmetry assessment in both typical and disordered growth. J. Anat. 219, 444–455. doi:10.1111/j.1469-7580.2011.01411.x

Clark, J.D., Mossey, P.A., Sharp, L., Little, J., 2003. Socioeconomic Status and Orofacial Clefts in Scotland, 1989 to 1998. Cleft Palate-Craniofacial J. 40, 481–485. doi:10.1597/1545-1569(2003)040<0481:SSAOCI>2.0.CO;2

Clark, S.L., Teichgraeber, J.F., Fleshman, R.G., Shaw, J.D., Chavarria, C., Kau, C.-H., Gateno, J., Xia, J.J., 2011. Long-Term Treatment Outcome of Presurgical Nasoalveolar Molding in Patients With Unilateral Cleft Lip and Palate. J. Craniofac. Surg. 22, 333–336. doi:10.1097/SCS.0b013e318200d874

Dado, D. V, Kernahan, D.A., 1985. Anatomy of the orbicularis oris muscle in incomplete unilateral cleft lip based on histological examination. Ann Plast Surg 15, 90–98.

Demke, J.C., Tatum, S.A., 2011. Analysis and evolution of rotation principles in unilateral cleft lip repair. J. Plast. Reconstr. Aesthetic Surg. 64, 313–318. doi:10.1016/j.bjps.2010.03.004

Devlin, M.F., Ray, A., Raine, P., Bowman, A., Ayoub, A.F., 2007. Facial Symmetry in Unilateral Cleft Lip and Palate Following Alar Base Augmentation With Bone Graft: A Three-Dimensional Assessment. Cleft Palate-Craniofacial J. 44, 391–395. doi:10.1597/06-179.1

Dindaroğlu, F., Kutlu, P., Duran, G.S., Görgülü, S., Aslan, E., 2016. Accuracy and reliability of 3D stereophotogrammetry: A comparison to direct anthropometry and 2D photogrammetry. Angle Orthod. 86, 487–494. doi:10.2319/041415-244.1

Djordjevic, J., Lewis, B.M., Donaghy, C.E., Zhurov, A.I., Knox, J., Hunter, L., Richmond, S., 2014a. Facial shape and asymmetry in 5-year-old children with repaired unilateral cleft lip and/or palate: an exploratory study using laser scanning. Eur. J. Orthod. 36, 497–505. doi:10.1093/ejo/cjs075

Djordjevic, J., Pirttiniemi, P., Harila, V., Heikkinen, T., Toma, A.M., Zhurov, A.I., Richmond, S., 2013. Three-dimensional longitudinal assessment of facial symmetry in adolescents. Eur. J. Orthod. 35, 143–151. doi:10.1093/ejo/cjr006

Djordjevic, J., Toma, A.M., Zhurov, A.I., Richmond, S., 2014b. Three-dimensional quantification of facial symmetry in adolescents using laser surface scanning. Eur. J. Orthod. 36, 125–132. doi:10.1093/ejo/cjr091

Drake, D., Colbert, S., 2017. Techniques for Cleft Lip Repair, in: Maxillofacial Surgery. Elsevier, pp. 948–971. doi:10.1016/B978-0-7020-6056-4.00067-8

Duffy, S., Noar, J.H., Evans, R.D., Sanders, R., 2000. Three-Dimensional Analysis of the Child Cleft Face. Cleft Palate-Craniofacial J. 37, 137–144. doi:10.1597/1545-1569(2000)037<0137:TDAOTC>2.3.CO;2

Ercan, I., Ozdemir, S.T., Etoz, A., Sigirli, D., Tubbs, R.S., Loukas, M., Guney, I., 2008. Facial asymmetry in young healthy subjects evaluated by statistical shape analysis. J. Anat. 213, 663–669. doi:10.1111/j.1469-7580.2008.01002.x

Fára, M., 1968. Anatomy and arteriography of cleft lips in stillborn children. Plast. Reconstr. Surg. 42, 29–36.

Farkas, L., 1994. Anthropometry of the Head and Face., 2nd ed. ed. New York: Raven Press.

Farkas, L.G., Cheung, G., 1981. Facial asymmetry in healthy North American Caucasians. An anthropometrical study. Angle Orthod. 51, 70–7. doi:10.1043/0003-3219(1981)051<0070:FAIHNA>2.0.CO;2

Farkas, L.G., Hajniš, K., Posnick, J.C., 1993. Anthropometric and Anthroposcopic Findings of the Nasal and Facial Region in Cleft Patients before and after Primary Lip and Palate Repair. Cleft Palate-Craniofacial J. 30, 1–12. doi:10.1597/1545-1569(1993)030<0001:AAAFOT>2.3.CO;2

Farkas, L.G., Posnick, J.C., Hreczko, T.M., 1992a. Growth Patterns of the Face: A Morphometric Study. Cleft Palate-Craniofacial J. 29, 308–315. doi:10.1597/1545-1569(1992)029<0308:GPOTFA>2.3.CO;2

Farkas, L.G., Posnick, J.C., Hreczko, T.M., Pron, G.E., 1992b. Growth Patterns of the Nasolabial Region: A Morphometric Study. Cleft Palate-Craniofacial J. 29, 318–324. doi:10.1597/1545-1569(1992)029<0318:GPOTNR>2.3.CO;2

Farronato, G., Kairyte, L., Giannini, L., Galbiati, G., Maspero, C., 2014. How various surgical protocols of the unilateral cleft lip and palate influence the facial growth and possible orthodontic problems? Which is the best timing of lip, palate and alveolus repair? literature review. Stomatologija 16, 53–60.

Ferrario, V.F., Sforza, C., Ciusa, V., Dellavia, C., Tartaglia, G.M., 2001. The effect of sex and age on facial asymmetry in healthy subjects: A cross-sectional study from adolescence to mid-adulthood. J. Oral Maxillofac. Surg. 59, 382–388. doi:10.1053/joms.2001.21872

Ferrario, V.F., Sforza, C., Poggio, C.E., Tartaglia, G., 1994. Distance from symmetry: A three-dimensional evaluation of facial asymmetry. J. Oral Maxillofac. Surg. 52, 1126–1132. doi:10.1016/0278-2391(94)90528-2

Ferris, H.C., 1927. Original photographic studies of orthodontic cases. Int. J.

Orthod. Oral Surg. Radiogr. 13, 627–637. doi:10.1016/S0099-6963(27)90118-5

Filho, L.C., Normando, A.D., da Silva Filho, O.G., 1996. Isolated Influences of Lip and Palate Surgery on Facial Growth: Comparison of Operated and Unoperated Male Adults with UCLP. Cleft Palate-Craniofacial J. 33, 51–56. doi:10.1597/1545-1569(1996)033<0051:IIOLAP>2.3.CO;2

Fisher, D.M., Lo, L.-J., Chen, Y.-R., Noordhoff, M.S., 1999. Three-Dimensional Computed Tomographic Analysis of the Primary Nasal Deformity in 3-Month-Old Infants with Complete Unilateral Cleft Lip and Palate. Plast. Reconstr. Surg. 103, 1826–1834. doi:10.1097/00006534-199906000-00003

Fitzsimons, K.J., Mukarram, S., Copley, L.P., Deacon, S.A., van der Meulen, J.H., 2012. Centralisation of services for children with cleft lip or palate in England: a study of hospital episode statistics. BMC Health Serv. Res. 12, 148. doi:10.1186/1472-6963-12-148

Fox, L.M., Stone, P.A., 2013. Examining the Team Process: Developing and Sustaining Effective Craniofacial Team Care, in: Berkowitz, S. (Ed.), Cleft Lip and Palate Management and Diagnosis. Springer Berlin Heidelberg, Berlin, Heidelberg, pp. 1–5. doi:10.1007/978-3-642-30770-6

Friede, H., 2007. Maxillary Growth Controversies After Two-Stage Palatal Repair With Delayed Hard Palate Closure in Unilateral Cleft Lip and Palate Patients: Perspectives From Literature and Personal Experience. Cleft Palate-Craniofacial J. 44, 129–136. doi:10.1597/06-037.1

Friede, H., Enemark, H., 2001. Long-Term Evidence for Favorable Midfacial Growth After Delayed Hard Palate Repair in UCLP Patients. Cleft Palate-Craniofacial J. 38, 323–329. doi:10.1597/1545-1569(2001)038<0323:LTEFFM>2.0.CO;2

Furlow, L.T., 1995. Cleft palate repair by double opposing z-plasty. Oper. Tech. Plast. Reconstr. Surg. 2, 223–232. doi:10.1016/S1071-0949(06)80036-3

Gallacher, M., Gillgrass, T., 2015. Cleft Care Scotland National Managed Clinical Network Annual Report 2014 / 2015. http://www.knowledge.scot.nhs.uk/media/CLT/ResourceUploads/4069636/55245f11-2b58-42e7-89ab-fc66643d21a4.pdf.

Garrahy, A., 2002. Three-dimensional assessment of dentofacial deformity in children with clefts. PhD thesis, University of Glasgow.

Gillies, H., Fry, W., 1921. A new principle in the surgical treatment of "congenital cleft palate'' and its mechanical counterpart. Br. Med. J. 5, 335–8.

Gomez, D.F., Donohue, S.T., Figueroa, A.A., Polley, J.W., 2012. Nasal Changes After Presurgical Nasoalveolar Molding (PNAM) in the Unilateral Cleft Lip Nose. Cleft Palate-Craniofacial J. 49, 689–700. doi:10.1597/11-007

Goodacre, T.E.E., Hentges, F., Moss, T.L.H., Short, V., Murray, L., 2004. Does Repairing a Cleft Lip Neonatally Have Any Effect on the Longer-Term Attractiveness of the Repair? Cleft Palate-Craniofacial J. 41, 603–608. doi:10.1597/03-028.1

Greene, D., 1931. Asymmetry of the head and face in infants and children. Arch. Pediatr. Adolesc. Med. 41, 1317. doi:10.1001/archpedi.1931.01940120054006

Gunther, E., Wisser, J.R., Cohen, M.A., Brown, A.S., 1998. Palatoplasty: Furlow's Double Reversing Z-Plasty Versus Intravelar Veloplasty. Cleft Palate-Craniofacial J. 35, 546–549. doi:10.1597/1545-1569(1998)035<0546:PFSDRZ>2.3.CO;2

Guo, J., Mei, X., Tang, K., 2013. Automatic landmark annotation and dense correspondence registration for 3D human facial images. BMC Bioinformatics 14, 232. doi:10.1186/1471-2105-14-232

Habel, A., Sell, D., Mars, M., 1996. Management of cleft lip and palate. Arch. Dis. Child. 74, 360–366. doi:10.1136/adc.74.4.360

Hajeer, M.Y., Ayoub, A.F., Millett, D.T., 2004a. Three-dimensional assessment of facial soft-tissue asymmetry before and after orthognathic surgery. Br. J. Oral Maxillofac. Surg. 42, 396–404. doi:10.1016/j.bjoms.2004.05.006

Hajeer, M.Y., Millett, D.T., Ayoub, A.F., Siebert, J.P., 2004b. Current Products and Practices. J. Orthod. 31, 154–162. doi:10.1179/146531204225020472

Hallac, R.R., Feng, J., Kane, A.A., Seaward, J.R., 2017. Dynamic facial asymmetry in patients with repaired cleft lip using 4D imaging (video stereophotogrammetry). J. Cranio-Maxillofacial Surg. 45, 8–12. doi:10.1016/j.jcms.2016.11.005

Hammond, P., 2007. The use of 3D face shape modelling in dysmorphology. Arch. Dis. Child. 92, 1120–1126. doi:10.1136/adc.2006.103507

Hammond, P., Hutton, T.J., Allanson, J.E., Campbell, L.E., Hennekam, R.C.M., Holden, S., Patton, M.A., Shaw, A., Temple, I.K., Trotter, M., Murphy, K.C., Winter, R.M., 2004. 3D analysis of facial morphology. Am. J. Med. Genet. 126A, 339–348. doi:10.1002/ajmg.a.20665

Harrison, J.A., Nixon, M.A., Fright, W.R., Snape, L., 2004. Use of hand-held laser scanning in the assessment of facial swelling: a preliminary study. Br. J. Oral Maxillofac. Surg. 42, 8–17. doi:10.1016/S0266-4356(03)00192-X

Hartmann, J., Meyer-Marcotty, P., Benz, M., Häusler, G., Stellzig-Eisenhauer,

A., 2007. Reliability of a Method for Computing Facial Symmetry Plane and Degree of Asymmetry Based on 3D-data. J. Orofac. Orthop. / Fortschritte der Kieferorthopädie 68, 477–490. doi:10.1007/s00056-007-0652-y

Heike, C.L., Cunningham, M.L., Hing, A. V, Stuhaug, E., Starr, J.R., 2009. Picture Perfect? Reliability of Craniofacial Anthropometry Using Three-Dimensional Digital Stereophotogrammetry. Plast. Reconstr. Surg. 124, 1261–1272. doi:10.1097/PRS.0b013e3181b454bd

Higgins, J.E., 2009. Curve Extraction and Facial Analysis Using Statistical Techniques. PhD thesis, University of Glasgow.

Hoffman, D., Dyleram, D., 2011. Comparison of the Millard and Fisher technique for closure of the unilateral cleft lip. Int. J. Oral Maxillofac. Surg. 40, e14. doi:10.1016/j.ijom.2011.07.1061

Hood, C.A., 2005. Three-Dimensional Assessment of Facial Morphology in infants with Cleft Lip and Palate. PhD thesis, University of Glasgow.

Hood, C.A., Bock, M., Hosey, M.T., Bowman, A., Ayoub, A.F., 2003. Facial asymmetry - 3D assessment of infants with cleft lip & palate. Int. J. Paediatr. Dent. 13, 404–410. doi:10.1046/j.1365-263X.2003.00496.x

Hood, C.A., Hosey, M.T., Bock, M., White, J., Ray, A., Ayoub, A.F., 2004. Facial Characterization of Infants With Cleft Lip and Palate Using a Three-Dimensional Capture Technique. Cleft Palate-Craniofacial J. 41, 27–35. doi:10.1597/02-143

Huang, A.H., Patel, K.B., Maschhoff, C.W., Huebener, D. V, Skolnick, G.B., Naidoo, S.D., Woo, A.S., 2015. Occlusal Classification in Relation to Original Cleft Width in Patients With Unilateral Cleft Lip and Palate. Cleft Palate-Craniofacial J. 52, 574–578. doi:10.1597/13-263

Huang, C.-S., Wang, W.-I., Jein-Wein Liou, E., Chen, Y.-R., Kao-Ting Chen, P., Noordhoff, M.S., 2002. Effects of Cheiloplasty on Maxillary Dental Arch Development in Infants With Unilateral Complete Cleft Lip and Palate. Cleft Palate-Craniofacial J. 39, 513–516. doi:10.1597/1545-1569(2002)039<0513:EOCOMD>2.0.CO;2

Huang, C.S., Liu, X.Q., Chen, Y.R., 2013. Facial asymmetry index in normal young adults. Orthod. Craniofac. Res. 16, 97–104. doi:10.1111/ocr.12010

Hurwitz, D.J., Ashby, E.R., Llull, R., Pasqual, J., Tabor, C., Garrison, L., Gillen, J., Weyant, R., 1999. Computer-Assisted Anthropometry for Outcome Assessment of Cleft Lip. Plast. Reconstr. Surg. 103, 1608–1623. doi:10.1097/00006534-199905060-00007

Inui, M., Fushima, K., Sato, S., 1999. Facial asymmetry in temporomandibular joint disorders. J. Oral Rehabil. 26, 402–406. doi:10.1046/j.1365-2842.1999.00387.x

Islam, S.M.S., Goonewardene, M.S., Farella, M., 2015. A Review on Three Dimensional Facial Averaging for the Assessment of Orthodontic Disorders. Innov. Adv. Comput. Informatics, Syst. Sci. Netw. Eng. Lect. Notes Electr. Eng. 313, 391–397.

James, J.N., Costello, B.J., Ruiz, R.L., 2014. Management of Cleft Lip and Palate and Cleft Orthognathic Considerations. Oral Maxillofac. Surg. Clin. North Am. 26, 565–572. doi:10.1016/j.coms.2014.08.007

Johnson, N., 2000. Initial cleft size does not correlate with outcome in unilateral cleft lip and palate. Eur. J. Orthod. 22, 93–100. doi:10.1093/ejo/22.1.93

Johnston, D.J., Millett, D.T., Ayoub, A.F., Bock, M., 2003. Are facial expressions reproducible? Cleft Palate-Craniofacial J. 40, 291–296. doi:10.1597/1545-

1569(2003)040<0291:AFER>2.0.CO;2

Joos, U., 1995. Skeletal growth after muscular reconstruction for cleft lip, alveolus, and palate. Br. J. Oral Maxillofac. Surg. 33, 139–144. doi:10.1016/0266-4356(95)90285-6

Ju, X., Siebert, J.P., 2001a. Individualising Human Animation Models, in: Eurographics Short Presentations. Manchester, UK.

Ju, X., Siebert, P., 2001b. Conforming Generic Animatable Models to 3D Scanned Data., in: International Conference of Numberisation 3D - Scanning. Paris, France.

Kamburoğlu, K., Kolsuz, E., Murat, S., Eren, H., Yüksel, S., Paksoy, C.S., 2013. Assessment of buccal marginal alveolar peri-implant and periodontal defects using a cone beam CT system with and without the application of metal artefact reduction mode. Dentomaxillofacial Radiol. 42, 20130176. doi:10.1259/dmfr.20130176

Karad, A., 2014. Clinical Orthodontics: Current Concepts, Goals and Mechanics, 2nd ed. Elsevier India.

Kasaven, C.P., McIntyre, G.T., Mossey, P.A., 2017. Accuracy of both virtual and printed 3-dimensional models for volumetric measurement of alveolar clefts before grafting with alveolar bone compared with a validated algorithm: a preliminary investigation. Br. J. Oral Maxillofac. Surg. 55, 31–36. doi:10.1016/j.bjoms.2016.08.016

Kau, C.H., Richmond, S., 2010. Three-Dimensional Imaging for Orthodontics and Maxillofacial Surgery. John Wiley & Sons, Ltd., West Sussex, UK. doi:10.1002/9781118786642

Kau, C.H., Richmond, S., Palomo, J.M., Hans, M.G., 2005a. Current Products and Practice. J. Orthod. 32, 282–293. doi:10.1179/146531205225021285

Kau, C.H., Richmond, S., Zhurov, A., Ovsenik, M., Tawfik, W., Borbely, P., English, J.D., 2010. Use of 3-dimensional surface acquisition to study facial morphology in 5 populations. Am. J. Orthod. Dentofac. Orthop. 137, S56.e1-S56.e9. doi:10.1016/j.ajodo.2009.04.022

Kau, C.H., Richmond, S., Zhurov, A.I., Knox, J., Chestnutt, I., Hartles, F., Playle, R., 2005b. Reliability of measuring facial morphology with a 3-dimensional laser scanning system. Am. J. Orthod. Dentofac. Orthop. 128, 424–430. doi:10.1016/j.ajodo.2004.06.037

Kau, C.H., Zhurov, A., Richmond, S., Bibb, R., Sugar, A., Knox, J., Hartles, F., 2006. The 3-Dimensional Construction of the Average 11-Year-Old Child Face: A Clinical Evaluation and Application. J. Oral Maxillofac. Surg. 64, 1086–1092. doi:10.1016/j.joms.2006.03.013

Kaufman, Y., Buchanan, E., Wolfswinkel, E., Weathers, W., Stal, S., 2012. Cleft nasal deformity and rhinoplasty. Semin. Plast. Surg. 26, 184–190. doi:10.1055/s-0033-1333886

Kernahan, D., 1971. The striped Y—a symbolic classification for cleft lip and palate. Plast Reconstr Surg 47, 469–470.

Kernhan, D.A., Stark, R.B., 1958. A new classification for cleft lip and cleft palate. Plast. Reconstr. Surg. 22, 435-.

Khambay, B., Nairn, N., Bell, A., Miller, J., Bowman, A., Ayoub, A.F., 2008. Validation and reproducibility of a high-resolution three-dimensional facial imaging system. Br. J. Oral Maxillofac. Surg. 46, 27–32. doi:10.1016/j.bjoms.2007.04.017

Khambay, B., Ullah, R., 2015. Current methods of assessing the accuracy of three-dimensional soft tissue facial predictions: technical and clinical considerations. Int. J. Oral Maxillofac. Surg. 44, 132–8. doi:10.1016/j.ijom.2014.04.007

Kolar, J., Salter, E., 1997. Craniofacial Anthropometry: Practical Measurement of the Head and Face for Clinical, Surgical and Research Use. Springfield,IL: Charles C. Thomas.

Kornreich, D., Mitchell, A.A., Webb, B.D., Cristian, I., Jabs, E.W., 2016. Quantitative Assessment of Facial Asymmetry Using Three-Dimensional Surface Imaging in Adults: Validating the Precision and Repeatability of a Global Approach. Cleft Palate-Craniofacial J. 53, 126–131. doi:10.1597/13-353

Koudelová, J., Brůžek, J., Cagáňová, V., Krajíček, V., Velemínská, J., 2015. Development of facial sexual dimorphism in children aged between 12 and 15 years: a three-dimensional longitudinal study. Orthod. Craniofac. Res. 18, 175–184. doi:10.1111/ocr.12096

Kriens, O., 1989. LAHSHAL—a concise documentation system for cleft lip, alveolus and palate diagnoses, in: Kriens OE, Ed. What Is a Cleft Lip and Palate? A Multidisciplinary Update. New York: Thieme Medical Publishers.

Krimmel, M., Kluba, S., Breidt, M., Bacher, M., Müller-Hagedorn, S., Dietz, K., Bülthoff, H., Reinert, S., 2013. Three-Dimensional Assessment of Facial Development in Children With Unilateral Cleft Lip With and Without Alveolar Cleft. J. Craniofac. Surg. 24, 313–316. doi:10.1097/SCS.0b013e318275ed60

Kuijpers-Jagtman, A.M., Long, R.E., 2000. The Influence of Surgery and Orthopedic Treatment on Maxillofacial Growth and Maxillary Arch

Development in Patients Treated for Orofacial Clefts. Cleft Palate-Craniofacial J. 37, 527–527. doi:10.1597/1545-1569(2000)037<0527:TIOSAO>2.0.CO;2

Kuijpers, M.A., Desmedt, D.J., Nada, R.M., Bergé, S.J., Fudalej, P.S., Maal, T.J., 2015. Regional facial asymmetries in unilateral orofacial clefts. Eur. J. Orthod. 37, 636–642. doi:10.1093/ejo/cju104

Kürkçüoğlu, A., Abbas, O.L., Ayan, D.M., Baykan, R., Demirkan, E., Özkan, Ö., Özkubat, I., Şimşek, M., 2016. Comparison of objective and subjective assessments for perception of facial symmetry. Anatomy 10, 94–98. doi:10.2399/ana.16.012

Kusnoto, B., Evans, C.A., 2002. Reliability of a 3D surface laser scanner for orthodontic applications. Am. J. Orthod. Dentofac. Orthop. 122, 342–348. doi:10.1067/mod.2002.128219

Laberge, L.C., 2007. Unilateral cleft lip and palate: Simultaneous early repair of the nose, anterior palate and lip. Can. J. Plast. Surg. 15, 13–18.

LaRossa, D., 2000. The State of the Art in Cleft Palate Surgery. Cleft Palate-Craniofacial J. 37, 225–228. doi:10.1597/1545-1569(2000)037<0225:TSOTAI>2.3.CO;2

Latham, R. a, Deaton, T.G., 1976. The structural basis of the philtrum and the contour of the vermilion border: a study of the musculature of the upper lip. J. Anat. 121, 151–60.

Lele, S., 1991. Some comments on coordinate-free and scale-invariant methods in morphometrics. Am. J. Phys. Anthropol. 85, 407–417. doi:10.1002/ajpa.1330850405

Lele, S., Richtsmeier, J.T., 1992. On comparing biological shapes: Detection of influential landmarks. Am. J. Phys. Anthropol. 87, 49–65. doi:10.1002/ajpa.1330870106

LeMesurier, A.B., 1949. A method of cutting and suturing the lip in the treatment of complete unilateral clefts. Plast. Reconstr. Surg. 4, 1–12. doi:10.1097/00006534-194901000-00001

Li, A.-Q., Sun, Y.-G., Wang, G.-H., Zhong, Z.-K., Cutting, C., 2002. Anatomy of the Nasal Cartilages of the Unilateral Complete Cleft Lip Nose. Plast. Reconstr. Surg. 109, 1835–1838. doi:10.1097/00006534-200205000-00009

Li, G., Wei, J., Wang, X., Wu, G., Ma, D., Wang, B., Liu, Y., Feng, X., 2013. Three-dimensional facial anthropometry of unilateral cleft lip infants with a structured light scanning system. J. Plast. Reconstr. Aesthetic Surg. 66, 1109–1116. doi:10.1016/j.bjps.2013.04.007

Li, H., Yang, Y., Chen, Y., Wu, Y., Zhang, Y., Wu, D., Liang, Y., 2011. Three-Dimensional Reconstruction of Maxillae Using Spiral Computed Tomography and Its Application in Postoperative Adult Patients With Unilateral Complete Cleft Lip and Palate. J. Oral Maxillofac. Surg. 69, e549–e557. doi:10.1016/j.joms.2011.07.024

Li, Y., Shi, B., Song, Q.-G., Zuo, H., Zheng, Q., 2006. Effects of lip repair on maxillary growth and facial soft tissue development in patients with a complete unilateral cleft of lip, alveolus and palate. J. Cranio-Maxillofacial Surg. 34, 355–361. doi:10.1016/j.jcms.2006.03.005

Liao, Y.-F., Mars, M., 2005. Long-Term Effects of Clefts on Craniofacial Morphology in Patients With Unilateral Cleft Lip and Palate. Cleft Palate-Craniofacial J. 42, 601–609. doi:10.1597/04-163R.1

Liao, Y.-F., Prasad, N.K.K., Chiu, Y.-T., Yun, C., Chen, P.K.-T., 2010. Cleft size at the time of palate repair in complete unilateral cleft lip and palate as an indicator of maxillary growth. Int. J. Oral Maxillofac. Surg. 39, 956–961. doi:10.1016/j.ijom.2010.01.024

Lindsay, W.K., Farkas, L.G., 1972. The use of anthropometry in assessing the cleft-lip nose. Plast. Reconstr. Surg. 49, 286–93.

Liou, E.J.-W., Subramanian, M., Chen, P.K.T., Huang, C.S., 2004. The Progressive Changes of Nasal Symmetry and Growth after Nasoalveolar Molding: A Three-Year Follow-Up Study. Plast. Reconstr. Surg. 114, 858–864. doi:10.1097/01.PRS.0000133027.04252.7A

Liu, Q., Yang, M.L., Li, Z.J., Bai, X.F., Wang, X.K., Lu, L., Wang, Y.X., 2007. A simple and precise classification for cleft lip and palate: A five-digit numerical recording system. Cleft Palate-Craniofacial J. 44, 465–468. doi:10.1597/06-140.1

Lübbers, H.-T., Medinger, L., Kruse, A., Grätz, K.W., Matthews, F., 2010. Precision and Accuracy of the 3dMD Photogrammetric System in Craniomaxillofacial Application. J. Craniofac. Surg. 21, 763–767. doi:10.1097/SCS.0b013e3181d841f7

Ma, L., Xu, T., Lin, J., 2009. Validation of a three-dimensional facial scanning system based on structured light techniques. Comput. Methods Programs Biomed. 94, 290–298. doi:10.1016/j.cmpb.2009.01.010

Maal, T.J.J., van Loon, B., Plooij, J.M., Rangel, F., Ettema, A.M., Borstlap, W.A., Bergé, S.J., 2010. Registration of 3-Dimensional Facial Photographs for Clinical Use. J. Oral Maxillofac. Surg. 68, 2391–2401. doi:10.1016/j.joms.2009.10.017

Mah, J.K., Danforth, R.A., Bumann, A., Hatcher, D., 2003. Radiation absorbed in maxillofacial imaging with a new dental computed tomography device. Oral Surgery, Oral Med. Oral Pathol. Oral Radiol. Endodontology 96, 508–513. doi:10.1016/S1079-2104(03)00350-0

Mao, Z., Ju, X., Siebert, J.P., Cockshott, W.P., Ayoub, A., 2006. Constructing dense correspondences for the analysis of 3D facial morphology. Pattern Recognit. Lett. 27, 597–608. doi:10.1016/j.patrec.2005.09.025

Markus, A.F., Smith, W.P., Delaire, J., 1992. Facial balance in cleft lip and palate. II. Cleft lip and palate and secondary deformities. Br. J. Oral Maxillofac. Surg. 30, 296–304. doi:10.1016/0266-4356(92)90179-M

Maull, D.J., Grayson, B.H., Cutting, C.B., Brecht, L.L., Bookstein, F.L., Khorrambadi, D., Webb, J.A., Hurwitz, D.J., 1999. Long-Term Effects of Nasoalveolar Molding on Three-Dimensional Nasal Shape in Unilateral Clefts. Cleft Palate-Craniofacial J. 36, 391–397. doi:10.1597/1545-1569(1999)036<0391:LTEONM>2.3.CO;2

Mcavinchey, G., 2013. The Perception of facial asymmetry. PhM thesis, University of Birmingham.

McBride, W.A., McIntyre, G.T., Carroll, K., Mossey, P.A., 2016. Subphenotyping and Classification of Orofacial Clefts: Need for Orofacial Cleft Subphenotyping Calls for Revised Classification. Cleft Palate-Craniofacial J. 53, 539–549. doi:10.1597/15-029

McBride, W.A., Mossey, P.A., McIntyre, G.T., 2013. Reliability, completeness and accuracy of cleft subphenotyping as recorded on the CLEFTSiS (Cleft Service in Scotland) electronic patient record. Surgeon 11, 313–318. doi:10.1016/j.surge.2013.05.003

McComb, H.K., 1975. Treatment of unilateral cleft lip nose. Plast. Reconstr. Surg. 55, 596–601.

McComb, H.K., Coghlan, B.A., 1996. Primary Repair of the Unilateral Cleft Lip Nose: Completion of a Longitudinal Study. Cleft Palate-Craniofacial J. 33, 23–31. doi:10.1597/1545-1569(1996)033<0023:PROTUC>2.3.CO;2

McIntyre, G.T., Mossey, P.A., 2002. Asymmetry of the parental craniofacial skeleton in orofacial clefting. J. Orthod. 29, 299–305. doi:10.1093/ortho/29.4.299

Meulstee, J.W., Verhamme, L.M., Borstlap, W.A., Van der Heijden, F., De Jong, G.A., Xi, T., Bergé, S.J., Delye, H., Maal, T.J.J., 2017. A new method for three-dimensional evaluation of the cranial shape and the automatic identification of craniosynostosis using 3D stereophotogrammetry. Int. J. Oral Maxillofac. Surg. 46, 819–826. doi:10.1016/j.ijom.2017.03.017

Meyer-Marcotty, P., Kochel, J., Boehm, H., Linz, C., Klammert, U., Stellzig-Eisenhauer, A., 2011. Face perception in patients with unilateral cleft lip and palate and patients with severe Class III malocclusion compared to controls. J. Cranio-Maxillofacial Surg. 39, 158–163. doi:10.1016/j.jcms.2010.05.001

Millard, D.R., 1968. Extensions of the rotation-advancement principle for wide unilateral cleft lips. Plast. Reconstr. Surg. 42, 535–44.

Millard, D.R., 1957. A primary camoulflage in the unilateral hairlip, in: Transactions of the International Congress of Plastic Surgeons, Williams and Wilkins, , Baltimore. p. 160.

Miller, L., Morris, D.O., Berry, E., 2007. Visualizing three-dimensional facial soft tissue changes following orthognathic surgery 29, 14–20.

doi:10.1093/ejo/cjl037

Mohler, L.R., 1987. Unilateral cleft lip repair. Plast Reconstr Surg 80, 511–517.

Morioka, D., Sato, N., Kusano, T., Muramatsu, H., Tosa, Y., Ohkubo, F., Yoshimoto, S., 2015. Difference in nasolabial features between awake and asleep infants with unilateral cleft lip: Anthropometric measurements using three-dimensional stereophotogrammetry. J. Cranio-Maxillofacial Surg. 43, 2093–2099. doi:10.1016/j.jcms.2015.09.002

Mortier, P.B., Martinot, V.L., Anastassov, V., Kulik, J.F., Duhamel, A., Pellerin, P.N., 1997. Evaluation of the Results of Cleft Lip and Palate Surgical Treatment: Preliminary Report. Cleft Palate-Craniofacial J. 34, 247–255. doi:10.1597/1545-1569(1997)034<0247:EOTROC>2.3.CO;2

Moss, J.P., Linney, A.D., Grindrod, S.R., Mosse, C.A., 1989. A laser scanning system for the measurement of facial surface morphology. Opt. Lasers Eng. 10, 179–190. doi:10.1016/0143-8166(89)90036-5

Moss, M.L., Young, R.W., 1961. A functional approach to craniology. Am. J. Orthod. 47, 928–931. doi:10.1016/0002-9416(61)90166-X

Mossey, P.A., Little, J., Munger, R.G., Dixon, M.J., Shaw, W.C., 2009. Cleft lip and palate. Lancet 374, 1773–1785. doi:10.1016/S0140-6736(09)60695-4

Mossey, P.A., Modell, B., 2012. Epidemiology of Oral Clefts 2012: An International Perspective, in: Frontiers of Oral Biology. pp. 1–18. doi:10.1159/000337464

Mulliken, J.B., Martínez-Pérez, D., 1999. The Principle of Rotation Advancement for Repair of Unilateral Complete Cleft Lip and Nasal Deformity: Technical Variations and Analysis of Results. Plast. Reconstr. Surg. 104, 1247–1460.

doi:10.1097/00006534-199910000-00003

Nahai, F.R., Williams, J.K., Burstein, F.D., Martin, J., Thomas, J., 2005. The Management of Cleft Lip and Palate: Pathways for Treatment and Longitudinal Assessment. Semin. Plast. Surg. 19, 275–285. doi:10.1055/s-2005-925900

Nakamura, N., Suzuki, A., Takahashi, H., Honda, Y., Sasaguri, M., Ohishi, M., 2005. A Longitudinal Study on Influence of Primary Facial Deformities on Maxillofacial Growth in Patients With Cleft Lip and Palate. Cleft Palate-Craniofacial J. 42, 633–640. doi:10.1597/03-151.1

Naqvi, Z., Ravi, S., Shivalinga, B., Munawwar, S., 2015. Effect of cleft lip palate repair on craniofacial growth. J. Orthod. Sci. 4, 59. doi:10.4103/2278-0203.160236

Naudi, K.B., Benramadan, R., Brocklebank, L., Ju, X., Khambay, B., The, A.A., 2013. The virtual human face : Superimposing the simultaneously captured 3D photorealistic skin surface of the face on the untextured skin image of the CBCT scan 393–400. doi:10.1016/j.ijom.2012.10.032

Nemtoi, A., Czink, C., Haba, D., Gahleitner, A., 2013. Cone beam CT: a current overview of devices. Dentomaxillofacial Radiol. 42, 20120443. doi:10.1259/dmfr.20120443

Nguyen, C.X., Nissanov, J., Ozturk, C., Nuveen, M.J., Tuncay, O.C., 2000. Three-dimensional imaging of the craniofacial complex. Clin. Orthod. Res. 3, 46–50. doi:10.1034/j.1600-0544.2000.030108.x

Noordhoff, M.S., 1984. Reconstruction of vermilion in unilateral and bilateral cleft lips. Plast. Reconstr. Surg. 73, 52–61.

Nord, F., Ferjencik, R., Seifert, B., Lanzer, M., Gander, T., Matthews, F., Rücker, M., Lübbers, H.T., 2015. The 3dMD photogrammetric photo system in cranio-maxillofacial surgery: Validation of interexaminer variations and perceptions. J. Cranio-Maxillofacial Surg. 43, 1798–1803. doi:10.1016/j.jcms.2015.08.017

O'Grady, K.F., Antonyshyn, O.M., 1999. Facial asymmetry: three-dimensional analysis using laser surface scanning. Plast. Reconstr. Surg. 104, 928–37.

Offerman, R.E., Cleall, J.F., Subtelny, J.D., 1964. Symmetry of lip activity in repaired unilateral clefts of lip. Cleft Palate J. 35, 347–56.

Ort, R., Metzler, P., Kruse, A.L., Matthews, F., Zemann, W., Grätz, K.W., Luebbers, H.-T., 2012. The Reliability of a Three-Dimensional Photo System-(3dMDface-) Based Evaluation of the Face in Cleft Lip Infants. Plast. Surg. Int. 2012, 1–8. doi:10.1155/2012/138090

Ovsenik, M., Perinetti, G., Zhurov, A., Richmond, S., Primozic, J., 2014. Three-dimensional assessment of facial asymmetry among pre-pubertal class III subjects: A controlled study. Eur. J. Orthod. 36, 431–435. doi:10.1093/ejo/cjt069

Ozsoy, U., 2016. Comparison of Different Calculation Methods Used to Analyze Facial Soft Tissue Asymmetry: Global and Partial 3-Dimensional Quantitative Evaluation of Healthy Subjects. J. Oral Maxillofac. Surg. 74, 1847.e1-1847.e9. doi:10.1016/j.joms.2016.05.012

Ozsoy, U., Sekerci, R., Ogut, E., 2015. Effect of sitting, standing, and supine body positions on facial soft tissue: detailed 3D analysis. Int. J. Oral Maxillofac. Surg. 44, 1309–1316. doi:10.1016/j.ijom.2015.06.005

Pai, B.C.-J., Ko, E.W.-C., Huang, C.-S., Liou, E.J.-W., 2005. Symmetry of the

Nose After Presurgical Nasoalveolar Molding in Infants With Unilateral Cleft Lip and Palate: A Preliminary Study. Cleft Palate-Craniofacial J. 42, 658–663. doi:10.1597/04-126.1

Pallanch, J., 2011. 3-D Imaging Technologies for Facial Plastic Surgery, An Issue of Facial Plastic Surgery Clinics, 1st ed. Saunders.

Palmer, A., Strobeck, C., 1992. Fluctuating asymmetry as a measure of developmental stability: implications of non-normal distributions and power of statistical tests. Acta Zool. Fenn. 191, 57–72. doi:10.1348/000712601162284

Park, B.-Y., Lew, D.-H., Lee, Y.-H., 1998. A Comparative Study of the Lateral Crus of Alar Cartilages in Unilateral Cleft Lip Nasal Deformity. Plast. Reconstr. Surg. 101, 915–920. doi:10.1097/00006534-199804040-00005

Park, C.G., Ha, B., 1995. The Importance of Accurate Repair of the Orbicularis Oris Muscle in the Correction of Unilateral Cleft Lip. Plast. Reconstr. Surg. 96, 780–788. doi:10.1097/00006534-199509001-00003

Patel, A., Islam, S.M.S., Murray, K., Goonewardene, M.S., 2015. Facial asymmetry assessment in adults using three-dimensional surface imaging. Prog. Orthod. 16, 36. doi:10.1186/s40510-015-0106-9

Peck, S., Peck, L., Kataja, M., 1992. The gingival smile line. Angle Orthod. 62, 91-100–2. doi:10.1043/0003-3219(1992)062<0091:TGSL>2.0.CO;2

Peck, S., Peck, L., Matti, K., 1991. Skeletal asymmetry in esthetically pleasing faces. Angle Orthod. 61, 43–48.

Peltomäki, T., Vendittelli, B.L., Grayson, B.H., Cutting, C.B., Brecht, L.E., 2001. Associations Between Severity of Clefting and Maxillary Growth in Patients

With Unilateral Cleft Lip and Palate Treated With Infant Orthopedics. Cleft Palate-Craniofacial J. 38, 582–586. doi:10.1597/1545-1569(2001)038<0582:ABSOCA>2.0.CO;2

Plooij, J.M., Swennen, G.R.J., Rangel, F.A., Maal, T.J.J., Schutyser, F.A.C., Bronkhorst, E.M., Kuijpers–Jagtman, A.M., Bergé, S.J., 2009. Evaluation of reproducibility and reliability of 3D soft tissue analysis using 3D stereophotogrammetry. Int. J. Oral Maxillofac. Surg. 38, 267–273. doi:10.1016/j.ijom.2008.12.009

Premkumar, S., 2011. Text book of craniofacial growth, First. ed. Jaypee Borther Medical Publisher LTD, New Delhi, St Louis, Panama City, London.

Primozic, J., Ovsenik, M., Richmond, S., Kau, C.H., Zhurov, A., 2009. Early crossbite correction: a three-dimensional evaluation. Eur. J. Orthod. 31, 352–356. doi:10.1093/ejo/cjp041

Proffit, W.R., 2013. Contemporary orthodontics, 5th ed. ed. Elsevier/Mosby, St. Louis, Mo, USA.

Ras, F., Habets, L.L.M.H., Van Ginkel, F.C., Prahl-Andersen, B., 1994. Three-Dimensional Evaluation of Facial Asymmetry in Cleft Lip and Palate. Cleft Palate-Craniofacial J. 31, 116–121. doi:10.1597/1545-1569(1994)031<0116:TDEOFA>2.3.CO;2

Ravishanker, R., 2006. Furlow's Palatoplasty for Cleft Palate Repair. Med. J. Armed Forces India 62, 239–242. doi:10.1016/S0377-1237(06)80010-9

Reddy, G.S., Webb, R.M., Reddy, R.R., Reddy, L. V, Thomas, P., Markus, a F., 2008. Choice of Incision for Primary Repair of Unilateral Complete Cleft Lip: A Comparative Study of Outcomes in 796 Patients. Plast. Reconstr. Surg. 121, 932–940. doi:10.1097/01.prs.0000299282.63111.3f

Reid, J., 2004. A Review of Feeding Interventions for Infants With Cleft Palate. Cleft Palate-Craniofacial J. 41, 268–278. doi:10.1597/02-148.1

Rogers, C.R., Meara, J.G., Mulliken, J.B., 2014. The Philtrum in Cleft Lip: Review of Anatomy and Techniques for Construction. J. Craniofac. Surg. 25, 9–13. doi:10.1097/SCS.0b013e3182a2dce4

Ross, R.B., 1987. Treatment variables affecting facial growth in complete unilateral cleft lip and palate. Cleft Palate J. 24, 5–77.

Roussel, L.O., Myers, R.P., Girotto, J.A., 2015. The Millard Rotation-Advancement Cleft Lip Repair: 50 Years of Modification. Cleft Palate-Craniofacial J. 52, e188–e195. doi:10.1597/14-276

Ryckman, M.S., Harrison, S., Oliver, D., Sander, C., Boryor, A.A., Hohmann, A.A., Kilic, F., Kim, K.B., 2010. Soft-tissue changes after maxillomandibular advancement surgery assessed with cone-beam computed tomography. Am. J. Orthod. Dentofac. Orthop. 137, S86–S93. doi:10.1016/j.ajodo.2009.03.041

Salyer, K.E., 1986. Primary correction of the unilateral cleft lip nose: a 15-year experience. Plast. Reconstr. Surg. 77, 558–68.

Salyer, K.E., Genecov, E.R., Genecov, D.G., 2004. Unilateral cleft lip-nose repair – long-term outcome. Clin. Plast. Surg. 31, 191–208. doi:10.1016/S0094-1298(03)00128-7

Salyer, K.E., Xu, H., Genecov, E.R., 2009. Unilateral Cleft Lip and Nose Repair; Closed Approach Dallas Protocol Completed Patients. J. Craniofac. Surg. 20, 1939–1955. doi:10.1097/SCS.0b013e3181b77d4d

Scarfe, W., Azevedo, B., Toghyani, S., Farman, A., 2017. Cone Beam Computed Tomographic imaging in orthodontics. Aust. Dent. J. 62, 33–50.

doi:10.1111/adj.12479

Scarfe, W., Li, Z., Aboelmaaty, W., Scott, S., Farman, A., 2012. Maxillofacial cone beam computed tomography: essence, elements and steps to interpretation. Aust. Dent. J. 57, 46–60. doi:10.1111/j.1834-7819.2011.01657.x

Schendel, S.A., 2000. Unilateral Cleft Lip Repair—State of the Art. Cleft Palate-Craniofacial J. 37, 335–341. doi:10.1597/1545-1569(2000)037<0335:UCLRSO>2.3.CO;2

Scheuer, H.A., Höltje, W.-J., Hasund, A., Pfeifer, G., 2001. Prognosis of facial growth in patients with unilateral complete clefts of the lip, alveolus and palate. J. Cranio-Maxillofacial Surg. 29, 198–204. doi:10.1054/jcms.2001.0227

Schwartz, S., Kapala, J.T., Rajchgot, H., Roberts, G.L., 1993. Accurate and systematic numerical recording system for the identification of various types of lip and maxillary clefts (RPL SYSTEM). Cleft Palate-Craniofacial J. doi:10.1597/1545-1569(1993)030<0330:AASNRS>2.3.CO;2

Schwenzer-Zimmerer, K., Boerner, B.-I., Schwenzer, N.F., Müller, A.A., Juergens, P., Ringenbach, A., Schkommodau, E., Zeilhofer, H.-F., 2009. Facial acquisition by dynamic optical tracked laser imaging: a new approach. J. Plast. Reconstr. Aesthetic Surg. 62, 1181–1186. doi:10.1016/j.bjps.2007.11.080

Schwenzer-Zimmerer, K., Chaitidis, D., Berg-Boerner, I., Krol, Z., Kovacs, L., Schwenzer, N.F., Zimmerer, S., Holberg, C., Zeilhofer, H.-F., 2008a. Quantitative 3D soft tissue analysis of symmetry prior to and after unilateral cleft lip repair compared with non-cleft persons (performed in Cambodia).

J. Cranio-Maxillofacial Surg. 36, 431–438. doi:10.1016/j.jcms.2008.05.003

Schwenzer-Zimmerer, K., Chaitidis, D., Boerner, I., Kovacs, L., Schwenzer, N.F., Holberg, C., Zeilhofer, H.-F., 2008b. Systematic Contact-Free 3D Topometry of the Soft Tissue Profile in Cleft Lips. Cleft Palate-Craniofacial J. 45, 607–613. doi:10.1597/07-116.1

Scott, J.H., 1958. The cranial base. Am. J. Phys. Anthropol. 16, 319–348. doi:10.1002/ajpa.1330160305

Scott, J.H., 1954. The growth of the human face. Proc. R. Soc. Med. 47, 91–100.

Scrimshaw, G.C., 1979. Lip adhesion--a passing fad? Ann. Plast. Surg. 2, 183–8.

Seckel, N.G., van der Tweel, I., Elema, G.A., Specken, T.F.J.M.C., 1995. Landmark Positioning on Maxilla of Cleft Lip and Palate Infant — a Reality? Cleft Palate-Craniofacial J. 32, 434–441. doi:10.1597/1545-1569(1995)032<0434:LPOMOC>2.3.CO;2

Seidenstricker-kink, L.M., Becker, D.B., Govier, D.P., Deleon, V.B., Lo, L., Kane, A.A., 2008. Comparative Osseous and Soft Tissue Morphology Following Cleft Lip Repair. Cleft Palate–Craniofacial J. 45, 511–517. doi:10.1597/07-001.1

Semb, G., Enemark, H., Friede, H., Paulin, G., Lilja, J., Rautio, J., Andersen, M., Åbyholm, F., Lohmander, A., Shaw, W., Mølsted, K., Heliövaara, A., Bolund, S., Hukki, J., Vindenes, H., Davenport, P., Arctander, K., Larson, O., Berggren, A., Whitby, D., Leonard, A., Neovius, E., Elander, A., Willadsen, E., Bannister, R.P., Bradbury, E., Henningsson, G., Persson, C., Eyres, P., Emborg, B., Kisling-Møller, M., Küseler, A., Granhof Black, B., Schöps, A., Bau, A., Boers, M., Andersen, H.S., Jeppesen, K., Marxen, D., Paaso, M., Hölttä, E., Alaluusua, S., Turunen, L., Humerinta, K., Elfving-Little, U., Tørdal, I.B., Kjøll, L., Aukner, R., Hide, Ø., Feragen, K.B.,

Rønning, E., Skaare, P., Brinck, E., Semmingsen, A.-M., Lindberg, N., Bowden, M., Davies, J., Mooney, J., Bellardie, H., Schofield, N., Nyberg, J., Lundberg, M., Karsten, A.L.-A., Larson, M., Holmefjord, A., Reisæter, S., Pedersen, N.-H., Rasmussen, T., Tindlund, R., Sæle, P., Blomhoff, R., Jacobsen, G., Havstam, C., Rizell, S., Enocson, L., Hagberg, C., Najar Chalien, M., Paganini, A., Lundeborg, I., Marcusson, A., Mjönes, A.-B., Gustavsson, A., Hayden, C., McAleer, E., Slevan, E., Gregg, T., Worthington, H., 2017. Scandcleft randomised trials of primary surgery for unilateral cleft lip and palate: 1. Planning and management. J. Plast. Surg. Hand Surg. 51, 2–13. doi:10.1080/2000656X.2016.1263202

Sforza, C., Laino, A., Grandi, G., Pisoni, L., Ferrario, V.F., 2010. Three-Dimensional Facial Asymmetry in Attractive and Normal People from Childhood to Young Adulthood. Symmetry (Basel). 2, 1925–1944. doi:10.3390/sym2041925

Shafi, M.I., Ayoub, a., Ju, X., Khambay, B., 2013. The accuracy of three-dimensional prediction planning for the surgical correction of facial deformities using Maxilim. Int. J. Oral Maxillofac. Surg. 42, 801–806. doi:10.1016/j.ijom.2013.01.015

Shah, S.M., Joshi, M.R., 1978. An assessment of asymmetry in the normal craniofacial complex. Angle Orthod. 48, 141–8. doi:10.1043/0003-3219(1978)048<0141:AAOAIT>2.0.CO;2

Sharma, P., Arora, A., Valiathan, A., 2014. Age Changes of Jaws and Soft Tissue Profile. Sci. World J. 2014, 1–7. doi:10.1155/2014/301501

Shkoukani, M.A., Chen, M., Vong, A., 2013. Cleft Lip – A Comprehensive Review. Front. Pediatr. 1, 53. doi:10.3389/fped.2013.00053

Sierra, F.J., Turner, C., 1995. of infants with cleft lip and palate. Pediatr. Dent. 17, 419–423.

Singh, G., Levy-Bercowski, D., Yáñez, M., Santiago, P., 2007. Three-dimensional facial morphology following surgical repair of unilateral cleft lip and palate in patients after nasoalveolar molding. Orthod. Craniofac. Res. 10, 161–166. doi:10.1111/j.1601-6343.2007.00390.x

Slade, P., Bishop, S.C., Jowett, R.A., 1995. Relationships between Cleft Severity and Attractiveness of Newborns with Unrepaired Clefts. Cleft Palate-Craniofacial J. 32, 318–322. doi:10.1597/1545-1569(1995)032<0318:RBCSAA>2.3.CO;2

Soncul, M., Bamber, M.A., 2004. Evaluation of facial soft tissue changes with optical surface scan after surgical correction of Class III deformities. J. Oral Maxillofac. Surg. 62, 1331–1340. doi:10.1016/j.joms.2004.04.019

Souccar, N.M., Kau, C.H., 2012. Methods of Measuring the Three-Dimensional Face. Semin. Orthod. 18, 187–192. doi:10.1053/j.sodo.2012.04.003

Spauwen, P.H.M., Goorhuis-Brouwer, S.M., Schutte, H.K., 1992. Cleft palate repair: Furlow versus von Langenbeck. J. Cranio-Maxillofacial Surg. 20, 18–20. doi:10.1016/S1010-5182(05)80190-8

Stauber, I., Vairaktaris, E., Holst, A., Schuster, M., Hirschfelder, U., Neukam, F.W., Nkenke, E., 2008. Three-dimensional Analysis of Facial Symmetry in Cleft Lip and Palate Patients Using Optical Surface Data. J. Orofac. Orthop. / Fortschritte der Kieferorthopädie 69, 268–282. doi:10.1007/s00056-008-0746-1

Suri, S., Tompson, B.D., 2004. A Modified Muscle-Activated Maxillary Orthopedic Appliance for Presurgical Nasoalveolar Molding in Infants With Unilateral

Cleft Lip and Palate. Cleft Palate-Craniofacial J. 41, 225–229. doi:10.1597/02-141.1

Suri, S., Utreja, A., Khandelwal, N., Mago, S.K., 2008. Craniofacial Computerized Tomography Analysis of the midface of patients with repaired complete unilateral cleft lip and palate. Am. J. Orthod. Dentofac. Orthop. 134, 418–429. doi:10.1016/j.ajodo.2006.09.065

Susami, T., Kamiyama, H., Uji, M., Motohashi, N., Kuroda, T., 1993. Quantitative Evaluation of the Shape and the Elasticity of Repaired Cleft Lip. Cleft Palate-Craniofacial J. 30, 309–312. doi:10.1597/1545-1569(1993)030<0309:QEOTSA>2.3.CO;2

Suzuki, A., Mukai, Y., Ohishi, M., Miyanoshita, Y., Tashiro, H., 1993. Relationship between Cleft Severity and Dentocraniofacial Morphology in Japanese Subjects with Isolated Cleft Palate and Complete Unilateral Cleft Lip and Palate. Cleft Palate-Craniofacial J. 30, 175–181. doi:10.1597/1545-1569(1993)030<0175:RBCSAD>2.3.CO;2

Talbert, L., Kau, C.H., Christou, T., Vlachos, C., Souccar, N., 2014. A 3D analysis of Caucasian and African American facial morphologies in a US population. J. Orthod. 41, 19–29. doi:10.1179/1465313313Y.0000000077

Tamada, I., Nakajima, T., 2010. Detailed assessment of cleft lip scar following straight line repair. J. Plast. Reconstr. Aesthetic Surg. 63, 282–288. doi:10.1016/j.bjps.2008.11.005

Taylor, H.O., Morrison, C.S., Linden, O., Phillips, B., Chang, J., Byrne, M.E., Sullivan, S.R., Forrest, C.R., 2014. Quantitative Facial Asymmetry. J. Craniofac. Surg. 25, 124–128. doi:10.1097/SCS.0b013e3182a2e99d

Tennison, C.W., 1952. The repair of the Unilateral cleft lip by the stencil

method. Plast. Reconstr. Surg. 9, 115–120. doi:00739888-195202000-00005

Theodorakou, C., Walker, A., Horner, K., Pauwels, R., Bogaerts, R., Jacobs Dds, R., 2012. Estimation of paediatric organ and effective doses from dental cone beam CT using anthropomorphic phantoms. Br. J. Radiol. 85, 153–160. doi:10.1259/bjr/19389412

Thomas, C., 2009. Primary Rhinoplasty by Open Approach With Repair of Bilateral Complete Cleft Lip. J. Craniofac. Surg. 20, 1715–1718. doi:10.1097/SCS.0b013e3181b3ef2c

Thompson, L.A., Malmberg, J., Goodell, N.K., Boring, R.L., 2004. The Distribution of Attention Across a Talker's Face. Discourse Process. 38, 145–168. doi:10.1207/s15326950dp3801_6

Thornhill, R., Gangestad, S.W., 2006. Facial sexual dimorphism, developmental stability, and susceptibility to disease in men and women. Evol. Hum. Behav. 27, 131–144. doi:10.1016/j.evolhumbehav.2005.06.001

Tibesar, R.J., Black, A., Sidman, J.D., 2009. Surgical repair of cleft lip and cleft palate. Oper. Tech. Otolaryngol. Neck Surg. 20, 245–255. doi:10.1016/j.otot.2009.10.010

Trotman, C.A., Faraway, J.J., Essick, G.K., 2000. Three-dimensional nasolabial displacement during movement in repaired cleft lip and palate patients. Plast. Reconstr. Surg. 105, 1273–83.

Trotman, C.A., Faraway, J.J., Losken, H.W., Van Aalst, J.A., 2007a. Functional outcomes of cleft lip surgery. Part II: Quantification of nasolabial movement. Cleft Palate-Craniofacial J. 44, 607–616. doi:10.1597/06-125.1

Trotman, C.A., Phillips, C., Essick, G.K., Faraway, J.J., Barlow, S.M., Losken,

H.W., van Aalst, J., Rogers, L., 2007b. Functional outcomes of cleft lip surgery. Part I: Study design and surgeon ratings of lip disability and need for lip revision. Cleft Palate. Craniofac. J. 44, 598–606. doi:10.1597/06-124.1

Trpkova, B., Prasad, N.G., Lam, E.W.N., Raboud, D., Glover, K.E., Major, P.W., 2003. Assessment of facial asymmetries from posteroanterior cephalograms: validity of reference lines. Am. J. Orthod. Dentofac. Orthop. 123, 512–520. doi:10.1016/S0889-5406(02)57034-7

Tse, R., 2013. Unilateral Cleft Lip: Principles and Practice of Surgical Management. Semin. Plast. Surg. 26, 145–155. doi:10.1055/s-0033-1333884

Tzou, C.H.J., Artner, N.M., Pona, I., Hold, A., Placheta, E., Kropatsch, W.G., Frey, M., 2014. Comparison of three-dimensional surface-imaging systems. J. Plast. Reconstr. Aesthetic Surg. 67, 489–497. doi:10.1016/j.bjps.2014.01.003

Uchida, J.J., 1971. A new approach to the correction of cleft lip nasal deformities. Plast. Reconstr. 47, 454–458.

Uchiyama, T., Kitamura, N., Watanabe, A., Suga, K., Nakano, Y., Hitoshi, O., Takagiwa, M., 2014. Quantification of Negative Aesthetic Ratings in Primary Unrepaired Unilateral Cleft Lip Infants by Modified Paired Comparison Method. Cleft Palate-Craniofacial J. 51, 30–35. doi:10.1597/11-124

Van der Geld, P., Oosterveld, P., Van Heck, G., Kuijpers-Jagtman, A.M., 2007. Smile Attractiveness. Angle Orthod. 77, 759–765. doi:10.2319/082606-349

van Loon, B., Maal, T.J., Plooij, J.M., Ingels, K.J., Borstlap, W.A., Kuijpers-Jagtman, A.M., Spauwen, P.H., Bergé, S.J., 2010. 3D Stereophotogrammetric assessment of pre- and postoperative volumetric

changes in the cleft lip and palate nose. Int. J. Oral Maxillofac. Surg. 39, 534–540. doi:10.1016/j.ijom.2010.03.022

van Loon, B., Reddy, S.G., van Heerbeek, N., Ingels, K.J.A.O., Maal, T.J.J., Borstlap, W.A., Reddy, R.R., Kuijpers-Jagtman, A.-M., Bergé, S.J., 2011. 3D stereophotogrammetric analysis of lip and nasal symmetry after primary cheiloseptoplasty in complete unilateral cleft lip repair. Rhinology 49, 546–53. doi:10.4193/Rhino.11.092

Veau, V., Borel, S., 1931. Division palatine. Masson et Cie, Paris.

Verhoeven, T., Xi, T., Schreurs, R., Bergé, S., Maal, T., 2016. Quantification of facial asymmetry: A comparative study of landmark-based and surface-based registrations. J. Cranio-Maxillofacial Surg. 44, 1131–1136. doi:10.1016/j.jcms.2016.07.017

Verhoeven, T.J., Coppen, C., Barkhuysen, R., Bronkhorst, E.M., Merkx, M.A.W., Bergé, S.J., Maal, T.J.J., 2013. Three dimensional evaluation of facial asymmetry after mandibular reconstruction: validation of a new method using stereophotogrammetry. Int. J. Oral Maxillofac. Surg. 42, 19–25. doi:10.1016/j.ijom.2012.05.036

Walters, M., Claes, P., Kakulas, E., Clement, J.G., 2013. Robust and regional 3D facial asymmetry assessment in hemimandibular hyperplasia and hemimandibular elongation anomalies. Int. J. Oral Maxillofac. Surg. 42, 36–42. doi:10.1016/j.ijom.2012.05.021

Wang, K.H., Heike, C.L., Clarkson, M.D., Mejino, J.L. V, Brinkley, J.F., Tse, R.W., Birgfeld, C.B., Fitzsimons, D.A., Cox, T.C., 2014. Evaluation and integration of disparate classification systems for clefts of the lip. Front. Physiol. 5, 1–11. doi:10.3389/fphys.2014.00163

White, J., 2005. A Longitudinal Study of Facial Growth in Infants using a Three-Dimensional Imaging Technique. PhD thesis, University of Glasgow.

White, J.E., Ayoub, A.F., Hosey, M.-T., Bock, M., Bowman, A., Bowman, J., Siebert, J.P., Ray, A., 2004. Three-Dimensional Facial Characteristics of Caucasian Infants Without Cleft and Correlation With Body Measurements. Cleft Palate-Craniofacial J. 41, 593–602. doi:10.1597/03-069.1

Wiggman, K., Larson, M., Larson, O., Semb, G., Brattstrom, V., 2013. The influence of the initial width of the cleft in patients with unilateral cleft lip and palate related to final treatment outcome in the maxilla at 17 years of age. Eur. J. Orthod. 35, 335–340. doi:10.1093/ejo/cjr144

Williams, A.C., Bearn, D., Clark, J.D., Shaw, W.C., Sandy, J.R., 2001. The delivery of surgical cleft care in the United Kingdom. J. R. Coll. Surg. Edinb. 46, 143–9.

Wong, J.Y., Oh, A.K., Ohta, E., Hunt, A.T., Rogers, G.F., Mulliken, J.B., Deutsch, C.K., 2008. Validity and Reliability of Craniofacial Anthropometric Measurement of 3D Digital Photogrammetric Images. Cleft Palate-Craniofacial J. 45, 232–239. doi:10.1597/06-175

Worasakwutiphong, S., Chuang, Y., Chang, H., Lin, H., Lin, P., Lo, L., 2015. Nasal changes after orthognathic surgery for patients with prognathism and Class III malocclusion: Analysis using three-dimensional photogrammetry. J. Formos. Med. Assoc. 114, 112–123. doi:10.1016/j.jfma.2014.10.003

Wu, J., Heike, C., Birgfeld, C., Evans, K., Maga, M., Morrison, C., Saltzman, B., Shapiro, L., Tse, R., 2016. Measuring Symmetry in Children With Unrepaired Cleft Lip: Defining a Standard for the Three-Dimensional Midfacial Reference Plane. Cleft Palate-Craniofacial J. 53, 695–704. doi:10.1597/15-

053

Wu, J., Tillett, R., McFarlane, N., Ju, X., Siebert, J.P., Schofield, P., 2004. Extracting the three-dimensional shape of live pigs using stereo photogrammetry. Comput. Electron. Agric. 44, 203–222. doi:10.1016/j.compag.2004.05.003

Wu, J., Tse, R., Heike, C.L., Shapiro, L.G., 2011. Learning to compute the plane of symmetry for human faces, in: Proceedings of the 2nd ACM Conference on Bioinformatics, Computational Biology and Biomedicine - BCB '11. ACM Press, New York, New York, USA, pp. 471–474. doi:10.1145/2147805.2147873

Wu, J., Tse, R., Shapiro, L.G., 2014. Learning to Rank the Severity of Unrepaired Cleft Lip Nasal Deformity on 3D Mesh Data, in: 2014 22nd International Conference on Pattern Recognition. IEEE, Los Alamitos, CA, pp. 460–464. doi:10.1109/ICPR.2014.88

Xiong, Y., Zhao, Y., Yang, H., Sun, Y., Wang, Y., 2016. Comparison Between Interactive Closest Point and Procrustes Analysis for Determining the Median Sagittal Plane of Three-Dimensional Facial Data. J. Craniofac. Surg. 27, 441–444. doi:10.1097/SCS.0000000000002376

Yamada, T., Mori, Y., Minami, K., Mishima, K., Sugahara, T., 2002a. Three-dimensional facial morphology, following primary cleft lip repair using the triangular flap with or without rotation advancement. J. Cranio-Maxillofacial Surg. 30, 337–342. doi:10.1054/jcms.2002.0320

Yamada, T., Mori, Y., Minami, K., Mishima, K., Tsukamoto, Y., 2002b. Surgical Results of Primary Lip Repair Using the Triangular Flap Method for the Treatment of Complete Unilateral Cleft Lip and Palate: A Three-Dimensional

Study in Infants to Four-Year-Old Children. Cleft Palate-Craniofacial J. 39, 497–502. doi:10.1597/1545-1569(2002)039<0497:SROPLR>2.0.CO;2

Yamada, T., Sugahara, T., Mori, Y., Minami, K., Sakuda, M., 1999. Development of a 3-D measurement and evaluation system for facial forms with a liquid crystal range finder. Comput. Methods Programs Biomed. 58, 159–73.

Zreaqat, M., Hassan, R., Halim, A.S., 2012. Facial dimensions of Malay children with repaired unilateral cleft lip and palate: a three dimensional analysis. Int. J. Oral Maxillofac. Surg. 41, 783–788. doi:10.1016/j.ijom.2012.02.003

Appendices

7 Appendices

7.1 Appendix 1 Publications

7.1.1 Journal papers

1. Al-Rudainy, D., Ju, X., Mehendale, F., Ayoub, A., 2017. Assessment of facial asymmetry before and after the surgical repair of cleft lip in unilateral cleft lip and palate cases. Int. J. Oral Maxillofac. Surg. 1–9. doi:10.1016/j.ijom.2017.08.007.

2. Al-Rudainy, D., Ju, X., Mehendale, F., Ayoub, A., 2017. Longitudinal evaluation of facial asymmetry of unilateral cleft lip and palate cases (UCLP). Cleft Palate-Craniofacial Journal. Submitted.

3. Al-Rudainy, D., Ju, X., Mehendale, F., Ayoub, A., 2017. Impact of facial expression on residual asymmetry of UCLP cases. Plastic and Reconstructive Surgery. Submitted.

4. Al-Rudainy, D., Ju, X., Mehendale, F., Ayoub, A., 2017. Quality of surgical care provided for UCLP patients, in comparison to the controls. Completed

7.1.2 Oral presentations

1. Scottish Oral and Maxillofacial Society Conference, 3rd November 2017, Glasgow, UK. *A novel approach for the evaluation of facial asymmetry of unilateral cleft lip and palate cases.*

2. British Association of Oral and Maxillofacial Surgeons Annual Scientific Meeting 28th – 30th June 2017, Birmingham, UK. *A novel approach for the three-dimensional evaluation of facial asymmetry of unilateral cleft lip and palate patients (UCLP).*

3. Craniofacial Society of Great Britain and Ireland Annual Scientific Conference, 5th – 7th April 2017, Newcastle upon Tyne, UK. Short oral presentation. *A novel approach for the evaluation of facial asymmetry following surgical repair of unilateral cleft lip and palate patients (UCLP), (a prospective study).*

4. Craniofacial Society of Great Britain and Ireland Annual Scientific Conference 20th -22nd April 2016, Nottingham, UK. *Facial asymmetry of unilateral cleft lip and palate infants before and after primary surgery*.

5. Scottish Craniofacial Research Group Meeting, 8th of March 2017, Glasgow, UK.

6. Postgraduate Research Prize Seminar, 10th of May 2017, Glasgow, UK.

7. Scottish Craniofacial Research Group Meeting, 16th of March 2016, Glasgow, UK.

8. Postgraduate Research Prize Seminar, 27th of April/ 2016, Glasgow, UK.

9. Oral presentation at the Children's Clinical Research Facility Edinburgh, Royal Hospital for Sick Children, 2016, Edinburgh, UK.

7.1.3 Poster presentations

1. The 93rd Congress of European Orthodontic Society June 5th - 10th of June 2017, Montreux, Switzerland. *A novel approach for the assessment of facial asymmetry before and after primary lip surgery of unilateral cleft lip and palate (UCLP).*

2. The 23rd Congress of the European Association for Cranio-Maxillofacial Surgery 13th -16th of September 2016, London, UK. *Evaluation of facial asymmetry before and after the surgical correction of unilateral cleft lip and palate UCLP infants.*

3. Craniofacial Society of Great Britain and Ireland Annual Scientific Conference, 5th – 7th April 2017, Newcastle upon Tyne, UK. *A novel approach for the evaluation of facial asymmetry following surgical repair of unilateral cleft lip and palate patients (UCLP), (a prospective study).*

4. NHS Research Scotland Annual Conference 26th October 2016, Glasgow, UK. *Surface registration of the preoperative and postoperative 3D facial images of unilateral cleft lip and palate UCLP patients.*

5. Postgraduate Induction Day, 5th October 2017, University of Glasgow, Glasgow, UK.

6. Postgraduate Induction Day, 3rd October 2016, University of Glasgow, Glasgow, UK.